

# NISTIR 5486-1

(supersedes NISTIR 5486)

---

---

## Technical Reference Guide for FPEtool Version 3.2

---

---

Scot Deal



**U.S. Department of Commerce**  
**Technology Administration**  
National Institute of Standards and Technology  
Gaithersburg, MD 20899



*Prepared for:*  
**General Services Administration**  
Public Building Service  
Office of Real Property Management  
Washington, DC 20405



# Technical Reference Guide for FPEtool Version 3.2

---

---

Scot Deal

April 1995  
Building and Fire Research Laboratory  
Gaithersburg, Maryland 20899

**U.S. Department of Commerce**  
Ronald H. Brown, *Secretary*  
**Technology Administration**  
Mary L. Good, *Under Secretary for Technology*  
National Institute of Standards and Technology  
Arati Prabhkar, *Director*

*Prepared for:*  
**General Services Administration**  
Roger W. Johnson, *Administrator*  
Public Building Service  
Kenneth R. Kimbrough, *Commissioner*  
Office of Real Property Management  
Washington, DC 20405

## Bibliographic Information

NISTIR 5486-1 includes errata to the original publication of NISTIR 5486 covering installation and operation of the FPEtool software described in section 1.4. The remainder of the report is identical to the original publication.

### Abstract

**FPEtool** is a collection of computer simulated procedures providing numerical engineering calculations of fire phenomena to the building designer, code enforcer, fire protection engineer and fire-safety related practitioner. Version 3.2 newly incorporates an estimate of smoke conditions developing within a room receiving steady-state smoke leakage from an adjacent space. Estimates of human viability resulting from exposure to developing conditions within the room are calculated based upon the smoke temperature and toxicity. There is no modeling of human behavior. Also new to this release is the estimation (in the **FIRE SIMULATOR** procedure) of the reduction in fire heat release rate due to sprinkler suppression.

### Keywords

computer programs, detector response, evacuation models, fire research, fire models, tenability, fire safety engineering, performance evaluation, sprinkler response

## Disclaimer

The U.S. Department of Commerce and the General Services Administration makes no warranty, express or implied, to the users of **FPEtool**, and accepts no responsibility for its use. Users of **FPEtool** assume sole responsibility under Federal and State law for determining the appropriateness of its use in any particular application, for any conclusions drawn from the results of its use, and for any actions taken or not taken as a result of analyses performed using **FPEtool**.

Users are warned that **FPEtool** is intended for use only by persons competent in the field of fire safety and is intended only to supplement the informed judgement of the qualified user.

## Intent and use

The algorithms, procedures, and computer programs described in this report constitute a prototype version of a methodology for predicting the consequences resulting from a specified fire. They have been compiled from the best knowledge and understanding currently available, but have important limitations that must be understood and considered by the user. The program is intended for use by persons competent in the field of fire safety and with some familiarity with personal computers. It is intended as a decision-making tool, but the scope of its use is exploratory.



## Acknowledgements

The General Services Administration provided leadership in funding and developing **FPEtool**. **FPEtool** was created by Harold Nelson while at NIST. **FPEtool** source code was written and many of this document's figures were produced by Charles Arnold. Contributions from the following individuals are acknowledged and deserved; these persons bear no responsibility for errors. Significant help was extended to Mr. Nelson by: James Quintiere and Dave Stroup (both then of NIST), and Dan Madrzykowski of NIST. Suggestions were used from the following individuals: Richard Bukowski, Henri Mitler and Richard Peacock of NIST. Help was also provided by: Robert Zalosh and Jonathan Barnett both of Worcester Polytechnic Institute. Additional help was provided by C. R. Barnett then of McDonald Barnett Partners, Ltd, Rick Parker of G.S.A., Elley Falsafi of Tom Van Rickley & Associates, Don Hoffman of Safety Engineering Laboratories, Inc., Brad Evans of Westinghouse-Hanford, Lennie Farello of Westinghouse-Savannah, Brian McGraw and Ed Mui both from HSB/Professional Loss Control. I apologize to those who helped but to whom I have forgotten. All contributions were appreciated and continue to be encouraged; they improve the product for future users.



# Contents

<b>1 INTRODUCTION</b>	1
1.1 Verification	1
1.2 Technical Support	1
1.3 Hardware and Software Requirements	2
1.4 Installation	2
1.5 History	3
1.6 Comparison with models	3
1.7 FPEtool Modules	4
1.8 FPEtool Hints	5
1.9 FPEtool Filenames	6
1.10 References	6
<b>2 SYSTEM PARAMETERS</b>	9
2.1 Application	9
2.2 Theory	9
2.3 Program Interface	9
<b>3 FIREFORM</b>	11
3.1 ASETBX ROOM MODEL	11
3.1.1 Application	11
3.1.2 Theory	11
3.1.3 Program Notes	17
3.1.4 Program Interface	19
3.1.5 References	20
3.2 ATRIUM SMOKE TEMPERATURE	21
3.2.1 Application	21
3.2.2 Theory	21
3.2.3 Program Notes	21
3.2.4 Program Interface	22
3.2.5 References	22
3.3 BUOYANT GAS HEAD	23
3.3.1 Application	23
3.3.2 Theory	23
3.3.3 Program Notes	23
3.3.4 Program Interface	24
3.3.5 References	24
3.4 CEILING JET TEMPERATURE	25
3.4.1 Application	25
3.4.2 Theory	25
3.4.3 Program Notes	26

3.4.4	Program Interface .....	27
3.4.5	References .....	27
3.5	CEILING PLUME TEMPERATURE .....	29
3.5.1	Application .....	29
3.5.2	Theory .....	29
3.5.3	Program Notes .....	29
3.5.4	Program Interface .....	30
3.5.5	References .....	31
3.6	EGRESS TIME .....	32
3.6.1	Application .....	32
3.6.2	Theory .....	32
3.6.3	Program Notes .....	34
3.6.4	Program Interface .....	35
3.6.5	References .....	36
3.7	FIRE/WIND/STACK FORCES ON A DOOR. ....	37
3.7.1	Application .....	37
3.7.2	Theory .....	37
3.7.3	Program Notes .....	38
3.7.4	Program Interface .....	39
3.7.5	References .....	40
3.8	LATERAL FLAME SPREAD .....	41
3.8.1	Application .....	41
3.8.2	Theory .....	41
3.8.3	Program Notes .....	41
3.8.4	Program Interface .....	42
3.8.5	References .....	42
3.9	LAW'S SEVERITY CORRELATION .....	43
3.9.1	Application .....	43
3.9.2	Theory .....	43
3.9.3	Program Notes .....	44
3.9.4	Program Interface .....	44
3.9.5	References .....	45
3.10	MASS FLOW THROUGH A VENT .....	46
3.10.1	Application .....	46
3.10.2	Theory .....	46
3.10.3	Program Notes .....	47
3.10.4	Program Interface .....	47
3.10.5	References .....	48
3.11	PLUME FILLING RATE .....	49
3.11.1	Application .....	49
3.11.2	Theory .....	49
3.11.3	Program Notes .....	49
3.11.4	Program Interface .....	50

3.11.5	References	50
3.12	RADIANT IGNITION OF A NEAR FUEL	52
3.12.1	Application	52
3.12.2	Theory	52
3.12.3	Program Notes	53
3.12.4	Program Interface	53
3.12.5	References	54
3.13	SMOKE FLOW THROUGH AN OPENING	55
3.13.1	Application	55
3.13.2	Theory	55
3.13.3	Program Notes	56
3.13.4	Program Interface	57
3.13.5	References	57
3.14	SPRINKLER/DETECTOR RESPONSE	58
3.14.1	Application	58
3.14.2	Theory	58
3.14.3	Program Notes	59
3.14.4	Program Interface	60
3.14.5	References	61
3.15	THOMAS'S FLASHOVER CORRELATION	63
3.15.1	Application	63
3.15.2	Theory	63
3.15.3	Program Notes	63
3.15.4	Program Interface	64
3.15.5	References	65
3.16	UPPER LAYER TEMPERATURE	66
3.16.1	Application	66
3.16.2	Theory	66
3.16.3	Program Notes	69
3.16.4	Program Interface	70
3.16.5	References	71
3.17	VENTILATION LIMIT	72
3.17.1	Application	72
3.17.2	Theory	72
3.17.3	Program Notes	72
3.17.4	Program Interface	73
3.17.5	References	73
<b>4</b>	<b>MAKEFIRE</b>	<b>75</b>
4.1	FORMULA	75
4.1.1	Application	75
4.1.2	Theory	75
4.1.3	Program Notes	76

4.1.4	Program Interface .....	76
4.1.5	References .....	79
4.2	FREEBURN .....	80
4.2.1	Application .....	80
4.2.2	Theory .....	80
4.2.3	Program Notes .....	83
4.2.4	Program Interface .....	84
4.2.5	References .....	85
4.3	LOOK-EDIT .....	86
4.3.1	Application .....	86
4.3.2	Theory .....	86
4.3.3	Program Notes .....	86
4.3.4	Program Interface .....	86
4.4	MYFIRE .....	88
4.4.1	Application .....	88
4.4.2	Theory .....	88
4.4.3	Program Notes .....	88
4.4.4	Program Interface .....	89
4.4.5	References .....	90
4.5	RATES .....	91
4.5.1	Application .....	91
4.5.2	Theory .....	91
4.5.3	Program Notes .....	91
4.5.4	Program Interface .....	91
4.5.5	References .....	91
<b>5</b>	<b>FIRE SIMULATOR .....</b>	<b>93</b>
5.1	Application .....	93
5.2	Theory .....	93
5.2.1	Flashover Definition .....	94
5.2.2	Neutral Plane Location and Smoke Layer Interface .....	94
5.2.3	Vent Mass Flow Rate .....	95
5.2.4	Entrainment .....	95
5.2.5	Fire Dimensions: Diameter, Virtual Origin and Flame Height .....	96
5.2.6	Compartment Combustion Chemistry, Pre-Flashover .....	96
5.2.7	Post-Flashover Burning Rate .....	99
5.2.8	Sprinkler Activation and Fire Suppression .....	101
5.2.9	Smoke Detector Activation .....	103
5.2.10	Heat Losses from the Smoke to the Compartment Barriers .....	103
5.3	Program Notes .....	105
5.4	Program Interface .....	107
5.4.1	Pre-Flashover .....	108
5.4.2	Post-Flashover .....	110

5.5	References	112
<b>6</b>	<b>CORRIDOR</b>	<b>115</b>
6.1	Application	115
6.2	Theory	115
6.3	Program Notes	118
6.4	Program Interface	119
6.5	References	120
<b>7</b>	<b>3rd ROOM</b>	<b>123</b>
7.1	Application	123
7.2	Theory	123
7.2.1	Vent Flows	123
7.2.2	Viability Analysis	125
7.3	Program Notes	128
7.4	Program Interface	130
7.4.1	Reference Parameters	130
7.4.2	Target Room Parameters	130
7.4.3	Exposing Space Parameters	131
7.4.4	Leakage Area Parameters	131
7.5	References	132
<b>8</b>	<b>INDEX</b>	<b>133</b>

# List of Figures

	page
Figure 1.11.1 List of <b>FPEtool</b> files by extension and module use. . . . .	6
Figure 2.3.1. <b>FPEtool</b> System Setup menu . . . . .	9
Figure 3.0.1. <b>FPEtool</b> sub-menu for <b>FIREFORM</b> . . . . .	11
Figure 3.1.0. Elevation schematic of <b>ASETBX</b> parameters. . . . .	13
Figure 3.4.1. Fire plume and jet characteristics. . . . .	25
Figure 3.16.1. Temperature pulse moving from a heated to an unheated surface . . . . .	67
Figure 4.0.1. <b>FPEtool</b> sub-menu for <b>MAKEFIRE</b> . . . . .	75
Figure 4.1.1. <b>FPEtool</b> sub-sub-menu for <b>MAKEFIRE's FORMULA</b> . . . . .	77
Figure 4.2.1. Illustration of fuel package geometries for <b>FREEBURN</b> . . . . .	81
Figure 4.2.2. Fuel package widths for <b>FREEBURN</b> . . . . .	81
Figure 4.2.3. <b>FREEBURN</b> internal representation of fuel package separation distances . . . . .	81
Figure 4.2.4. <b>FPEtool</b> sub-menu of the <b>FREEBURN</b> procedure . . . . .	84
Figure 5.2.1. <b>FIRE SIMULATOR</b> geometrical descriptions . . . . .	95
Figure 5.2.2. Warm-air plume entrainment interactions with smoke layer interface elevation . . . . .	101
Figure 5.2.3. Conceptual procedure for warm-air plume entrainment . . . . .	103
Figure 6.0.1. <b>CORRIDOR</b> geometry in cross-section . . . . .	115
Figure 7.0.1. <b>3rd ROOM</b> input parameter geometries. . . . .	123
Figure 7.0.2. Delineation of vent-flow slabs and cross-vent pressure profiles . . . . .	124
Figure 7.0.3. Convective heat transfer exponential dependence upon temperature . . . . .	125
Figure 7.0.4. Effect of human activity on time to incapacitation via CO toxicity . . . . .	129

# Technical Reference Guide for **FPEtool**, Version 3.2

Scot Deal

Building and Fire Research Laboratory  
National Institute of Standards and Technology  
Gaithersburg, MD 20899

## 1 INTRODUCTION

**FPEtool** is a collection of computer simulated procedures providing numerical engineering calculations of fire phenomena to the building designer, code enforcer, fire protection engineer and fire-safety related practitioner. Version 3.2 newly incorporates an estimate of smoke conditions developing within a room receiving steady-state smoke leakage from an adjacent space. Estimates of human viability resulting from exposure to developing conditions within the room are calculated based upon the smoke temperature and toxicity. There is no modeling of human behavior. Also new to this release is the estimation (in the **FIRE SIMULATOR** procedure) of the reduction in fire heat release rate due to sprinkler suppression.

### 1.1 Verification

Formal verification of **FPEtool** has not been conducted. However, many of the components of **FPEtool** are based upon experimental data, and predictions from previous versions of **FPEtool** have been compared with data from a number of experiments [11,12,13,14,18,19]. Users may find it appropriate to compare the predictions of **FPEtool** with those from other models and/or experimental data. In addition, a sensitivity analysis of **FPEtool** output to variations in the input data may be desirable.

### 1.2 Technical Support

There are several databases within **FPEtool**. One provides information for designing input fire files (this database is found in **RATES/MAKEFIRE**), another provides information on wall thermophysical properties (this database is found in **FIRE SIMULATOR**), and another provides information on flame spread rates of various fuels (this database is found in **FREEBURN/MAKEFIRE**). References containing these types of data may be found in the Fire Protection Handbook [20], the SFPE Handbook [21], the Handbook for Fire Engineers [22] and standard engineering handbooks [15,16].

Inquires concerning **FPEtool** should be directed to the manager of the Fire Research Information Services, Building and Fire Research Laboratory, National Institute of Standards and Technology, Building 224, Room A-252, Gaithersburg, MD 20899, (301) 975-6862.

### 1.3 Hardware and Software Requirements

Your package should contain a 3.5-inch diskette, *Technical Reference Guide for FPEtool, Version 3.2*, and a registration card. If the package is incomplete, contact the vendor or the Building and Fire Research Laboratory at the National Institute of Standards and Technology.

An IBM PC<sup>1</sup> compatible computer with DOS version 3.1 or later will operate the **FPEtool Version 3.2** code (The Macintosh and UNIX platforms do not support **FPEtool**). A math co-processing chip is not required, but will significantly improve calculation speed. A minimum of 640 kBytes RAM are required and 3 MBytes of hard-disk space is recommended. The graphics display driver supports CGA or better monitors.

### 1.4 Installation

To install **FPEtool**, place the diskette into an available 3.5-inch diskette drive and type the drive letter of the 3.5-inch drive, followed by a colon, a backslash, and the word install. For example, if your 3.5-inch drive is drive A, type

```
a:\install
```

and press the enter key. You will be asked several questions about your computer and how you wish to install **FPEtool**. You may answer none, some or all of the questions as appropriate for your specific needs. Follow the directions on the screen closely and provide answers to questions as desired. Usually, the defaults provided by the program will be sufficient and you may simply press the enter key to accept the default selection.

To start **FPEtool**, change to the directory where the program is installed and type fpetool followed by the enter key. For example, for the default installation, the following DOS commands can be used

```
cd \fpetool  
fpetool
```

---

1. The use of company or trade names within this report is made solely for the purpose of identifying those computer hardware or software products operationally compatible with the **FPEtool** product. Such use does not constitute any endorsement of those products by the National Institute of Standards and Technology.

## 1.5 History

Simple (algebraic) equations have been a mainstay of engineering handbooks for as long as they have existed. With the advent of modern calculators and then computers, the complexity of these equations has increased, since it was no longer necessary to refer to tables of logarithms to evaluate them. Today we can perform fully time-dependent calculations with systems of differential equations on our desktops at the push of a button.

Individual equations which relate to fire phenomena have been around a long time as well, often representing correlations to experimental data and observations. In 1984 Bukowski suggested that a *series* of individual calculations could be used to evaluate a complex, interactive process (i.e., a fire hazard analysis). This was followed by a demonstration of the technique for plenum cables in a paper published in 1985 [2]. A broader series of equations applicable to fire growth estimates was also published in 1985 [3].

The proliferation of personal computers in the 1980's led to the programming of these collections of equations into packages which prompted the user for a few, simple inputs and provided for tabular and simple, graphical outputs. Soon, software<sup>2</sup> like FIREFORM [4] (US), ASKFRS (UK) [5], and FIRECALC [6] (Australia) appeared on desktop computers around the world. These packages have become the engineering handbook type of calculation for the modern practice of fire safety engineering.

## 1.6 Comparison with models

Persons just learning about these calculational methods often wonder how these tools differ from the growing number of computer fire models appearing on the scene. An appropriate distinction is that the simple tools generally give *steady-* or *quasi-steady state* solutions to time dependent problems and predict a *single* parameter (e.g., layer temperature, filling time, doorway flow, radiation at a point). Models give time varying results of several parameters which are inter-dependent. Most (e.g. HARVARD V [7]) apply a *quasi-steady* approximation to do so (FAST [8] solves the differential equations, so is fully time-dependent). With the tools, the user may need to perform calculations and thread results together to obtain a prediction for the scenario under study.

This interaction is an important distinction since fire can be a highly interactive process. In some circumstances such as early in a room fire while there is only a single item burning and little enhancement of the burning rate by radiation feedback from the upper layer, the model prediction should approach the steady-state solutions produced by the some of the equations in **FIREFORM**.

---

2. While these software packages contain a number of individual equations they include simple one- or even two-room models as well, such as the well known ASET model.

However, later, as radiation from the upper layer and room surfaces and lowered oxygen concentrations alter burning rates, appropriately designed models should maintain their predictive accuracy while the steady-state equations become invalid.

However, users of both models and steady-state equations must always keep in mind the ranges of validity of each. All such techniques are approximations which often involve empirical relationships derived from limited sets of observations. It is not that the relation is *known* to be invalid outside the stated range, but rather that it is *not known* to be correct -- an important distinction<sup>3</sup>.

## 1.7 FPEtool Modules

**FPEtool** is a compilation of several modules grouped into 5 categories. These categories are:

**SYSTEM SETUP**  
**FIREFORM**  
**MAKEFIRE**  
**FIRE SIMULATOR**  
**CORRIDOR**  
**3rd ROOM**

**SYSTEM SETUP** is a utility routine. It allows the user to change file destination and source directories, change operating units and to alter screen colors. The menu choices are presented in Figure 2.0.1 as they appear to the user. This manual uses SI (System International or metric system) as the default unit set.

**FIREFORM** is a predominantly a collection of quick procedures designed to solve single-parameter questions (see Section 1.8). Such questions might be "How hot is the ceiling jet 3 meters from the center of plume impingement? How long will it take for 50 people to evacuate from the 7th floor to the ground floor of this building? When will this second fuel item ignite?"

**MAKEFIRE** is a collection of routines that create and edit fire files. These files have 3 columns of data: time, fire heat release rate and fuel pyrolysis rate. The users can create their own fires, use prescribed 't-squared' fires, and let the program determine when the primary fire ignites a secondary object.

**FIRE SIMULATOR** is a procedure that predicts the effects of fire growing in a one-room, two-vent, compartment with sprinkler and detector, using a two-zone model.

---

<sup>3</sup> The author acknowledges R.W. Bukowski for contributing these preceding paragraphs.

**CORRIDOR** is a procedure that predicts the characteristics of a moving smoke wave; the procedure works best in spaces with large length to width ratios that receive smoke flows with minimal entrainment.

**3rd ROOM** is a procedure that predicts smoke conditions developing in a room and the subsequent reduction in human viability resulting from exposure to such conditions.

The last 3 modules may be used sequentially. **FIRE SIMULATOR** predicts fire generated effects within the room of origin. Smoke outflow from **FIRE SIMULATOR** may be used as smoke inflow to the **CORRIDOR** module. Smoke conditions predicted with the **CORRIDOR** module can be used to define conditions on the 'fire-side' of the door to the **3rd ROOM**. In the following chapters, each of the above-mentioned modules will be explained in further detail.

## 1.8 FPEtool Hints

Input files for the **FREEBURN**, **FIRE SIMULATOR**, and **3rd ROOM** routines may be created 'from scratch'. It is usually easier to edit an existing file than create one.

An index provided in Section 8 provides assistance in obtaining some contextual definitions.

If one desires to reverse their direction or to move backwards in the input process (and thus return to a higher branch in the menu structure), this can be accomplished by simultaneously pressing the 'Control' and 'Q' keys. The only time when this command will not work is when the program expects to receive a DOS file name as input.

The figures and diagrams presented in this guide are for edification purposes, not measurement reconstruction. The figures do not necessarily convey accurate scaling.

## 1.9 FPEtool Filenames

Figure 1.11.1 is presented to explain the relationship between the files and file names used by **FPEtool**.

DOS File Name Extension	Procedure that generates the DOS file	Procedure that uses the DOS file	File Type	Description
*.FIR	<b>MAKEFIRE</b> or user created in <b>FIRE SIMULATOR</b>	<b>ASETBX, UPPER LAYER TEMPERATURE FREEBURN, FIRE SIMULATOR, CORRIDOR</b> <sup>□</sup>	ASCII	3 columns of data, time (s), actual heat release rate of the fire (kW), and pyrolysis rate (g/s)
*.DAT	<b>FREEBURN</b>	<b>FREEBURN</b>	ASCII	Input file for <b>FREEBURN</b>
*.IN	<b>FIRE SIMULATOR</b>	<b>FIRE SIMULATOR</b>	ASCII	Input file for <b>FIRE SIMULATOR</b> , see <i>INPUT</i> section of <b>FIRE SIMULATOR</b> for a list of variables.
*.WK1	<b>FIRE SIMULATOR</b> or <b>CORRIDOR</b>	LOTUS <sup>®</sup> and compatible spreadsheet programs	Binary	Output file from <b>FIRE SIMULATOR</b> and <b>CORRIDOR</b> .
*.HSL	<b>3rd ROOM</b>	<b>3rd ROOM</b>	Binary	Input file for <b>3rd ROOM</b>
*.OUT	<b>3rd ROOM</b>	<b>3rd ROOM</b>	ASCII	Output file from <b>3rd ROOM</b>

<sup>□</sup> Citation of LOTUS<sup>®</sup> and compatible spreadsheet software is not an endorsement of these products.

Figure 1.11.1 List of **FPEtool** files by extension and module use.

## 1.10 References

- [1] Bukowski, R.W., "Strawman Procedure for Assessing Toxic Hazard." In Summary preliminary report of the advisory committee on the toxicity of the products of combustion. NFPA, Quincy, MA; June 1984.
- [2] Bukowski, R.W., "Toxic Hazard Evaluation of Plenum Cables", *Fire Technology*, 21(4), 252-266, November 1985.

- [3] Lawson, J.R. and Quintiere, J.G., "Slide-rule Estimates of Fire Growth," Nat. Bur. Stand. (U.S.), NBSIR 85-3196, Gaithersburg, MD, pp. 56. 1985.
- [4] Nelson, H.E., "FIREFORM: A Computerized Collection of Convenient Fire Safety Computations", Nat. Bur. Stand. (U.S.), NBSIR 86-3308, Gaithersburg, MD, 1986.
- [5] Chitty, R. and Cox, G., "ASKFRS: An Interactive Computer Program for Conducting Engineering Estimations," HMSO, London, 1988.
- [6] Anonymous, "FIRECALC Computer Software for the Fire Engineering Professional," CSIRO Division of Building, Construction, and Engineering, North Ryde, NSW, Australia, 1991.
- [7] Mitler, H.E. and Emmons, H.W., "Documentation for CFC V, the Fifth Harvard Computer Fire Code," Nat. Bur. Stand. (U.S.), NBS GCR 81-344, 187p, 1981.
- [8] Jones, W.W. and Peacock, R.D., "Technical Reference Guide for FAST: version 18", Nat. Inst. Stand. Tech. (U.S.) TN 1262, Gaithersburg, MD, 1989.
- [9] Hall, J.R., "How to Tell Whether What You Have is a Fire Risk Analysis Model," Fire Hazard and Risk Assessment, ASTM Publication STP 1150, Marcelo Hirschler, ed., Philadelphia, PA 19103, pp. 131-5, 1992.
- [10] McGrattan, K.B., et al., "Boussinesq Algorithm for Buoyant Convection in Polygonal Domains," Nat. Inst. Stand. Tech. (U.S.), NISTIR 5273, Gaithersburg, MD 20899, 1993.
- [11] Notarianni, K.A., Davis, W.D., "Use of Computer Models to Predict Temperature and Smoke Movement in High Bay Spaces," Nat. Inst. Stand. Tech. (U.S.), NISTIR 530, Gaithersburg, MD 20899, 1993.
- [12] Walton, W.D., Notarianni, K.A., "Comparison of Ceiling Jet Temperatures Measured in an Aircraft Hanger Test Fire with Temperatures Predicted by the DETACT-QS and LAVENT Computer Models," Nat. Inst. Stand. Tech. (U.S.), NISTIR 4947, Gaithersburg, MD 20899, 1993.
- [13] Nelson, H.E., Deal, S., "Comparison of Four Fires with Four Fire Models," Proceedings of 3rd International Symposium, IAFSS, Edinburg, Scotland, pp. 719-728, 1992.
- [14] Peacock, R.D. et al., "Verification of a Model of Fire and Smoke Transport," Fire Safety Journal: Vol. 21(2), pp. 89-129, 1993.

- [15] Perry, J.H., Chilton, C., Chemical Engineers' Handbook, McGraw-Hill, New York, pp. 3-151, 1973.
- [16] Baumeister, T., "Mark's Standard Handbook for Mechanical Engineers, 8th Ed.," Editor-in-chief, Mc-Graw Hill, NY, 1978.
- [17] Quintiere, J., Cleary T., "A Framework for Utilizing Fire Test Properties," Nat. Inst. Stand. Tech. (U.S.), NISTIR 4619, Gaithersburg, MD 20899, 1991.
- [18] Heskestad, G. and Hill, J.P., "Experimental Fires in Multi-Room/Corridor Enclosures," NBS-GCR-86-502, Gaithersburg, MD 20899, 1986.
- [19] Hinkley, P.L., "Work by the Fire Research Station on the Control of Smoke in Covered Shopping Centers," proceedings of the Conseil International du Bâtiment (CIB) W14/163/76 (U.K.) 24 p. September 1975.
- [20] Cote, A.E., Editor-in-chief, Fire Protection Handbook, National Fire Protection Association, Quincy, MA 02269, 1991.
- [21] DiNunno, P., Editor-in-chief, The Society of Fire Protection Engineers Handbook of Fire Protection Engineering, National Fire Protection Association, Quincy, MA, 1988.
- [22] Edgerley, P.G., Editor-in-chief, Handbook for Fire Engineers, Wheaton & Co. Ltd., Exeter, England, 1989.



Units: metric/U.S. enginr. Allows user to switch between metric ( $\text{kg}\cdot\text{m}\cdot\text{s}\cdot^\circ\text{C}$ ) and American customary units ( $\text{lb}_m\cdot\text{ft}\cdot\text{s}\cdot^\circ\text{F}$ ).

*OUTPUT* -- none



listed in the *OUTPUT* section of this report. To obtain these output, **ASETBX** solves the fundamental conservation equations. The solutions to these equations provide answers to basic properties (temperature and mass) of the smoke resulting from the fire. These basic properties then are used in turn to provide answers about subsequently more detailed descriptions of the smoke.

The conservation equations are mathematical accounting procedures. These accounting procedures record where a quantity has come from, where the quantity is, and where the quantity is going at each time step. The conservation laws state that a quantity can not appear or disappear without proper accounting. The accounting procedures can be exploited to predict an array of fire related output because nature obeys the conservation laws. There are three conservation laws: mass, momentum and energy. When speaking about conserved quantities it is necessary to clearly define the system (or control volume) to avoid confusion about the appearance, consumption and movement of conserved quantities. If a quantity appears, it is because it was generated or transported into the system. If a quantity disappears, it is because it was consumed or transported out of the system. In the context of a defined system, when a quantity appears at a rate exceeding the rate of disappearance, a net accumulation results. The converse also is true. While simple in theory, the conservation laws can be somewhat difficult to apply in practice. Perhaps this difficulty arises from an unfamiliarity with 'visualizing' generation, consumption and movement of energy and/or momentum. Perhaps the difficulty is due to the unrecognized and simultaneous influence that the three conservation laws exert upon one other. Despite these apparent difficulties with 'thinking' in terms of conservation laws, there are distinct advantages to familiarizing one's self with them. As is true in most areas of endeavor when a new or difficult situation arises, the solution can often be achieved through strong application of the fundamentals.

In reality--mass, momentum and energy quantities are conserved, however, in **ASETBX** only energy and mass are conserved (momentum is ignored because vent flows are assumed unidirectional). These conserved quantities are introduced below as concepts and then converted to mathematical equations of the form solved by **ASETBX**. The mathematical equations are not solved analytically owing to their non-linearity; the equations are solved numerically. The development of energy conservation can be drawn from analogy to the following presentation of mass conservation.

$$\left[ \begin{array}{l} \text{rate of mass flow} \\ \text{into the control volume} \end{array} \right] + \left[ \begin{array}{l} \text{rate of mass generation} \\ \text{in the control volume} \end{array} \right] - \left[ \begin{array}{l} \text{rate of mass flow} \\ \text{out of the control volume} \end{array} \right] - \left[ \begin{array}{l} \text{rate of mass consumption} \\ \text{in the control volume} \end{array} \right] = \left[ \begin{array}{l} \text{rate of mass accumulation} \\ \text{within the control volume} \end{array} \right] \quad (1)$$

$$\dot{m}_{out} = \frac{(1-\lambda_c)\dot{Q}}{c_{p_\infty} T_\infty} \quad z_{inf} > -z_{fire}$$

$$\frac{(1-\lambda_c)\dot{Q}}{c_{p_\infty} T} \quad z_{inf} = -z_{fire} \quad (2)$$



$$\begin{aligned}
& (-\dot{m}_{out} - \dot{m}_{plume}); & 0 < z_{intf} \leq z_{ceil}, & \quad (a) \\
\rho_{\infty} A_{floor} \frac{dz_{intf}}{dt} = & -\dot{m}_{out}; & -z_{fire} < z_{intf} \leq 0, & \quad (b) \\
& 0; & z = -z_{fire}, & \quad (c)
\end{aligned} \tag{5}$$

$$\tau = \frac{t}{t_o}; \quad \zeta = \frac{z_{intf}}{L_c}; \quad \phi = \frac{T}{T_{\infty}}; \quad \dot{q} = \frac{\dot{Q}}{\dot{Q}_o} \tag{6}$$

$$\begin{aligned}
& -c1\dot{q} - c2\dot{q}^{\frac{1}{3}}\zeta^{\frac{5}{3}}; & 0 < \zeta \leq \zeta_{ceil}, & \quad (a) \\
\frac{d\zeta}{d\tau} = & -c1\dot{q}; & -\zeta_{fire} < \zeta \leq 0, & \quad (b) \\
& 0; & \zeta = -\zeta_{fire}, & \quad (c)
\end{aligned} \tag{7}$$

The change of variables defined in eq (6) were made in such a way [4] that the **ASETBX** program output could be generalized to any unit system. This generalization required nondimensionalizing. The nondimensionalized terms were substituted into eq (5) to produce eq (7), the mathematical form of the mass conservation law used in **ASETBX**.

$$\rho_{\infty} T_{\infty} = constant \tag{8}$$

$$\bar{\rho} = \frac{1}{(z_{ceil} - z_{intf})} \int_{z_{intf}}^{z_{ceil}} \rho(s) ds \tag{9}$$

By analogy and by using eqs (8) and (9) one may also obtain the mathematical equation for the energy conservation law used in **ASETBX** eq (10).

$$\begin{aligned}
\frac{d\phi}{d\tau} = & \frac{\phi[c1\dot{q} - (\phi-1)c2\dot{q}^{\frac{1}{3}}\zeta^{\frac{5}{3}}]}{(\zeta_{ceil} - \zeta)}; & 0 < \zeta \leq \zeta_{ceil} & \quad (10) \\
& \frac{c1\phi\dot{q}}{(\zeta_{ceil} + \zeta)}; & -\zeta_{fire} \leq \zeta \leq 0 &
\end{aligned}$$

$$c1 = \frac{(1-\lambda_c)t_c\dot{Q}_0}{\rho_{\infty}c_pT_{\infty}A_{floor}L_c} \tag{11}$$

$$c_2 = \left[ \frac{0.21 t_c}{A_{floor}} \right] \left[ \frac{(1-\lambda_r) \dot{Q}_0 * g * L_c^2}{(\rho_\infty c_p T_\infty)} \right]^{\frac{1}{3}} \quad (12)$$

Conservation of energy is applied to a system around the hot, smokey gases--not the lower ambient gases. Eqs (7) and (10) are first-order, non-linear, non-homogeneous, coupled, ordinary differential equations (ODE's). The coupling (dependency upon one another) is evident through the layer height term ( $\zeta$ ) appearing in both equations. This dependency is resolved by determining answers for eqs (7) and (10) simultaneously.

Even after nondimensionalizing, eqs (7) and (10) may still be seen to possess terms representative of physical processes. The first term in eq (7) represents mass contribution from the pyrolyzate. The second term in eq (7) represents mass contribution from plume entrainment. Similarly, the first term in the top equation of eq (10) represents energy contributed from the burned fuel. The second term in top equation of eq (10) represents energy contributed from plume-entrained air. The top equation in eq (10) represents energy conservation when the smoke layer interface is higher than the pyrolyzing fuel. The bottom equation in eq (10) represents energy conservation when the smoke layer interface is at or lower than the fuel level.

Conceptually, the plume acts as a pump entraining pyrolyzates and cool air into the upper layer. The energy for entrainment comes from the fire. Entrainment is the process whereby a surrounding fluid is drawn into a stream of moving fluid. The moving fluid stream can be buoyancy or momentum driven; for most compartment fire applications, the moving steam is buoyancy driven. The entrainment process is quite complex and only beginning to be analytically computed. Most 2-zone fire models therefore represent entrainment correlationally [2,7]. The correlation is strongly dependent upon height within the plume (Section 5.2.4), and to a lesser extent the buoyancy of the plume. The entrainment process will cease when the stream of fluid stops moving, either through loss of buoyancy or loss of momentum.

The surrounding fluid is drawn into the rising plume by mixing occurring at the plume edges. This mixing occurs primarily because of friction (between the moving hot gases and the nonmoving, cool surrounding air) and to a lesser extent because of diffusion. Vortices are sheared back and away from the moving fluid stream and as this occurs, cool, ambient air is drawn into the low pressure area formed behind the circulating eddy/vortex. As ambient air is drawn in with the turbulent, buoyant combustion gases, and the resulting mixture expands, cools and slows as it rises in what is called the fire plume.

The gases in the fire plume rise because the hot gases are buoyant and therefore pushed up (similar to why a helium balloon is pushed up) by the colder, denser, surrounding air. The plume expands, cools and slows as it rises. The plume expands because entrainment introduces more mass into the plume. The additional mass more than compensates for the contraction of gases as they cool. The gases cool because the entrained air is colder than the fire products. The plume gases slow because

conservation of momentum dictates a larger plume mass moves at a slower velocity. Friction with the surrounding air also takes kinetic energy from the rising gases.

The plume extends from the location where entrainment begins to the location where entrainment and plume rise cease. Entrainment height is an important factor in modeling fire effects because the amount of cool air entrained within the plume is proportional to the entrainment height raised to the 5/3 power [2]. **ASETBX** and most other 2-zone fire models ask the user to define the location where entrainment begins. In the *INPUT* section of 3.1.3, the model asks for the height at the base of the flames. Appropriate input is therefore important for the *'base of the fuel'* parameter.

$$\zeta_{\tau=0} = \zeta_{ceil} \quad (a)$$

$$\phi_{\tau=0} = 1 + \frac{c1}{c2} \zeta_{ceil}^{-\frac{5}{3}} \quad (b)$$

$$\frac{d\phi}{d\tau_{\tau=0}} = \left[ \frac{c1}{c2} \right] \left[ \frac{2\dot{Q}_{t=0} + 5(c1 + \zeta_{ceil}^{\frac{5}{3}}c2)}{6\zeta_{ceil}^{\frac{8}{3}}} \right] \quad (c) \quad (13)$$

The form of the mathematical equations solved by **ASETBX** take a slightly different form than seen in eq (7) and eq (10). This difference results from using a numerical rather than an analytical solution. One result of the numerical approach is the quasi-steady state assumption. This assumption states that conditions related to the fire and the fire's effects are constant between computational timesteps. Differences between a real fire and the numerical solution can occur if the time steps are too large to account for detail in the real fire that occur between computations.

In order to solve differential equations, boundary conditions must be provided. Initial-value boundary conditions are applied because conditions at the onset of the fire are generally better known than conditions during the fire. The initial conditions define the initial upper-air layer temperature ( $\phi$ ) and the mass of the lower layer [accounted for with the layer position ( $\zeta$ )]. Although  $d\phi/d\tau^*_{\tau=0}$  appears indeterminate at time  $\tau$  equal to zero [eq (10)], a value has been found by Cooper [3] and this appears in eq (13).

$A_{floor}$	Floor area (m <sup>2</sup> )
$c_{p,\infty}$	Ambient air heat capacity, (kJ/(kg·ΔK))
$g$	Earth's surface gravitational constant, (m/s <sup>2</sup> )
$\Delta H_c$	Heat of combustion (kJ/(kg·K))
$L_c$	Characteristic length (m)
$m$	Mass of the lower air layer (kg)
$\dot{m}_{exit}$	Mass of air exiting the room from the lower air layer (kg/s)
$\dot{m}_{plume}$	Mass of air leaving the lower air layer into the plume (kg/s)

$\dot{q}$	Nondimensional heat release rate, $Q/Q_0$
$Q$	Fire heat release rate (kW)
$Q_0$	Initial value of the heat release rate, (0.95 kW)
$s$	Dummy variable of integration
$t$	Virtual simulation time (seconds)
$t_c$	Characteristic time (1 second)
$T$	Smoke temperature (K)
$T_\infty$	Ambient air temperature
$z$	Elevation (m)
$z_{\text{inf}}$	Elevation change from smoke layer interface to lowest point of burning fuel (m)
$z_{\text{fire}}$	Elevation of the bottom of the fuel flames above the room floor (m)
$z_{\text{ceil}}$	Elevation of the ceiling above the fuel height (m)
$\lambda_c$	Fraction of upper layer energy lost by heat transfer into room barrier surfaces
$\lambda_r$	Fraction of actual heat release rate directed into radiative energy
$\rho_\infty$	Ambient air density (1.2 kg/m <sup>3</sup> )
$\tau$	Nondimensional time, $t/t_{\text{characteristic}}$
$\zeta$	Nondimensional elevation, $z/L_c$
$\phi$	Nondimensional temperature, $T/T_\infty$
$\chi_A$	Combustion efficiency

### Energy Flow out of the Hot Gases and into the Walls

In applying conservation of energy to the upper air layer, the rate of energy flow out of the this hot gas volume leaving by radiation and convection and moving into the room barrier surfaces is assumed to be a fixed fraction. This fraction ( $\lambda_c$ ) is unchanged throughout the simulation duration. This fraction also is user specified and has a default value of 0.65.

#### 3.1.3 Program Notes

The heat losses to the wall surfaces are a fixed fraction of the heat contained in the upper, hot gas layer. This ratio can change with time, fire conditions, room geometry and wall material though. The user specifies this wall heat-loss fraction.

The fire growth rate is not enhanced by radiation feedback from the hot layer.

$$\dot{Q} = \Delta H_c \dot{m}_{\text{pyrolysis}} \quad (14)$$

The heat release rate of the fire should be specified to the **ASETBX** input fire file. The heat release rate can be determined from eq (14) utilizing either the theoretical heat of combustion or the effective

heat of combustion. Sometimes the effective heat of combustion is called the chemical heat of combustion. The theoretical heat of combustion is the maximum heat release rate possible per unit mass of fuel under specific conditions. The effective heat of combustion is less than the theoretical heat of combustion since it reflects inefficiencies in actual combustion scenarios. Using theoretical heat of combustion will therefore result in a larger heat release rate for a given mass loss rate compared with the effective heat of combustion.

The fuel area is an important factor in entrainment. **ASETBX** and many other 2-zone fire models use plume correlations [2,7] that assume a point-source fire. The error in this assumption is that line-fires [8], liquid pool fires and large fires of irregular area (e.g., sofas, tables) will entrain differently than a point-source fire model. Line-fires have long, narrow geometries. Examples of line fires are a flammable liquid fire on a pipe-run wetted from a leak, or a cable tray fire.

The plume is unconfined: the distance from the walls to the vertical axis running through the fire-center should be  $\geq 0.2$  height of  $(z_{\text{ceiling}} - z_{\text{fire}})$ .

There is no modeling of oxygen starvation, hence post-flashover modeling is inappropriate.

Mass conservation occurs on the lower layer; this can possibly induce numerical inaccuracies when the lower layer becomes small relative to the larger layer. This fact is another reason why it is not recommended to use **ASETBX** for post-flashover fire analysis.

Pressure accumulation is not mathematically considered, this implies that openings of sufficient size must exist below the level of the smoke layer to allow outflow of the lower layer gases as the smoke expands to fill the room.

The upper layer temperature prediction from 2-zone fire models is a characteristic temperature. Temperatures near the ceiling will be hotter and temperatures near the smoke layer bottom will be cooler than the predicted temperature. The **ASETBX** (and most other 2-zone fire model) temperature predictions result from an integrated average of energy contained in the upper layer.

The quasi steady-state fire assumption holds if the actual fire heat release rate does not change substantially between computational time-steps. The simulated fire linearly interpolates fire heat release rate for time steps between data points in the input fire file.

Standard pressure (101,325 Pa), room temperature (21 °C) and ambient gas concentrations (21% O<sub>2</sub>, 79% N<sub>2</sub>) are assumed.

Radiative loss fractions from the fire are assumed at 35% and remains fixed for all fuels regardless of soot volume-fraction generation rate.

This procedure is not appropriate for rooms with floor aspect ratios (width:length) greater than 10:1 [9] during early stages of fire growth where smoke has not traversed the entire length of the room.

This procedure also may not be appropriate for rooms with a height to minimum horizontal ratio, in excess of 1 [3].

This procedure is not appropriate for large fires relative to the compartment containing the hot layer [5].

### 3.1.4 Program Interface

#### *INPUT*

Heat loss fraction	Fraction of upper layer energy lost to the room surfaces, ( $\lambda_c$ )
Fire radiative fraction	Fraction of actual fire heat release rate dispersed via radiation, ( $\lambda_r$ )
Height at Base of Flames	Lowest elevation of the burning fuel that can freely entrain air (m)
Room ceiling height	Height of the ceiling above the floor (m)
Room floor area	(m <sup>2</sup> or ft <sup>2</sup> )
Printout interval	(sec)
Next input screen	
File Description	User selected, pre-existing valid DOS fire file name
Enter a fire	User created fire file (see Section 4.1 and 4.4)

#### *OUTPUT*

T(t)	Smoke temperature as a function of time (°C)
Layer height(t)	Elevation of the bottom of the smoke layer above the floor (m)
$Q_{\text{fire}}$	Fire heat release rate (kW)
Graphs	Temperature vs time (°C, sec) Layer depth vs time (m, sec) Fire heat release rate vs time (kW, sec)

### 3.1.5 References

- [1] Alpert, R.L., and Ward, E. J.; "Evaluating Unsprinklered Fire Hazards; SFPE Technology Report 83-2;" Society of Fire Protection Engineers: Boston, MA, 1983.
- [2] Zukoski, E.E., Kubota, T., Cetegen, B., "Entrainment in the Near Field of a Fire Plume. Final Report," Nat. Bur. Stand. (U.S.), NBS-GCR-81-346, Gaithersburg, MD 29899, November 1981.
- [3] Cooper, L.Y., and Stroup, D.W., "Calculating Available Safe Egress Time from Fires," Nat. Bur. Stand. (U.S.), NBSIR 82-2587, Gaithersburg, MD 20899, 1982.
- [4] Cooper, L.Y., "A Mathematical Model for Estimating Available Safe Egress Time in Fires," Fire and Materials, (6), No. 3 & 4, pp. 135-44, 1982.
- [5] Walton, W.D., "ASET-B, A Room Fire Program for Personal Computers," Nat. Bur. Stand. (U.S.), NBSIR- 85-3144-1, Gaithersburg, MD 20899, 1985.
- [6] Nelson, H.E., "FPETOOL: Fire Protection Engineering Tools for Hazard Estimation," Nat. Inst. Stand. Tech. (U.S.), NISTIR 4380, Gaithersburg, MD 20899, 1990.
- [7] McCaffrey, B.J. "Purely Buoyant Diffusion Flames: Some Experimental Results," Nat. Bur. Stand. (U.S.), NBSIR 79-1910, Gaithersburg, MD 20899, 1979.
- [8] Grella, J.J. and Faeth, G.M., "Measurements in a Two-Dimensional Thermal Plume along a Vertical Adiabatic Wall," Journal of Fluid Mechanics, 21, pp. 701, 1975.
- [9] Cooper, L.Y. "Estimating Safe Available Egress Time from Fires," Nat. Bur. Stand. (U.S.) NBSIR 80-2172, Gaithersburg, MD 20899, 1981.

## 3.2 ATRIUM SMOKE TEMPERATURE

### 3.2.1 Application

This procedure estimates the average temperature in the smoke layer developing from a fire within an atrium or other large space.

### 3.2.2 Theory

$$T_{atria} = \frac{220}{1 + 39.8 \left\{ \frac{z^{5/3}}{\dot{Q}^{2/3}} \right\}} \quad (1)$$

The atrium smoke temperature is derived from the **ASETBX** plume equation [1] that had its own origins from Zukoski [3]. Given an entrainment height and a fire heat release rate, the procedure then determines the maximum temperature in the plume.

$T_{atria}$	Temperature rise in atria hot gas layer (°C)
$Q$	Fire heat release rate (kW)
$z$	Elevation between lowest point of entrainment and height of interest (m)

### 3.2.3 Program Notes

The plume theory used in this routine does not apply to the case where plume gases expand to the point where they touch the room walls [2]. To ensure that the plume does not touch the wall in the modeled case, the following restriction may be reviewed. The restriction assumes a plume expansion angle of 15° from the vertical.

$$H_{room} \leq \frac{W_{room}}{2 \cdot \sin 15^\circ}$$

Wall heat losses should be negligible. To ensure modeled wall heat-losses are negligible, either the plume should not touch the walls or the smoke layer should have a temperature below 105 °C (220 °F).

Cooper [2] suggests an upper limit on the fire heat release rate (kW) for maintaining moderate wall heat loss. The variable 'z' is defined in eq (1). At fire sizes larger than  $Q_{limit}$ , heat from the gases lost to the walls can produce temperatures cooler than predicted.

$$\dot{Q}_{limit} = 333z^{5/2}$$

The heat release rate is steady-state.

The fire is assumed to be a point-source; i.e. no line fires.

The program does not accurately model small fires and/or short entrainment heights.

### 3.2.4 Program Interface

#### *INPUT*

Clear Height	Entrainment distance from the point where entrainment begins (usually the base of the flames) to the elevation of interest to the user (m)
Fire size	Fire heat release rate (kW)

#### *OUTPUT*

Appr. temperature	Plume temperature at clear height above where entrainment begins (°C)
Largest fire size	Largest actual fire heat release rate that can be used with this correlation for valid temperature approximations.

### 3.2.5 References

- [1] Walton, W. D., "ASET-B, A Room Fire Program for Personal Computers," Nat. Bur. Stand. (U.S.), NBSIR 85-3144, Gaithersburg, MD 20899, 1985.
- [2] Cooper, L. Y., and Stroup, D. W., "Calculating Available Safe Egress Time from Fires," Nat. Bur. Stand. (U.S.), NBSIR 82-2587; Gaithersburg, MD, 20899, 1982.
- [3] Zukoski, E. E.; "Development of a Stratified Ceiling Layer in the Early Stages of a Closed-Room Fire", Fire and Materials, Vol. 2, No. 2, 1978.

### 3.3 BUOYANT GAS HEAD

#### 3.3.1 Application

This procedure calculates the pressure difference between two laterally adjacent gases of different density. In fire safety applications, these density differences are created by differences in smoke and clean air temperatures, but the density differences could also be due to differences in molecular weights of adjacent gases.

#### 3.3.2 Theory

The equation used is directly extracted from the manual *Design of Smoke Control Systems in Buildings* [1]. The ambient colder gas volume is assumed to be 21 °C (70 °F). The pressure differential is calculated between the adjacent gases at an elevation coincident with the base of the least dense gas volume.

- $\Delta P_{c-h}$  Pressure difference between the cold and warm gas (Pa)
- $T_c$  Temperature of the colder gas (294 K)
- $T_h$  Temperature of the hotter gas (K)
- $T_\infty$  Reference gas temperature (294 K)
- $z$  Thickness of the least dense (hot) gas volume (m)
- $\rho_\infty$  Reference gas density (1.2 kg/m<sup>3</sup>)

#### 3.3.3 Program Notes

Conditions are steady-state: temperature in the hotter (least dense) gas layer is uniform throughout and the height of the hotter gas volume is constant.

There are no mechanical ventilation/pressurization connections with the hot layer.

Air is the surrounding fluid with a density of 1.2 kg/m<sup>3</sup> (0.075 lb/ft<sup>3</sup>) at 21 °C. Use of this formula in environments where the surrounding gas has a molecular weight or pressure substantially different than a warm-gas layer of air at standard pressure will result in errors.

### 3.3.4 Program Interface

#### *INPUT*

$T_h$  Hot (least dense) smoke temperature ( $^{\circ}\text{C}$ )

$z$  Thickness of the warm air layer (m)

#### *OUTPUT*

$\Delta P$  (Pa or in.  $\text{H}_2\text{O}$ ) Pressure difference at base of the hotter (least dense) gas volume

### 3.3.5 References

- [1] Klote, J.H., Milke, J.A., *Design of Smoke Control Management Systems*, ASHRAE & SFPE, Atlanta, GA 30329, 1992.

### 3.4 CEILING JET TEMPERATURE

#### 3.4.1 Application

With this procedure's estimate of ceiling jet temperature one can determine the likelihood of ignition or heat-induced damage at locations *outside* the plume impingement zone.

#### 3.4.2 Theory

The likelihood of igniting ceiling combustibles may be determined from ceiling jet temperature estimates provided by this routine [1]. Gas jet temperatures are estimated for radial locations outside the plume impingement zone on the ceiling; the plume impingement radius is 0.2 of the plume clear entrainment height. The procedure will adjust the temperature of the gas to recognize the changed entrainment characteristics of wall- or corner-positioned fires. The entrainment adjustment is per the method of reflection [5,3] (Figure 3.4.1). The procedure also recognizes that any hot gas layer development beneath the ceiling will create an underestimate bias in the temperature predictions. As a precaution to this bias, the procedure approximates the time when this hot layer development will become influential [4].

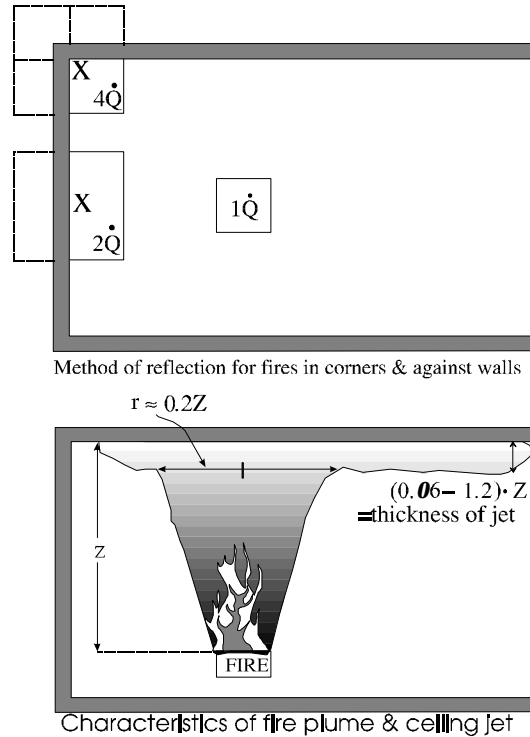


Figure 3.4.1. Fire plume and jet characteristics.

$$T = T_{\infty} + 6.81 \frac{\left(\frac{K \dot{Q}}{r}\right)^{\frac{2}{3}}}{z} ; \quad \text{for } \frac{r}{z} > 0.2 \quad (1)$$

$$t = \frac{4.1 A_{ceiling}}{\frac{\dot{Q}}{z} z^{2/3}} \frac{1}{1.06 \cdot 3048} \quad (2)$$

A	Area (m <sup>2</sup> )
D	Fire diameter (m)
K	Entrainment factor (1 for axisymmetric, 2 for wall-fire, 4 for corner fire)

Q	Total theoretical fire heat release rate (kW)
r	Radial distance from center of the fire to point of interest outside the plume (m)
z	Vertical distance between ceiling and lowest point of the burning fuel (m)
t	Time (second)
T	Jet temperature at height, z, and radial distance, r, from the fire (°C)
T <sub>∞</sub>	Ambient temperature (°C)

### 3.4.3 Program Notes

The total theoretical (and not the actual) heat release rate should be used to describe the fire in this and other ceiling/plume correlations by Alpert. The total theoretical heat release rate may be obtained by multiplying the mass pyrolysis rate by the theoretical heat of combustion. Mass pyrolysis rates can be obtained through experimental measurement using load cells. Theoretical heats of combustion are available from handbooks (see Section 1.4). This fire specification is documented per Alpert's work [1,5].

Points considered for examination should be at radial distances greater than 0.2 times the entrainment height from the vertical axis of the fire.

The entrainment height is the vertical distance between the ceiling and the lowest elevation where flaming combustion occurs.

The fire heat release rate is assumed to be steady state. The test fires used in developing the correlation were buoyancy dominated diffusion flames arising from various fuels: wood cribs and pool fires of liquid heptane and ethanol. This procedure is not intended for momentum-dominated jet fires.

The fire is assumed to be a point source; line fires geometries are not considered.

The plume is considered to be unconfined up to the time of predicted layer development.

The method of reflection is appropriately used when flames are attached to a wall or a corner. When the fire is next to but not against the walls, and flames are not touching the wall surfaces, then the reduction in entrainment was not significant [3].

This routine does not consider combustible wall surfaces.

Standard pressure (101,325 Pa) and normal atmospheric gas concentrations (79% N<sub>2</sub>, 21% O<sub>2</sub>) exist.

This procedure is valid up to the point of hot gas layer development. The actual time to hot layer development can be less than predicted by eq (1) for values of  $z/D_{\text{fire}} \gg 1$ . In addition, eq (2) does not consider fires against a wall or in a corner. The estimated time to hot layer development is



- [2] Evans, D., "Ceiling Jet Flows," The SFPE Handbook of Fire Protection Engineering, National Fire Protection Association, Quincy, MA 02269, 1988, pp. 1-138 to 1-145.
- [3] Zukoski, E.E., Kubota, T., Cetegen, B., "Entrainment in the Near Field of a Fire Plume. Final Report," Nat. Bur. Stand. (U.S.), NBS-GCR-81-346, Gaithersburg, MD 29899, November 1981.
- [4] Nelson, H.E., "FPETOOL: Fire Protection Engineering Tools for Hazard Estimation," Nat. Inst. Stand. Tech. (U.S.), NISTIR 4380, Gaithersburg, MD 20899, 1990.
- [5] Alpert, R.L., "Turbulent Ceiling-Jet Induced by Large-Scale Fires", Factory Mutual Research, Tech. Report No. 22357-2, Norwood, MA, 02062, 1974.

## 3.5 CEILING PLUME TEMPERATURE

### 3.5.1 Application

This procedure estimates fire-plume gas temperatures from the height of the continuous flames to the height of the ceiling. This routine compliments CEILING JET TEMPERATURE.

### 3.5.2 Theory

The equation was developed by Alpert and Ward [1983] and may be used to estimate the damages caused by the hot plume gases. For this reason, the plume temperatures predicted in this routine are conservatively hotter than the plume temperatures predicted in SPRINKLER/DETECTOR RESPONSE. Figure 3.4.1 in **CEILING JET TEMPERATURE** illustrates some of the plume geometry variables used in eq (1).

$$T = T_{\infty} + 22.2 \frac{(K \dot{Q}_{fire})^{\frac{2}{3}}}{z^{\frac{5}{3}}}; \quad \text{for } \frac{r}{z} \leq 0.2 \quad (1)$$

$$t = \frac{4.1 A_{ceiling}}{\frac{\dot{Q}}{1.06} \frac{z}{.3048}^{2/3}} \quad (2)$$

A	Area (m <sup>2</sup> )
D <sub>fire</sub>	Fire diameter (m)
K	Entrainment factor (1 for axisymmetric, 2 for wall-fire, 4 for corner fire)
Q	Total theoretical fire heat release rate (kW)
r	Radial distance from the center of the fire to the point of interest (m)
z	Entrainment height: vertical distance between the ceiling and the lowest point of the burning fuel (m)
t	Time (second)
T	Jet temperature at height, z, and radial distance, r, from the fire (°C)
T <sub>∞</sub>	Ambient temperature (°C)

### 3.5.3 Program Notes

The total theoretical (and not the actual) heat release rate should be used to describe the fire in this and other ceiling/plume correlations by Alpert. The total theoretical heat release rate may be obtained

by multiplying the mass pyrolysis rate with the theoretical heat of combustion. Mass pyrolysis rates can be obtained through experimental measurement using load cells. Theoretical heats of combustion are available from handbooks (see Section 1.4). This fire specification is documented per Alpert's work [1].

The heat release rate of the fire is simulated as steady-state. The fire is modeled as a point source; no line fires are considered.

Radial locations from the vertical axis of the fire should be less than 0.2 times the height the plume.

Radial location should be no further from the vertical axis of the fire than the shortest dimension of the room.

Temperature is conservative on the high side compared with experiments used to develop this correlation [1].

The continuous flame height is located at the base of the intermittent flaming region. The temperature of the continuous flaming region is about 800 °C in buoyancy-dominated diffusion flames, but may be as hot as the adiabatic flame temperature under ideal conditions (approximately 1800 °C). The height of the continuous flaming region is below the mean flame height. The mean flame height is defined as the elevation where flames appear 50% of the time [3,4].

The temperature predictions from wall and corner configurations are theoretical.

The fire must be close enough to a wall that flames touch the surface before the user decides to chose the 'Fire near a wall or corner' option. Combustible walls are not considered in this routine.

Standard pressure (101,325 Pa) conditions are used.

Time to hot layer development can be less than predicted for values of  $z/D_{\text{fire}} \gg 1$ .

A hot layer of gas has not developed at the ceiling.

### 3.5.4 Program Interface

#### *INPUT*

Nearby Walls	Entrainment factor whose value may be 1, 2 or 4 depending upon whether the fire is located away from any walls, against a wall or in a corner. Experiments have shown [2] that in order for reflection to apply, the fire flames must <b>touch</b> the wall, K
--------------	----------------------------------------------------------------------------------------------------------------------------------------------------------------------------------------------------------------------------------------------------------------

Ambient T	Room temperature at pre-fire conditions, $T_{\infty}$ ( $^{\circ}\text{C}$ ).
Distance from Fuel to Ceiling	Elevation difference between the lowest height where flames exist and where air can freely be entrained into the fire, and the height of the ceiling $z$ , (m)
Ceiling Area	( $\text{m}^2$ )
Fire Burn Rate	Total theoretical fire heat release rate, $Q$ (kW)
Radial Distance	Lateral distance across ceiling from a point directly over the fire to the point of interest in the ceiling jet, $r$ (m)

### *OUTPUT*

$T_{\text{plume}}$	Plume temperature ( $^{\circ}\text{C}$ )
$t$	Time when a layer of hot gas that develops under the ceiling can interfere with the 'no layer' assumption

### **3.5.5 References**

- [1] Alpert, R.L., and Ward, E. J.; "Evaluating Unsprinklered Fire Hazards; SFPE Technology Report 83-2," Society of Fire Protection Engineers: Boston, MA, 1983.
- [2] Zukoski, E.E., Kubota, T., Cetegen, B., "Entrainment in the Near Field of a Fire Plume. Final Report," Nat. Bur. Stand. (U.S.), NBS-GCR-81-346, Gaithersburg, MD 29899, November 1981.
- [3] Heskestad, G. "Fire Plumes," The SFPE Handbook of Fire Protection Engineering, National Fire Protection Association, Quincy, MA 02269, 1988, pp. 1-107 to 1-109.
- [4] McCaffrey B.J. "Flame Height," The SFPE Handbook of Fire Protection Engineering, National Fire Protection Association, Quincy, MA 02269, 1988, pp. 1-298 to 1-305.

## 3.6 EGRESS TIME

### 3.6.1 Application

This procedure estimates the time needed for a person or group of people to exit an area. The egress movement may be vertical or horizontal and include the use of doorways, stairs, ramps, and corridors. Elevator transportation is not considered.

### 3.6.2 Theory

Theory assumes that evacuees will travel at user-designated speeds on flat and vertical pathways. These speeds will be altered if the user designates a reduced travel efficiency for the slowest person in the evacuating population. The default travel speed on flat pathways is 76.2 m/min (250 ft/min). The default travel speed on stairs is 12.2 m/min (40 ft/min). Travel time on vertical pathways may be further altered by deviations in standard-stair design measurements. The assumed standard-stair design measurement is a tread depth of 280 mm (11 in.) and a riser height of 178 mm (7 in.). The base speed on stairs is increased for several user-defined parameters. These parameters are increased tread depth, decreased riser height and increased effective width [1] of the stairway. The assumed exitway flow rate is 60 persons/min/m<sub>W-effective</sub> (18.3 persons/min/ft<sub>W-effective</sub>). The rate of travel through enclosed exitways is limited by the flowrate through the doors or door-leaves in the enclosure opening. The doorway calculations assume a default movement rate of one person per second per door-leaf. The standard door-leaf width is 0.76 m (30 in.).

In the equations below, eq (1) represents the time needed for one individual to complete unimpeded egress. Eqs (2) - (4) support eq (1). Eq (5) represents the time to move the entire building population through the exterior exit doors. Eq (6) represents the time to move the entire building population through and out of the stairway enclosures. In eq (6) the limit to flow is the  $W_{\text{effective}}$ . The  $W_{\text{effective}}$  may be either the stairway enclosure exit door width or it could be the width of the stairway itself (protruding handrails or other projections).

Together, eqs (1), (5) and (6) provide a first-order estimate of area evacuation times; the user, however, should be aware of assumptions in arriving at the results. The egress estimates assume the most efficient exit paths are chosen. The procedure does not account for investigation, verification, 'way-finding,' or assistance. Flow is assumed to proceed ideally and without congestion. There are no adjustments to flow speed in response to evacuee flow density. In light of these inefficiencies, it would be reasonable to expect evacuation times to be two to three times greater than the nominal evacuation time [3]. The nominal evacuation time varies. If any evacuation time from eqs (1), (5) or (6) was an order-of-magnitude greater than the other two evacuation times, then this would be the nominal evacuation time estimate. If the unimpeded evacuation time, ( $t_{\text{unimpeded}}$ ) is close to one or both estimates of eqs (5) or (6), then  $t_{\text{unimpeded}}$  plus a fraction of eqs (5) or (6) is the nominal evacuation

time. Conversely, if eq (5) or (6) exceeds  $t_{unimpeded}$ , then the nominal evacuation time is the time in eqs (5) or (6) plus a fraction of  $t_{unimpeded}$ . To determine what value these fractions should be, it is necessary to conduct a more detailed analysis of the evacuation flow [3].

$$t_{unimpeded} = \frac{(t_{horizontal} + t_{vertical})}{\chi_{mobility}} \quad (1)$$

$$\chi_{mobility} = \frac{X}{100} \quad (2)$$

$$t_{horizontal} = \frac{X_{horizontal}}{v_{able}} \quad (3)$$

$$t_{vertical} = \frac{z_{vertical}}{v_{stair}} \sqrt{\frac{11}{7} \frac{z_{riser}}{x_{tread}}} \quad (4)$$

$$t_{exit-opening} = \frac{N_{people}}{N_{exitleaves}} \left( \frac{\text{exit leaf} \cdot \text{sec}}{1 \text{ person}} \right) \quad (5)$$

$$t_{stair} = \frac{N_{people}}{W_{effective}} \frac{1}{\dot{Q}_{stair}} \quad (6)$$

$N_{exit\ leaves}$	Total number of door leaves from the building to the outside
$N_{people}$	Total evacuating population
$Q_{stair}$	People flow rate in a stairway enclosure (default 60 people/min/m <sub>w, eff</sub> )
$t$	Exit time (sec)
$W_{effective}$	Effective width of an exit passageway (see Section 3.6.3) (m)
$X_{horizontal}$	Total horizontal distance traversed by the evacuee (m)
$v_{able}$	Speed of an able evacuee moving on flat, dry surface (m/s)
$v_{stair}$	Speed of an able evacuee moving in a vertical means of egress (m/s)
$x_{tread}$	Depth of the tread from riser to riser (m)
$X$	Speed of the slowest evacuee as a percentage of able evacuee speed
$z_{riser}$	Height of the riser from tread to tread (m)
$z_{vertical}$	Total vertical traverse distance (not distance along a sloped incline) (m)

### 3.6.3 Program Notes

Door leaves less than 5/6 of a standard-door width (0.76 m) should not be considered as an additional leaf available for evacuee egress movement.

Flow rates through door leaves are assumed at one person per second per door leaf. If the door leaf is less than 0.86m (34 in.) then the flow rate may be less. The exitway flow rate is user adjustable. For exit openings substantially larger than 0.86m (34 in.) per door leaf, the flow rate can exceed one person per second. To reflect this potential the user should modify the parameter 'Flow rate per door leaf.'

Effective flow width for stairs measures wall-to-wall, minus projection of artifacts, minus a clearance distance from the artifacts. This clearance distance is artifact dependent [3]. Typical stairwell effective width is 0.305 m (1 ft) less than actual width. This accounts for the 0.076 m (3 in.) projection of each handrail plus 0.076 m clearance for each handrail.

Turnstiles can have flow rates 1/3 of values for stairwell doorways (20 people/min/m<sub>W, effective</sub>).

Stair flow rate is roughly 60 persons per minute per meter of effective width (18.3 persons/min/ft). This flow rate is user adjustable.

If there is more than one stairway and these widths differ, an average width is needed to represent these egress paths because only one stairway width may be entered to this routine. This average width may be calculated such that when multiplied by the number of stairways, it yields a net width equal to the sum of the individual stairway widths.

Emergency travel speed on flat, dry, uncongested surfaces is 76 m/min (250 ft/min). The flow rate is user adjustable; one application follows:

The Americans with Disabilities Act [2] suggest flow rates of 28 m/min (90 ft/min) for disabled evacuees. This represents a speed 37 percent of that assumed for an able person. However, after every 30.5 m (100 ft) of travel, the ADA further suggests that the evacuee will pause for 2 minutes, presumably to rest.

The output parameter 'Time required to pass persons through the (building) exit doors...' predicts the waiting time the **last** person in line will experience when completing one of the last parts of their egress path--that of moving from inside to outside of the building. The rate of movement through the exterior-access doors is a function of the number and effective width of these doors. The building population is equally distributed among the specified exterior-access exit doors. A wait during this part of the egress can be caused by insufficient exit doors, inadequate door widths, or a larger-than-anticipated building population.

The output parameter 'Time required to pass persons through the stairwell exit doors...' is calculated analogous to 'Time required to pass persons through the (building) exit doors...'

### 3.6.4 Program Interface

#### *INPUT*

Travel speed on level routes	(m/min)
Vertical travel speed on stairs	(people/min/m $W_{\text{effective}}$ )
Flow rate through doors	(people/min/exit door leaf)
Flow rate on stairway	(people/min/m $W_{\text{effective}}$ )
Population	Total number of evacuees using the evacuation routes
Evacuees are able/disabled	Choice between default and modified travel speeds
Speed of the slowest evacuee	Disabled speed as a percentage of able-bodied speed
Exit door leaves avail. to evacuees	This number is rounded-off to an integer. To obtain results reflecting additional exit width beyond 0.86m (34 in.) adjust the parameter pertaining to 'Flow rate through doors'
Total length of route that is level	(m)
Portion of travel over stairs	Vertical distance moved via stairwell travel. This is not the same as the distance moved along the slope of a stairway but the vertical distance between the starting and the stopping locations (m)
Number of stairways used	
Stairway width	Total width ( <b>not</b> effective flow width: $W_{\text{effective}}$ )
Stairway riser height	(mm)
Stairway tread depth	(mm)

## *OUTPUT*

Horizontal and stair travel time	Time estimated for a person to traverse all stair and horizontal paths exclusive of any queuing (queuing or line-waiting is considered by the following two output parameters). Doorways are assumed open and no other evacuees are considered to impede travel rates (min)
Time required to pass persons through the (building) exit doors	Time for the entire building population to pass through the available building exit doors (min)
Time required to pass persons through the stairway exit doors	Time for the entire building population to pass through the available building stairwell exit doors (min)

### **3.6.5 References**

- [1] Pauls, J., "Movement of People," SFPE Handbook of Fire Protection Engineering," NFPA, Quincy, MA 02269, pp. 1-246, 1988.
- [2] United States Department of Justice, "Nondiscrimination on the Basis of Disability by Public Accommodations and in Commercial Facilities: Americans with Disabilities Act 28 CFR Part 36, Final Rule, Federal Register, July 26, 1991.
- [3] Nelson, H.E., McLennan, H.A., "Emergency Movement," The Society of Fire Protection Engineers Handbook of Fire Protection Engineering, NFPA, Quincy, MA 02269, pp. 2-214, 1988.

## 3.7 FIRE/WIND/STACK FORCES ON A DOOR.

### 3.7.1 Application

This procedure estimates forces imposed on a door from up to three combined pressure sources: buoyancy, wind and stack effects.

### 3.7.2 Theory

Fluid movement in general and gas movement in particular, is initiated by pressure differences. Pressure differences are created by energy sources. The energy source for buoyancy-induced pressure differences comes from the fire, [eq (1)] [3]. The energy source for wind-induced pressure is contained in the kinetic energy of the air molecules [eq (2)] [1,4]. The energy source for stack-effected pressure differences is maintained in the potential energy of the building's climate-controlled air [eq (3)] [4].

$$\Delta P_{buoyancy} = \Delta \rho g z = \frac{P(MW)}{R} \left( \frac{1}{T_{bldg}} - \frac{1}{T_{fire}} \right) g z \quad (1)$$

$$\Delta P_{wind} = \frac{C \rho_{wind} (v_{initial}^2 - v_{final}^2)}{2} \quad (2)$$

$$\Delta P_{stack} = \Delta \rho g z_{neutralplane} = \frac{P(MW)}{R} \left| \left( \frac{1}{T_{outside}} - \frac{1}{T_{building}} \right) \right| g (z_{neutralplane} - z_o) \quad (3)$$

$$\Sigma M_{hinge} = 0; \quad \int_0^{W_{door}} (F'(x) \cdot x) dx - F_{latch} W_{door} = 0 \quad (4)$$

$$F_{latch} = \frac{1}{W_{door}} \int_0^{W_{door}} (\Delta P z_{door} \cdot x) dx \quad (5)$$

In order to determine the net force required to open the door at the latch, the net pressure acting upon the door is needed. The net pressure acting upon the door is obtained by summing the individual pressure contributions cited above in eqs [(1) - (3)]. Once the net acting pressure is determined, the opening force required at the latch is obtained by summing the moments about the door hinge [eqs (4) and (5)].

C	Coefficient accounting for non-ideal flow, particularly about orifice edges
F	Force (N)
g	Gravitational acceleration constant at Earth's surface (9.81 m/s <sup>2</sup> )
$\Sigma M_{\text{hinge}}$	Sum of the moments about a door hinge (m)
MW	Molecular weight of the gas (~29 g/(g·mole) for air)
P	Pressure (Pa)
$\Delta P$	Pressure difference over some interval of distance (Pa)
R	Universal gas constant (8.314 J/((g·mole)K))
T	Temperature of a gas (K)
$W_{\text{door}}$	Door width (m)
x	Distance along the width of a door with the origin at the latch (m)
z	Height of a gas volume adjacent to another gas volume of different density (m)
$z_{\text{door}}$	Height of the door (m)
$z_{\text{floor}}$	Elevation of bldg. floor above lowest significant building opening to outside (m)
$z_{\text{neutral plane}}$	Elevation of building neutral plane above lowest major opening to outside (m)
$z_o$	Elevation of interest above the lowest significant building opening to outside (m)
v	Gas velocity, wind speed, (m/s)
$\rho$	Gas density (kg/m <sup>3</sup> )
$\Delta\rho$	Density difference between two gas volumes (kg/m <sup>3</sup> )

### 3.7.3 Program Notes

$$z_{\text{virtual building height}} = \frac{3}{2} |(z_{\text{neutral plane}} - z_{\text{floor}})| \quad (6)$$

The stack effect calculations assume the elevation of interest is located 2/3 of the building height vertically distant from the neutral plane. To model conditions when the door-of-interest is located a vertical distance other than 2/3 of the building height from the neutral plane the user can enter a 'virtual building height' instead of the actual building height. Eq (6) is presented for the user to calculate this 'virtual building height.' Eq (6) presumes the user knows the elevation of the building's neutral plane.

All pressures are additive. This is not necessarily true in all cases, but it is a conservative simplification of theory. The resulting force an individual must apply at the latch of a door experiencing one or more of these pressure forces is the sum of the forces calculated from this procedure plus the force required to open the door against the door-closing mechanism.

One application is determining the force an individual needs to exert on the latch edge of a door located at the top of a building stairwell experiencing a strong winter-stack effect.

There are no pressure differences across the width of the door. This implies the net force acting on the door per differential width,  $F'(x)$  or  $\Delta Pz_{\text{door}}$ , is constant.

The density difference,  $\Delta\rho$ , is due to a temperature difference between 2 gas volumes of similar molecular weight. This procedure does not apply to density differences originating from 2 gas volumes of differing molecular weight.

The fire gases impacting the door of consideration are at a single temperature across the full width of the door.

None of the forces being measured are constrained by a 'tight building' or other situation that would constrict gas flow or development of the full theoretical force predicted by the wind pressure equation.

Wind assumedly impacts the building with a pressure coefficient of 0.8 [1]. If wind effects are being considered upon a door, then the assumption is that the wind strikes the door in such a direction as to contribute to the pressure effects generated by buoyancy and stack.

The temperature of air inside the building is 21 °C (70 °F).

The building height may be considered the elevation difference between the lowest and highest opening to the outside.

Bernoulli flow assumptions were used in this procedure. These assumptions were: no viscosity, steady-state flow, an incompressible fluid (for air at room temperature). Significant deviations from incompressibility occur around 1,013,250 Pa [2].

This procedure can consider the stack effect created by winter and summer conditions [1].

If one uses eq (3) for a 'hand-calculation' then  $z_{\text{neutral plane}}$  measures the distance from the building neutral plane to the elevation of interest in the building [1].

### 3.7.4 Program Interface

#### *INPUT*

Building Height	(m or ft)
Door Height	(m or ft)
Door Width	(m or ft)

Ceiling Height	Measured from the floor (m or ft)
Smoke Depth	Depth of the smoke measured from the ceiling (m or ft)
Wind Speed	(km/hr or mph)
$T_{\text{bldg}}$	Building temperature ( $^{\circ}\text{C}$ or $^{\circ}\text{F}$ )
$T_{\text{fire}}$	Fire temperature, values for this parameter may be obtained from characteristic hot-layer temperature predictions from <b>FIRE SIMULATOR</b> or <b>ASETBX</b> . ( $^{\circ}\text{C}$ or $^{\circ}\text{F}$ )
$T_{\text{outside}}$	Outside temperature ( $^{\circ}\text{C}$ or $^{\circ}\text{F}$ )

### *OUTPUT*

Pressure on the door	Pressure on door (Pa or $\text{lb}_f/\text{ft}^2$ )
Latch Edge Force	Force at latch edge of door (N or $\text{lb}_f$ )

### **3.7.5 References**

- [1] Klote, J.H., Milke, J.A., Design of Smoke Management Systems, ASHRAE, Atlanta, GA 30329, 1992.
- [2] Perry, J.H., Chilton, C. Chemical Engineers Handbook, McGraw-Hill, New York, pp. 3-151, 1973.
- [3] Fang, J.B., "Static Pressures Produced by Room Fires," Nat. Bur. Stand. (U.S.), NBSIR 80-1984, Gaithersburg, MD 20899, 1980.
- [4] Tamura, G.T., Klote, J.H., "Experimental Fire Tower Studies on Elevator Pressurization Systems for Smoke Control," ASHRAE Transactions, 93(2), pp. 2235-2257, 1988.
- [5] Klote, J.H. "Fire Experiments of Zoned Smoke Control at the Plaza Hotel in Washington, D.C.," ASHRAE Transactions 96(2), 1990.

## 3.8 LATERAL FLAME SPREAD

### 3.8.1 Application

This procedure estimates the lateral spread of an attached flame along the surface of a thermally thick fuel. 'Wind-aided' flame spread is an inappropriate application of this procedure; the procedure is appropriate for flame spread in a direction that is opposite--or normal to--the direction of the propagating flame front.

### 3.8.2 Theory

The equations used in this program were developed by Quintiere and Harkelroad [1984]. The material properties required by these equations may be experimentally obtained from the Lateral Ignition and Flame spread Test (LIFT) apparatus using procedures outlined in the above reference. The properties include the fuel flame spread parameter ( $\phi$ ), the fuel piloted-ignition temperature ( $T_{\text{ignition, pilot}}$ ), and the fuel thermal inertia ( $k\rho c_v$ ).

$$v_{\text{flame, lateral}} = \frac{\phi}{k\rho c_v} \cdot \frac{1}{(T_{\text{ig}} - T_{\text{surface}})^2} \quad (1)$$

The equation for lateral flame spread appears in eq (1). The piloted-ignition temperature for many fuels is quite similar, as the software reference provided with this routine demonstrates.

$v_{\text{flame, lateral}}$	Lateral rate of attached flame spread (m/s or ft/s)
$\phi$	Ignition factor from flame spread test data ( $\text{kW}^2/\text{m}^3$ )
$k\rho c_v$	Fuel thermal inertia at flame preheat conditions ( $\text{kW}^2\cdot\text{s}/(\text{m}^4\cdot\text{K}^2)$ )
$T_{\text{ignition, pilot}}$	Piloted fuel ignition temperature ( $^{\circ}\text{C}$ or $^{\circ}\text{F}$ )
$T_{\text{surface}}$	Unignited, ambient-surface temperature ( $^{\circ}\text{C}$ or $^{\circ}\text{F}$ )

### 3.8.3 Program Notes

Because temperature is raised to the second power, its impact on the estimated flame velocity is relatively large.

Thermal inertia ( $k\rho c_v$ ) of the fuel is best measured as a single value and at elevated temperatures that accurately simulate conditions during actual flame spread.

It is strongly recommended that data for  $\phi$  and  $k\rho c_v$  be obtained from a single test per the suggestions of Quintiere and Harkelroad.

An inappropriate use of this model is for upward flame spread on a wall where unignited fuel in the 'shadow' of the flamesheet receives significant preheating.

Experiments have shown correlation with this procedure for lateral extension on a horizontal fuel surface and downward flame extension on a vertical fuel surface [1,2].

This procedure may not be appropriate for vertically-oriented fuel surfaces that drip when burning.

### 3.8.4 Program Interface

#### *INPUT*

List values	Example materials and their values for $\phi$ and $T_{\text{ignition, pilot}}$
Ignition temperature	$T_{\text{ignition, pilot}}$ ( $^{\circ}\text{C}$ or $^{\circ}\text{F}$ )
Surface temperature	$T_{\text{surface}}$ ( $^{\circ}\text{C}$ or $^{\circ}\text{F}$ )

#### *OUTPUT*

Flame spread rate	Lateral attached flame spread rate (m/s or ft/s)
-------------------	--------------------------------------------------

### 3.8.5 References

- [1] Quintiere, J.G., Harkelroad, M.F., "New Concepts for Measuring Flame Spread Properties," Symposium on Application of Fire Science to Fire Engineering: American Society for Testing and Materials and Society of Fire Protection Engineers, Denver, CO, 27 June 1984.
- [2] Quintiere, J.G., "A Semi-Quantitative Model for the Burning of Solid Materials," Nat. Inst. Stand. Tech. (U.S.), NISTIR 4840, Gaithersburg, MD 20899, 1992.
- [3] Standard Test Method for Surface Flammability of Materials Using a Radiant Heat Energy Source, ASTM E-162, Annual Book of ASTM Standard, Volume 04.07, American Society for Testing and Materials, 1988.

## 3.9 LAW'S SEVERITY CORRELATION

### 3.9.1 Application

This procedure provides a systematic method whereby two fires (one a 'real' fire, the other a standard, time-temperature fire) may be compared for equivalence regarding the structural damage they impose. Effectively, the procedure answers the question, 'given a known fire, what standard-fire resistance is needed to protect insulated structural members?' The standard, time-temperature fire follows the European specification [1], a close approximation to the ASTM E-119 standard time-temperature curve. The breadth of data from which this correlation was developed [2,3] as well as the length of time over which the correlation has been successfully used testifies to its robustness.

### 3.9.2 Theory

The point of comparison between the 'real' fire and the 'standard' fire is the point in time that a critical temperature is achieved on the surface of a thermally-thick insulated structural element. Law chose 550 °C (1220 °F) as the critical temperature (because at this temperature steel's modulus of elasticity (strength) is dramatically reduced; however, other critical temperatures could have been chosen just as readily, the net result being a relationship bearing the same form as eq (1), only with

$$t_{\text{effective resistance}} = \frac{m_{\text{fuel}}}{\sqrt{A_{\text{vent}} A_{\text{room}}}} \quad (1)$$

different constants. The author demonstrated that other thermally-thick-insulated elements, (e.g. concrete, heavy-timber) could be analyzed with this method. Although these other insulated-elements may not fail at the 'critical' temperature assumed with this procedure, these elements would nonetheless experience a similar surface temperature of approximately 550 °C.

$t_{\text{effective}}$	Duration of exposure to the ISO standard time-temperature fire-resistance test that is correlationally equivalent to the 'real' fire exposure. (min)
$A_{\text{vent}}$	Effective area of all vents. When more than one vent exists, use the method outlined in Section 3.15.2 for calculating an equivalent area. (m <sup>2</sup> )
$A_{\text{room}}$	Area of the compartment surfaces. The calculations <i>do</i> include the floor and ceiling area, as well as the area of the walls, less $A_{\text{vent}}$ . (m <sup>2</sup> )
$m_{\text{fuel}}$	Mass of dry wood burning in a crib configuration that is equivalent to the total energy released by the 'real' fire. (kg)

### 3.9.3 Program Notes

This procedure requires as input, a mass of wood fuel ( $m_{\text{fuel}}$ ) releasing an equivalent energy upon completion of burning as from complete burning of the 'actual' fuel. The mass of wood fuel needed as input for the **Fire Load** input parameter described in Section 3.9.4 may be determined from eq (2). Informed and/or engineering judgement is needed to determine what are appropriate and prudent values for the heats of combustion used in eq (2).

$$m_{\text{wood}} = \frac{m_{\text{fuel,actual}} \Delta H_{c_{\text{fuel,actual}}}}{\Delta H_{c_{\text{wood}}}} \quad (2)$$

The concept that an exposure time in a standard time-temperature fire can be related to a different exposure time in an actual fire hinges upon the premise that a thermally-protected steel column within each exposure attains the same temperature at the completion of each fire.

The correlation assumes the materials providing the estimated fire resistance protection are thermally thick. Thermally thin protection or exposed steel members may not be a valid application for this correlation [2].

The tests used for development of the correlation were conducted in small- and full-scale rooms with concrete and fibre-board insulated walls and a variety of ventilation sizes. Various fuels (tires, liquids, wood cribs, and furniture) were used in correlating eq (1) [2,3].

The test configurations all contained open vents. It is recommended that the compartment being investigated possess at least a 0.4 m<sup>2</sup> (4 ft<sup>2</sup>) opening. This recommendation is based upon engineering judgement [5].

### 3.9.4 Program Interface

#### *INPUT*

Length of space	Length of the room (m or ft)
Width of space	Width of the room (m or ft)
Height of space	Height of the room (m or ft)
Height of opening	Height of the (equivalent) vent (m or ft)
Width of opening	Width of the (equivalent) vent (m or ft)
Fire load	Mass of wood producing a fire 'equal' to the actual fire (kg or lb <sub>m</sub> )

Fire load (density)                      Fire load per unit floor area. This value is entered by toggling the ENTER key on the line *underneath* Fire Load (kg/m<sup>2</sup> or lb<sub>m</sub>/ft<sup>2</sup>)

### *OUTPUT*

t<sub>effective fire resistance</sub>                      Exposure time in the standard fire test that is equivalent to the time of exposure in a 'real' fire (min)

### **3.9.5 References**

- [1] Fire Resistance Tests of Structures, International Organization for Standardization Recommendation R834, 1968.
- [2] Law, M., "Prediction of Fire Resistance"; Proceedings, Symposium No. 5, Fire-resistance Requirements for Buildings - A New Approach; Joint Fire Research Organization, London, Her Majesty's Stationery Office, 1973.
- [3] Thomas, P.H., Heseldon, A.J.M., "Fully-developed fires in single compartments. A cooperative research programme of the Conseil International du Bâtiment," Joint Fire Research Organization Fire Research Note No. 923, 1972.
- [4] National Fire Protection Association Handbook, "Standard Methods of Fire Tests of Building Construction and Materials," NFPA 251, NFPA, Quincy, MA 02669, 1989.
- [5] Nelson, H.E., "FPETOOL: Fire Protection Engineering Tools for Hazard Estimation," Nat. Inst. Stand. Tech. (U.S.), NISTIR 4380, Gaithersburg, MD 20899, 1990.

## 3.10 MASS FLOW THROUGH A VENT

### 3.10.1 Application

This procedure uses an iterative process to determine an approximate solution for mass flow into and out of a single, naturally-ventilated opening to a room with a steady-state fire in it. This routine is similar to, but not identical with, **SMOKE FLOW THROUGH AN OPENING**.

### 3.10.2 Theory

$$\{\text{Generation Rate}\} + \dot{m}_{in} - \dot{m}_{out} = \frac{d[m_{cv}]}{dt} \quad (1)$$

$$z_{neutral\ plane} = \frac{1}{1 + \left[\frac{T}{T_{\infty}}\right]^{\frac{1}{3}} \left[1 + \frac{\dot{m}_{pyrolysis}}{\dot{m}_{in}}\right]^{\frac{2}{3}}} \quad (2)$$

$$M_o = \frac{\sqrt{\theta}}{1 + \theta} (1 + z_{neutral\ plane}^{3/2}), \quad \text{where } \theta = \frac{T - T_{\infty}}{T_{\infty}} \quad (3)$$

$$\dot{m}_{out} = \frac{2}{3} C M_o A_{vent} \rho_{\infty} \sqrt{2g z_{vent}} \quad (4)$$

Conservation of mass is used to solve numerically the gas-mass flow rate into a naturally ventilated room with steady-state elevated temperatures [eq (1)]. **MASS FLOW THROUGH A VENT** is solved using the conservation of mass principal, **SMOKE FLOW THROUGH AN OPENING** is solved using Bernoulli flow and orifice equation assumptions (Section 3.13). This solution process begins with the user-specified fuel pyrolysis rate [the {generation rate} term in eq (1)]. The procedure then 'guesses' a mass inflow rate based upon door width. This inflow rate is then used to calculate the neutral-plane elevation ( $z_{neutral-plane}$ ) via eq (2). The neutral plane elevation is subsequently used to calculate the mass outflow rate [eq (4)] [3]. If mass conservation [eq (1)] does not close within the specified criteria then the bisection numerical technique guesses again and the process repeats until convergence or excess iterations are achieved [1]. Some of the first work on these vent flow rates was presented by Kawagoe [2].

In the conservation of mass equation, the pyrolysis rate is a source term, and as such its value is inserted in the {generation rate} term of eq (1). Since this procedure assumes a steady-state elevated temperature in the control volume (the room), the net rate-of-change in mass within the room ( $d[m_{cv}]/dt$ ) is zero.

$\dot{m}_{\text{pyrolysis}}$	Mass generation rate of the fuel (g/s)
$\dot{m}_{\text{cv}}$	Net mass of gas within the control volume (the control volume is the room air-volume not including the wall/ceiling materials).
$Z_{\text{vent}}$	Height of the vent opening from soffit to sill (m)
$Z_{\text{neutral plane}}$	Height of the neutral plane in the vertical opening of the door (m)
$T$	Temperature of the hot gas layer (K)
$T_{\infty}$	Temperature of the ambient, outside air (K)
$\theta$	Non-dimensionalized temperature variable $(T - T_{\infty})/T_{\infty}$

### 3.10.3 Program Notes

Air flows are motivated by buoyancy forces only: no mechanical pressurization, stack effect or wind effects are considered.

Conditions are steady state: pyrolysis rate is constant, layer temperatures are constant, layer heat losses are constant, momentum flow across the vent is constant. Examples of steady-state conditions could be flashover, or fuel controlled burning when the fire is not growing.

The gas in the room is either at a uniform temperature (e.g. flashover) or is in a ventilation-limited condition. This procedure is inappropriate for early stages in a fire when a hot layer increases in thickness and the expansion of gases causes only an outflow from the room.

There is either one opening in the space or all of the openings are at reasonably the same level in the space. If openings must be combined, they should be combined per the method used in Section 3.17.

### 3.10.4 Program Interface

#### *INPUT*

Convergence Criterion	Criterion for numerical solution of eq (2)
Upper layer temperature	Temperature of the hot, upper layer of gas ( $^{\circ}\text{C}$ )
External temperature	Temperature of the ambient, outside temperature ( $^{\circ}\text{C}$ )
burning rate	Fuel pyrolysis rate (g/s)

## *OUTPUT*

$\dot{m}_{\text{out}}$	Fluid flow rate out of the room (g/s)
$\dot{m}_{\text{in}}$	Fluid flow rate into the room (g/s)
$h_{\text{neutral plane}}$	Absolute height of the neutral plane above the bottom of the vent. This variable is also expressed as the nondimensional height of the neutral plane in the door (m)

### **3.10.5 References**

- [1] Lawson, J.R. and Quintiere, J.G., "Slide-rule Estimates of Fire Growth," Nat. Bur. Stand. (U.S.), NBSIR 85-3196, Gaithersburg, MD, pp. 56, 1985.
- [2] Kawagoe, K. D. & Sekine, T., "Estimation of Fire Temperature-Time Curve for Rooms," BRI Occasional Report No. 11, Building Research Institute, Ministry of Construction, Japanese Government, June 1963.
- [3] Rockett, J. "Fire Induced Gas Flow in an Enclosure," Combustion Science Technology, (12), pp. 165-75, 1976.

### 3.11 PLUME FILLING RATE

#### 3.11.1 Application

This procedure estimates the volume flow of smoke and entrained air in a plume at a point above the flames of a fire of constant heat release rate.

#### 3.11.2 Theory

There are currently several models [3,4,5,6] that estimate entrainment into a rising buoyant plume. Each model provides roughly the same accuracy with no individual model clearly outperforming the others in all cases. This procedure uses a model originated by Zukoski and later modified by Cooper & Stroup [2]. A version of this plume model was incorporated by Walton [1] into **ASETBX**.

The equation in **PLUME FILLING RATE** is

$$\dot{V}(z) = 2.60(1-\chi_r)\dot{Q} + 60.5[(1-\chi_r-\chi_o)\dot{Q}]^{1/3}z^{5/3} \quad (1)$$

$\dot{V}(z)$	Volumetric flow rate of all gases in the plume at height z (Liters/s)
$\dot{Q}$	Theoretical fire heat release rate (kW/s)
$\chi_r$	Fraction of $\dot{Q}$ released through radiative heat transfer
$\chi_o$	Fraction of $\dot{Q}$ not released via radiative or convective heat into the plume
$z$	Height in the plume where $\dot{V}(z)$ is calculated (m)

#### 3.11.3 Program Notes

This procedure applies to steady-state fires.

The input parameter  $\chi_o$  may be used to account for combustion inefficiencies and/or heat from the fire that is expended in pyrolyzing fuel. If  $\chi_o$  is non-zero, then the sum of  $\chi_o$  and  $\chi_r$  should be less than one.

This procedure should not be applied at heights equal to or less than the mean flame height. The mean flame height is that elevation on the central fire axis where flames appear 50% of the time. The mean flame height also correlates with an average gas temperature of 500 °C. [3].

Other plume models have been verified in large atria [7].

The approximate conversion between Liters/s and cubic feet per minute is 2.12. To convert from L/s to cfm, multiply the number representing flow in L/s by 2.12.

The fire is considered a point source; i.e. no line fires or fire areas in a distributed sense are considered.

This procedure does not consider wall or corner fires.

The buoyant gas has no appreciable horizontal momentum.

There is no contact between the walls of the compartment and the plume (mathematically the walls are a distance,  $r$ , from the fire:  $r \geq 0.2 * H$ ).

This procedure should not be used on predominantly momentum-driven plumes.

The plume is not tilted from the vertical and the plume is not experiencing wind- or mechanically-aided entrainment.

### 3.11.4 Program Interface

#### *INPUT*

Burning rate	Fire heat release rate (kW)
Radiant fraction	Fraction of Q distributed via radiative energy [10]
Additional loss fraction	Fraction of Q not convected and not radiatively distributed
Height above fire	Elevation difference between the point of interest in the plume and the lowest height where entrainment begins (for diffusion flames this is usually the base of the flames. (m)

#### *OUTPUT*

Volumetric flow rate	Volumetric flow rate in the plume at elevation (z) above the fire (m <sup>3</sup> /s or scfm)
----------------------	-----------------------------------------------------------------------------------------------

### 3.11.5 References

- [1] Walton, W. D., "ASET-B A Room Fire Program for Personal Computers," Nat. Bur. Stand. (U.S.), NBSIR 85-3144, Gaithersburg, MD 20899, 1985.
- [2] Cooper, L. Y., and Stroup, D. W., "Calculating Available Safe Egress Time from Fires," Nat. Bur. Stand. (U.S.), NBSIR 82-2587, Gaithersburg, MD 20899, 1982.

- [3] McCaffrey, B.J., "Purely Buoyant Diffusion Flames: Some Experimental Results," Combustion Institute: Eastern States Section, November 1978.
- [4] Zukoski E., "Development of a Stratified Ceiling Layer in the Early Stages of a Closed-Room Fire," Fire and Materials, Vol. 2, No. 2, 1978.
- [5] Morton, B.R., Taylor, G., Turner, J.S., "Turbulent Gravitational Convection from Maintained and Instantaneous Sources," Proceedings of the Royal Society of London, Series A, No. 1196, London, England, 1956.
- [6] Heskestad, G., "Engineering Relations for Fire Plumes," Fire Safety Journal, Vol. 7, pp. 25-32, 1984.
- [7] Grubitts, S., Shestopal, V.O., "Computer Program for an Uninhibited Smoke Plume and Associated Computer Software," Fire Technology, Vol 29, (3), pp. 246-67, 1993.
- [8] Heskestad, G., "Fire Plumes,"The SFPE Handbook of Fire Protection Engineering," National Fire Protection Association, Quincy, MA 02269, pp. 1-107 to 1-109, 1988.
- [9] McCaffrey, B.J., "Flame Height,"The SFPE Handbook of Fire Protection Engineering," National Fire Protection Association, Quincy, MA 02269, pp. 1-301, 1988.
- [10] Tewarson, A., "The SPFE Handbook of Fire Protection Engineering," National Fire Protection Association, Quincy, MA 02269, pp. 1-186, 1988.

## 3.12 RADIANT IGNITION OF A NEAR FUEL

### 3.12.1 Application

This is a quick, simplistic estimation method for determining what size fire will radiatively ignite a nearby fuel; no flame impingement is assumed.

### 3.12.2 Theory

The equations in this procedure were obtained through correlation of experimental data [1]. The experiments examined the fire sizes necessary to ignite a second, remote, initially non-burning fuel item that was not in direct contact with the flame or convective flow of the original fire. The experimental data provided a correlation between the peak heat release rate of the first-burning item and the maximum distance to a second non-burning fuel item that would result in ignition. Babrauskas found the second item could usually be categorized into one of three groups--based upon material and size:

- 1). **Easily Ignited** - material ignites when it receives a radiant flux of 10 kW/m<sup>2</sup> or greater. Example are thin materials such as curtains or draperies.

$$\dot{Q}_{fire} = 30.0 \times 10 \left( \frac{Distance + 0.08}{0.89} \right) \quad (1)$$

- 2). **Normally Resistant to Ignition** - material ignites when it receives a radiant flux of 20 kW/m<sup>2</sup> or greater. Examples are upholstered furniture and other materials with significant mass but small thermal inertia ( $k\rho c_p$ ).

$$\dot{Q}_{fire} = 30 \left( \frac{Distance + 0.05}{0.019} \right) \quad (2)$$

- 3). **Difficult to Ignite** - material ignites when it receives a radiant flux of 40 kW/m<sup>2</sup> or greater. Examples are thermoset plastics and other thick materials (greater than 0.013 m [ ½ in.]) with substantial thermal inertia ( $k\rho c_p$ ).

$$\dot{Q}_{fire} = 30 \left( \frac{Distance + 0.02}{0.0092} \right) \quad (3)$$

$Q_{\text{fire}}$	Fire heat release rate (kW)
$\alpha$	Regression coefficient of experimentally measured data (m)
$\beta$	Regression coefficient of experimentally measured data (m)

### 3.12.3 Program Notes

The least accuracy is obtained when analyzing 'Easy to ignite' items. This is because the required heat release rates for igniting these types of fuels are low enough that small changes in fuel properties can result in large percentage changes for the required ignition heat release rates.

Target fuels do not have flame impingement considered in the ignition analysis.

The distance between the exposed fuel item and the initial burning fuel is small enough to nullify a point source radiation assumption. The target-fuel item assumedly sees a broad fire such as that produced by a free-standing upholstered chair or side of a couch.

Fuel types included in the experimental correlation were: wood, plywood, plywood laminates, paper, polyurethane and polyethylene. These fuel types have a radiative fraction varying from 0.6 for polyurethane to 0.3 for wood pine [2].

Another procedure for predicting radiative ignition of target fuels may be found in **FREEBURN**.

### 3.12.4 Program Interface

#### *INPUT*

Separation of fuel packages (mm or in.)

Fuel resistance to ignition For easily ignitable fuels the energy flux is 10 kW/m<sup>2</sup>, for normal fuels the energy flux is 20 Kw/m<sup>2</sup>, and for hard to ignite fuels, the energy flux is 40 kW/m<sup>2</sup>.

#### *OUTPUT*

$Q_{\text{fire}}$  Fire size of the initially burning fuel needed to ignite the second fuel source.

### 3.12.5 References

- [1] Babrauskas, V., "Will the Second Item Ignite," Nat. Bur. Stand. (U.S.), NBSIR 81-2271, Gaithersburg, MD, 1982.
- [2] Tewarson, A., "Generation of Heat and Chemical Compounds in Fires," The SFPE Handbook of Fire Protection Engineering, National Fire Protection Association, Quincy, MA 02269, pp. 1-186, 1982.

### 3.13 SMOKE FLOW THROUGH AN OPENING

#### 3.13.1 Application

This procedure estimates the steady-state volumetric flow rate of heated gas at elevated temperatures through an opening from an enclosure. It is appropriate for measuring post-flashover or steady-state smoke leakage through open doors or cracks around closed doors. Whereas this procedure solves for the volumetric smoke flow rate at a given temperature, **MASS FLOW THROUGH A VENT** solves for the vent flow in terms of mass.

#### 3.13.2 Theory

The theory for smoke flow through an opening due to buoyancy forces is developed in *Design of Smoke Control Management Systems*, [1]. The derivation foundation is the classical orifice eq (1); in contrast **MASS FLOW THROUGH A VENT** iterates on a solution satisfying mass conservation.

The velocity term in eq (1) may be substituted for by rearranging the Bernoulli expression [eq (2)] and solving for velocity in terms of the other parameters [eq (2b)]. The assumptions for Bernoulli flow are presented in Section 3.13.3. The pressure term in eq (2b) is solved through rearranging the ideal gas law [eq (3)] with pressure expressed in gas density terms.

$$\dot{V} = CA_{vent}v \quad (1)$$

$$\frac{\Delta P_1}{\rho_1} + \frac{v_1^2}{2} + gz_1 = \frac{\Delta P_2}{\rho_2} + \frac{v_2^2}{2} + gz_2 \quad (2a)$$

$$v_2 = \sqrt{\frac{\Delta P_{(1-2)}}{\rho_2}} \quad (2b)$$

$$\Delta P_{1-2} = \Delta\rho_{1-2}gh \quad (3)$$

$$\Delta\rho_{1-2} = \frac{P(MW)}{R} \left| \frac{1}{T_1} - \frac{1}{T_2} \right| \quad (3b)$$

$$\dot{V} = CA_{vent} \sqrt{\frac{2ghP(MW)}{\rho_2 R} \left| \frac{1}{T_1} - \frac{1}{T_2} \right|} \quad (4)$$

$A_{\text{vent}}$	Area of the vent that allows smoke movement ( $\text{m}^2$ )
$C$	Orifice coefficient (0.8)
$g$	Acceleration constant equal to Earth's surface gravity ( $9.81 \text{ m/s}^2$ )
$h$	Height of the neutral plane (m)
$MW$	Ambient fluid molecular weight ( $28.95 \cdot 10^{-3} \text{ kg air/(g}\cdot\text{mole)}$ )
$P$	Standard pressure (101,325 Pa)
$\Delta P_{1-2}$	Pressure difference across the vent (Pa)
$R$	Universal gas constant ( $8.314 \text{ J/((g}\cdot\text{mole})\cdot\text{K)}$ )
$T$	Air temperature (K)
$T_{\infty}$	Ambient air temperature (294 K)
$V$	Volumetric vent flow rate ( $\text{m}^3/\text{s}$ )
$z$	Elevation difference (m)
$v$	Smoke velocity (m/s)
$\Delta\rho_{1-2}$	Density difference across the vent ( $\text{kg}/\text{m}^3$ )

#### Subscript

1	Location inside the room
2	Location just beyond the vent

### 3.13.3 Program Notes

Assumes uniform depth of smoke in the vent area.

Steady-state flow conditions were assumed.

Bernoulli fluid is: steady-state, incompressible, nonviscous.

Only buoyancy driven smoke flow was considered.

Standard pressure, no stack effect, no air-handling systems, no wind forces, no unrelieved pressure-volume work by the expanding, hot smoke.

Standard gravitational acceleration at Earth's surface, i.e. smoke flow is not considered in systems undergoing additional accelerations. The heated smoke layer is quiescent away from the vent.

Inappropriate for duct-like openings where the passage length is significantly greater than the narrow dimension of the opening.

Air is the ambient gas (or any other ambient gas should have a similar molecular weight) at a temperature of 21 °C (70 °F).

The temperature should characterize the average conditions throughout the smoke layer.

### 3.13.4 Program Interface

#### *INPUT*

Smoke flow area	Vent area (m <sup>2</sup> )
Smoke T	Temperature of the smoke (°C)
Depth of Smoke	Depth of the smoke (m)

#### *OUTPUT*

Smoke flow	Smoke flow rate out of the vent area (L/s)
------------	--------------------------------------------

### 3.13.5 References

- [1] Klote, J.H., Milke, J.A., *Design of Smoke Control Management Systems*, ASHRAE & SFPE, Atlanta, GA 30329, pp. 21-32, 1992.

## 3.14 SPRINKLER/DETECTOR RESPONSE

### 3.14.1 Application

This procedure calculates the thermal response of a detector or sprinkler located at or near a ceiling whose area is large enough to neglect the effects of smoke layer development.

### 3.14.2 Theory

The equations in this procedure were originally distributed in a program written by Evans and Stroup [1] entitled DETACT-QS. The correlations for jet temperatures and velocities were developed from data by Alpert [2]. The theory and documentation for sprinkler activation are presented by Evans [3].

The results of this procedure predict time of thermal detector activation. In order to make this prediction, time-dependent events from the fire must be linked to events resulting in the heating of the detector from ambient to its activation temperature. The heat source is accounted for by a user-specified, time varying-fire<sup>4</sup>. The time-lag associated with heating the detector is accounted for with the RTI parameter [eq (2)]. The RTI parameter considers the detector's ability to absorb heat and the ambient environment's ability to provide heating. Ambient environmental heating is modeled with only forced convection. The temperature and velocity of the convecting air are predicted from correlations assembled from experimental data of full-scale steady-state and growing fires [2] [eqs (1) - (4)]. The actual heat release rate of the fire should be used with both radiative and convective fractions. When  $T_{D,t+\Delta t}$  equals or exceeds the value in  $T_{D, \text{activation}}$ , then detector response is predicted.

$$T_{D,t+\Delta t} = (T_{jet,t+\Delta t} - T_{D,t})(1 - e^{-\frac{1}{\tau}}) + (T_{jet,t+\Delta t} - T_{jet,t})\tau(e^{-\frac{1}{\tau}} + \frac{1}{\tau} - 1) \quad (1)$$

$$\tau = \frac{RTI}{\sqrt{v_{jet,t}}} \quad (2)$$

$$v_{jet,t} = 0.95\left(\frac{\dot{Q}}{Z}\right)^{\frac{1}{3}}, \quad \text{for } \frac{r}{Z} \leq 0.15 \quad (3)$$

---

4 See Section 4.4, 4.5, or 4.6.

$$v_{jet,t} = 0.2 \frac{\dot{Q}^{\frac{1}{3}} z^{\frac{1}{2}}}{r^{\frac{5}{6}}}, \quad \text{for } \frac{r}{z} > 0.15 \quad (4)$$

$$T_{jet,t} = T_{\infty} + \frac{16.9 \dot{Q}^{\frac{2}{3}}}{z^{\frac{5}{3}}}, \quad \text{for } \frac{r}{z} \leq 0.18 \quad (5)$$

$$T_{jet,t} = T_{\infty} + \frac{5.38}{z} \left( \frac{\dot{Q}}{r} \right)^{\frac{2}{3}}, \quad \text{for } \frac{r}{z} > 0.18 \quad (6)$$

Q	Total theoretical fire heat release rate (kW)
r	Radial distance of the sprinkler from the vertical axis of the fire (m)
RTI	Response Time Index: $(mc_p)_{detector} / (hA) \cdot v_{jet}^{1/2}$ a characterization of the detector's thermal sensitivity; a measure of how quickly a detector link reaches its activation temperature.
$T_{jet,t+\Delta t}$	Temperature of the jet at the next time step, $t+\Delta t$ ( $^{\circ}\text{C}$ )
$T_{jet,t}$	Same as $T_{jet,t+\Delta t}$ , but at the previous time step, $t$ ( $^{\circ}\text{C}$ )
$T_{\infty}$	Ambient space and initial sprinkler temperature ( $^{\circ}\text{C}$ )
$T_{D,t}$	Detector or link temperature at time, $t$ ( $^{\circ}\text{C}$ )
$v_{jet,t}$	Velocity of the ceiling jet gases as a function of the parameters on the right-hand side of eqs (2) and (3) at time step, $t$ (m/s)
z	Vertical entrainment distance; the difference between the height of the ceiling and the base of the flames (m)

### 3.14.3 Program Notes

The total theoretical heat release rate should describe the fire in this correlation [2,5]. The total theoretical heat release rate may be obtained by multiplying the mass pyrolysis rate by the theoretical heat of combustion. Mass pyrolysis rates can be obtained through experimental measurement using load cells or by analogy with previously burned exemplars. Theoretical heats of combustion are

available from handbooks (see Section 1.4).

The program assumes a quasi-steady-state fire and ceiling jet behavior. This assumption limits the accuracy most when the fire heat release rate changes very rapidly.

The procedure assumes an unconfined ceiling jet and plume. If a smoke layer should develop under the ceiling (as is the case when the fire is large relative to the room), **SPRINKLER** procedure within **FIRE SIMULATOR** will consider entrainment of hot gases into the fire plume whereas this procedure will not. The plume should not experience a reduction in entrainment, such as when flames attach to a wall or corner.

If the detector is located significantly below the bottom of the ceiling jet, then this procedure should not be used. The ceiling jet thickness is estimated between 6 - 12% of the entrainment height (z).

The procedure assumes the detector is located such that it is exposed to both the maximum ceiling jet velocity and temperature.

Correlations for ceiling jet temperature and velocity were determined from limited experimental data: (no beam or truss ceilings, no cathedral ceilings, only smooth, horizontal unconfined ceilings).

Sprinklers or heat detectors located on a wall or on a ceiling next to a wall may have activation times significantly later than predicted activation times. This delay is due to the dissipation of ceiling jet velocity at the wall and wall/ceiling intersection. The dissipation effect may be especially true in room corners. Within the **FIRE SIMULATOR** procedure, the ceiling jet velocity may be adjusted to better model these special flow effects; this capability is not provided within **SPRINKLER/DETECTOR RESPONSE**.

Rate-of-rise heat detectors are not simulated, only fixed-temperature detectors are simulated.

Radiation and conduction are not accounted for explicitly, but because these phenomena participated in the correlational experiments--to the degree that simulated fire conditions reproduce experimental fire conditions--the radiation/conduction effects are implicitly accounted for. The experimental fire conditions involved wet-pipe sprinklers exposed to cotton, wood, polyurethane, polyvinyl chloride, and liquid heptane fires [1,4].

#### **3.14.4 Program Interface**

##### *INPUT*

Printout interval

Effects hardcopy output

Height of ceiling above fuel	The difference between the elevation of the lowest point of the fire that can freely entrain air and the elevation of the ceiling (m or ft)
Distance of detector from fire axis	Horizontal distance of the detector location from a vertical axis running through the center of the fire (m or ft)
Initial room temperature	$T_{\infty}$ , Ambient and initial sprinkler temperature ( $^{\circ}\text{C}$ or $^{\circ}\text{F}$ )
Detector activation temperature	$T_{D, \text{activation}}$ , Detector link activation temperature ( $^{\circ}\text{C}$ or $^{\circ}\text{F}$ )
Detector response time index	RTI, Response Time Index ( $[\text{m}\cdot\text{s}]^{1/2}$ or $[\text{ft}\cdot\text{s}]^{1/2}$ )
RHR(t)	Total theoretical fire heat release rate (kW)

### *OUTPUT*

Jet Temperature(t)	Temperature in the ceiling jet at radial distance, r ( $^{\circ}\text{C}$ )
Head Temperature(t)	Temperature of the sprinkler/detector link ( $^{\circ}\text{C}$ )

### Graphical Output

RHR	Total theoretical fire heat release rate (kW)
$T_{\text{jet}}$	Temperature in ceiling jet at detector radial position ( $^{\circ}\text{C}$ )
$T_{\text{head}}$	Temperature of the detector head ( $^{\circ}\text{C}$ )

### 3.14.5 References

- [1] Evans, D. D. and Stroup, D. W., "Methods to Calculate the Response of Heat and Smoke Detectors Installed Below Large Unobstructed Ceilings," Nat. Bur. Stand. (U.S.), NBSIR 85-3167, Gaithersburg, MD, 1985.
- [2] Alpert, R. L., "Calculation of Response Time of Ceiling-Mounted Fire Detectors," Fire Technology, Vol 8:(3), National Fire Protection Association, Quincy, MA, pp. 181-195, 1972.
- [3] Evans, D. D., "Calculating Fire Plume Characteristics in a Two-Layer Environment," Fire Technology, Vol. 20:(3), National Fire Protection Association, Quincy, MA, pp. 39-63, 1984.

- [4] Heskestad, G., Delicatsios, M.A., "Environments of Fire Detectors--Phase I. Effect of Fire Size, Ceiling Height and Material," Nat. Bur. Stand. (U.S.), NBS-GCR-77-86, Gaithersburg, MD 20899, 1977.
- [5] Alpert, R.L., and Ward, E. J.; "Evaluating Unsprinklered Fire Hazards; SFPE Technology Report 83-2;" Society of Fire Protection Engineers: Boston, MA, 1983.

## 3.15 THOMAS'S FLASHOVER CORRELATION

### 3.15.1 Application

This procedure quickly estimates the amount of energy needed to produce flashover in a compartment.

### 3.15.2 Theory

This procedure [1] results from simplifications applied to a hot-layer energy balance on a room with a fire. These simplifications resulted in eq (1). There is a term representing heat losses to the "...total internal surface area of the compartment..." , and a term representing energy flow out of the vent opening. The two constants in eq (1) represent values correlated to experimental flashover conditions.

$$\dot{Q} = 7.8A_{room} + 378(A_{vent}\sqrt{H_{vent}})_{equivalent} \quad (1)$$

$$A_{room} = A_{floor} + A_{ceiling} + A_{walls} - A_{vents_{equivalent}} \quad (2)$$

$$A_{vents_{equivalent}} = H_{vent_{equivalent}} \cdot W_{vent_{equivalent}} \quad (3)$$

$$W_{vent_{equivalent}} = \frac{(A_{vent}\sqrt{H_{vent}})_1 + (A_{vent}\sqrt{H_{vent}})_2 + \dots}{H_{vent_{equivalent}}^{\frac{3}{2}}} \quad (4)$$

$Q =$  Fire heat release rate (kW)

$A_{vent} =$  Area of the vent (m<sup>2</sup>)

$H_{vent, equivalent} =$  The difference between the elevation of the highest point among all of the vents and the lowest point among all of the vents (m).

$W_{vent, equivalent} =$  The width of a virtual vent that has an area equivalent (for the purposes of determining flashover) to the combined area of all individual vents from the room of consideration (m).

### 3.15.3 Program Notes

The formulation of the energy balance considered heat losses from the hot gas layer and heated walls to the cooler lower walls and floor surfaces. The term  $A_{room}$  should include all surfaces inside the room, exclusive of the vent area.

The fire area should not be subtracted from the floor area as the fire will conduct and convect heat into the floor underneath the fuel footprint.

The equation does not know where the vent is located, nor whether the vent is a window or a door; however, the equation was developed from tests that included window venting.

The equation does not consider whether the walls are insulated or not. Use of the equation for compartments with thin metal walls may therefore be inappropriate. The experiments included compartments with thermally thick walls and fires of wood cribs. The equation was later verified in gypsum lined rooms with furniture fires [2].

Verification with fast growing fires: the correlation was developed from fast not slow growing fires.

This procedure was correlated from experiments conducted in rooms not exceeding 16 m<sup>2</sup> in floor area.

The equation predicts flashover in spaces without ventilation. This prediction is unlikely due to oxygen starvation of the fire.

#### **3.15.4 Program Interface**

##### *INPUT*

Room Length (m or ft)

Room Width (m or ft)

Room Height (m or ft)

Vent Height Height of the (equivalent) vent (m or ft)

Vent Width Width of the (equivalent) vent (m or ft)

##### *OUTPUT*

$Q_{\text{flashover}}$  = Estimated fire heat release rate that will create flashover (kW)

$Q_{\text{door}}$  = Estimated energy losses from gas flow out of the door (kW)

$Q_{\text{wall}}$  = Estimated energy losses from gas to room wall surfaces (kW)

### 3.15.5 References

- [1] Thomas, P. H., "Testing Products and Materials for Their Contribution to Flashover in Rooms," *Fire and Materials*, 5, pp. 103-111; 1981.
- [2] Babrauskas, V., "Upholstered Furniture Room Fires--Measurements, Comparison with Furniture Calorimeter Data, and Flashover Predictions," *Journal of Fire Sciences*, Vol. 2, 5, 1984.

## 3.16 UPPER LAYER TEMPERATURE

### 3.16.1 Application

This procedure is a fast, rugged method for predicting pre-flashover upper-layer gas temperatures in a compartment fire with a door and/or window.

### 3.16.2 Theory

The procedure was developed from a regressional fit to a large number of experimentally measured fire data. This large database is, in large part, a reason for the procedure's robustness. The authors of this method are McCaffrey, Quintiere and Harkelroad [1].

The prediction of upper layer temperature begins with an energy balance about a control volume. This control volume includes the hot pyrolyzates and entrained air that together rise and form the gaseous 'smoke layer' within the room. The control volume does not include the barrier surfaces (ceiling and walls); the control volume extends to, but not beyond the openings from the vents. By applying conservation of energy to this control volume, a general expression for the temperature of the upper layer in the room becomes available [eq (1)]. The two terms in eq (1),  $\dot{m}_{out}$  [2] and  $Q_{surface}$ , are substituted with eqs (2) and (3). After further algebraic manipulation, eq (4) is obtained.

$$\dot{Q}_{fire} = \dot{m}_{out} c_p (T - T_{\infty}) + \dot{Q}_{surface} \quad (1)$$

$$\dot{m}_{out} = \frac{2}{3} C_D W_{vent} H_{vent}^{\frac{3}{2}} \rho_{\infty} \sqrt{2g \frac{T_{\infty}}{T} (1 - \frac{T_{\infty}}{T})} (1 - \frac{N}{H_{vent}})^{\frac{3}{2}} \quad (2)$$

$$\dot{Q}_{surface} = h_k A_{surface} (T - T_{\infty}) \quad (3)$$

$$\frac{\Delta T}{T_{\infty}} = \frac{\dot{Q}/(c_p T_{\infty} \dot{m}_{vent})}{1 + h_k A_{surface}/(c_p \dot{m}_{vent})} \quad (4)$$

The three terms appearing in eq (1) also are present in eq (5), albeit in slightly rearranged manner. These terms are:  $Q_{fire}$ , the energy source term;  $h_k A_{surface}$ , the heat loss term (to the ceiling and walls); and  $g^{1/2} c_p \rho_{\infty} T_{\infty} (A \cdot H^{1/2})_{vent}$ , the energy flow term. The form of the regression in eq (5) was motivated by the derived physical relationships in eq (4). Numerical values for the terms C, n and m in eq (6) were provided directly from the regressional fit. Quintiere et al. [1] discovered that the heat losses from the control volume to the floor surface ( $Q_{surface}$ ) were minor in pre-flashover burning. Eq (4) therefore is presented without consideration of floor area in  $A_{surface}$ .

$$\frac{\Delta T}{T_{\infty}} = C \left( \frac{\dot{Q}}{\sqrt{g} c_p \rho_{\infty} T_{\infty} (A\sqrt{H})_{vent}} \right)^n \left( \frac{h_k A_{surface}}{\sqrt{g} c_p \rho_{\infty} (A\sqrt{H})_{vent}} \right)^m \quad (5)$$

$$C = 480^{\circ}C, \quad n = \frac{2}{3}, \quad m = -\frac{1}{3} \quad (6)$$

### Surface heat loss coefficient, $h_k$

The surface heat loss coefficient,  $h_k$  is derived from an assumption of a thermally thick compartment barrier [1]. This assumption implies the duration that a slab is exposed to a heat source must be less than the time when 16 percent of the energy entering the slab's heated surface begins to exit the slab from the unexposed surface. Figure 3.16.1 illustrates that the amount of energy leaving the slab (or wall) from the cool side changes with time as a

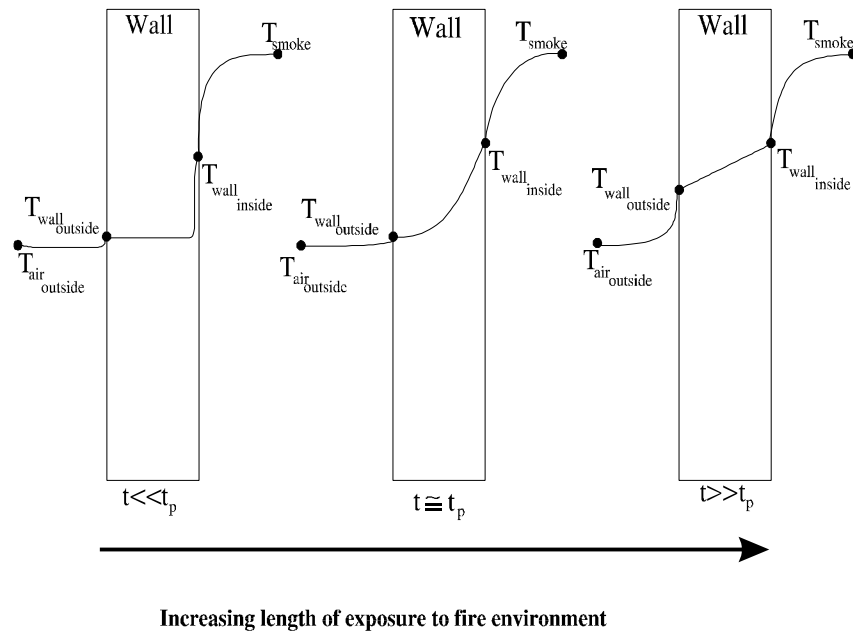


Figure 3.16.1. Temperature pulse moving from a heated to an unheated surface

result of the temperature pulse moving through the slab (or wall). This temperature pulse moves in a manner similar to that of a wave. As the temperature wave moves through the slab, more energy is conducted into the barrier interior. Eventually the interior slab temperatures increase to the point that the temperature profile becomes linear, and the amount of heat leaving the cool side no longer increases. The heat transfer coefficient,  $h_k$ , is calculated using the transient formula [eq (7)], up to the point when the heat exiting the back surface is greater than 16 percent of the heat entering the exposed surface. After this point,  $h_k$  is calculated using the steady-state assumption [eq (8)]. The elapsed time up to this transition point between unsteady and steady-state heat loss is called the thermal penetration time; it is calculated from eq (9). A barrier with a long thermal penetration time is said to be 'thermally thick.'

$$h_k = \frac{A_{wall}}{A_{total}} \sqrt{\frac{\rho_{\infty} c_p k}{t}}|_{wall} + \frac{A_{ceiling}}{A_{total}} \left( \frac{1}{\sqrt{\frac{\rho c_p k}{t}}|_{ceiling_1} + \sqrt{\frac{\rho c_p k}{t}}|_{ceiling_2}} \right)^{-1} \quad (7)$$

$$h_k = \frac{A_{wall}}{A_{total}} \left( \frac{1}{\left(\frac{k}{\delta}\right)|_1 + \left(\frac{k}{\delta}\right)|_2} \right)^{-1} + \frac{A_{ceiling}}{A_{total}} \left(\frac{k}{\delta}\right)|_1 \quad (8)$$

$$t_{thermal\ penetration} = \frac{\rho_{\infty} c_p}{k} \left(\frac{\delta}{2}\right)^2 \quad (9)$$

In the above scheme, an accounting for the fact that walls and ceiling may be built from different materials is incorporated into the equation through the ratio of the respective surface areas and material properties. It is also possible to account for surfaces that are layered together in a manner analogous to a sandwich. The subscript  $\cdot_k$  denotes this latter type of sandwich arrangement. Up to five layers are considered, but approximations can be acceptably written through representing only those layers with the highest thermal conductivity. The subscripts  $\cdot_1$  and  $\cdot_2$  denote the layer whose surface is visible from inside the room and the layer immediately behind that, respectively. If only one layer exists, subscripted terms in eqs (8) and (9) with values greater than one vanish.

$A_{surface}$	Area of surface denoted by subscript, excluding vent areas (m <sup>2</sup> )
$(A\sqrt{H})_{vent}$	Width · Height <sup>3/2</sup> of the vent
C	Linear constant of regression
$C_D$	Orifice discharge coefficient
$c_p$	Heat capacity of slab denoted by subscript (kJ/kg/ΔK)
$\delta$	Thickness of a slab denoted by subscript (m)
g	Earth's surface gravitational constant (9.81 m/s <sup>2</sup> )
$h_k$	Overall surface heat transfer coefficient (kW/m <sup>2</sup> /ΔK)
$H_{vent}$	Vent height (m)
k	Thermal conductivity of slab denoted by subscript (kW/m/ΔK)
$\dot{m}_{out}$	Mass flow rate of hot gas out of the room (kg/s)
N	Layer neutral plane height in the doorway (m)
$\rho_{\infty}$	Density of slab denoted by subscript (kg/m <sup>3</sup> )
$Q_{fire}$	Fire heat release rate into the control volume (kW)
$Q_{surface}$	Heat lost from the control volume to the room surfaces (except floor) (kW)
$t_{thermal\ penetration}$	Time when a fixed percentage of the heat entering a surface from one side transfers through the slab and exits from the back surface (sec)
T	Temperature of the control volume (smoke) gases (K)
$T_{\infty}$	Temperature of the ambient room air at simulation start (K)

$\Delta T$	Temperature difference ( $T - T_{\infty}$ ) (K)
$W_{\text{vent}}$	Vent width (m)

subscripts

1	Surface 1, surface visible from the inside of the room
2	Surface 2, directly behind surface 1 (from a point of view inside the room)
p	thermal penetration time
$\infty$	Ambient and/or starting conditions

### 3.16.3 Program Notes

The database robustness along with regression as the choice of correlational fit have ensured good utility from this procedure in predicting temperatures up to flashover or up to the vent-controlled burning regime. The database included over 100 experiments of both full- and small-scale rooms and ventilation that included doors or windows or both. The fires included wood, gas and plastics in crib, burner or furniture configurations [1].

For fires that are small relative to the room, the ventilation parameter will tend to overestimate vent flows and therefore underestimate layer temperatures.

The simulated fire should be described with the actual heat release rate (radiative and convective). If the change in fire heat release rate is significant between the one-second time steps of the simulation or the datapoints in the fire file, then errors can result in the output from this procedure. The fire is considered to be a point source; no line fires, wall fires or fires of significantly distributed area are considered.

Predictions become hotter than experimentally measured when the vent area approaches zero. An example of a poor application could be smoke leakage past a crack in a doorway.

This procedure has no method to account for the location of the vent with respect to its elevation within the wall.

Ventilation through the ceiling or floor is not simulated.

This regressional correlation was developed with some reduced-scale enclosures having length scales as small as 0.5 meter on a side. Below this size however, results can not be assured.

This correlation has been adapted for post-flashover predictions [3], but agreement with post-flashover experimental results were not satisfactory per the comments of McCaffrey, Quintiere et al. For post-flashover predictions, **FIRE SIMULATOR** is a recommended tool.

When thermally thin walls are modeled, predictions of temperatures may be higher than reality. One example of thermally thin walls is bare metal.

When modeling room barriers containing multiple layers, those layers with thermal conductivities one or more orders of magnitude smaller than other layers may be disregarded from eq (7) and (8).

### 3.16.4 Program Interface

#### *INPUT*

Printout interval	(s)
Initial room temperature	(°C or °F)
Maximum Run Time	Duration of the simulation (sec)
Barrier Material Properties	Up to 5 layers simulating multiple-layered, back-to-back composite
$A_{\text{surface}}$	Material surface area (m <sup>2</sup> or ft <sup>2</sup> )
$\delta$	Material thickness (m or ft)
$k$	Material thermal conductivity (kW/(m·K))
$c_p$	Material heat capacity (kJ/(kg·ΔK))
$\rho$	Material density (kg/m <sup>3</sup> )
Vents	A door and/or a window may be described here (m <sup>2</sup> or ft <sup>2</sup> )
Fire file	A pre-existing fire file (*.fir) may be specified or a fire file can be generated at run-time. To exit from the fire file generation process, use the ESCAPE key.
Next Input Screen	The option to enter a descriptive title for the simulation may be entered here

#### *OUTPUT*

$Q_{\text{fire}}(t)$	(kW)
$T(t)$	(°C or °F)
Ventilation Limit	Determined as in Section 3.17 (kg/s)
$T(t_{\text{flashover}})$	Determined when the temperature increase of the control volume gases (smoke) increases 600 °C (1200 °F) above $T_{\infty}$ (°C)

### 3.16.5 References

- [1] McCaffrey, B.J., Quintiere, J.G., Harkelroad, M.H. "Estimating Room Temperatures and the Likelihood of Flashover using Fire Test Data Correlations," *Fire Technology*, Vol. 17, No. 2, 98-119, May 1981.
- [2] Rockett, J.A., "Fire Induced Gas Flow in an Enclosure," *Combustion Science and Technology*, Vol. 12 (1976), p. 165.
- [3] Kawagoe, K.D. & Sekine, T., "Estimation of Fire Temperature-Time Curve for Rooms," *BRI Occasional Report No. 11*, Building Research Institute, Ministry of Construction, Japanese Government, June 1963.

## 3.17 VENTILATION LIMIT

### 3.17.1 Application

This procedure estimates the maximum post-flashover fire size sustainable in a room based upon the ventilation geometry. Vent geometry can control the fire size because vent geometry can limit the amount of air entering the room and hence limit the amount of oxygen that may combine with the fuel.

### 3.17.2 Theory

Kawagoe [1] originally presented the idea that fire heat release rate within a compartment could be limited by ventilation geometry. This idea was borne out by Kawagoe's original--and many subsequent--post-flashover experiments [2,3]. The equation for VENTILATION LIMIT is presented in eq (1) where the mass flow rate of air into the room  $\frac{1}{2}A_oH_o^{1/2}$  is in kg/s.

$$\dot{Q}_{VL} = \chi_A \Delta H_{c,air} \frac{1}{2} A_o \sqrt{H_o} \quad (1)$$

$\dot{Q}_{VL}$	Limit of fire heat release rate supportable by a naturally ventilated room (kW)
$\chi_A$	Combustion efficiency
$A_o$	Area of the opening (m <sup>2</sup> )
$H_o$	Height of opening (m)
$\Delta H_{c,air}$	Fuel heat of combustion per kilogram of air that oxidizes fuel (~3000 kJ/kg).

### 3.17.3 Program Notes

It is possible to calculate the dimensions of a single vent that will sustain the fire burning rate allowed by several individual vents each contributing air (oxidizer) to the fire up to the limit supported by their geometrical size. The dimensions of this equivalent vent are obtainable from eq (3) in Section 3.15.

The equivalent vent dimension approach is not appropriate for use when vents are located at significantly different elevations in the wall.

This routine is not applicable to the early times in the growth of a compartment fire when fuel-limited burning occurs. In this situation, more than enough air needed to sustain burning passes through the vent and reaches the fuel

Ventilation limit will calculate the heat released inside the room; however, it is possible that additional heat may be released outside of the room that is unaccounted for by this procedure. This can occur if during ventilation limited burning, the fire pyrolyzes more fuel than the air is capable of burning.

The unburned pyrolyzate will be carried out the vent and may burn in a 'door or window jet' providing that the pyrolyzate concentrations are high enough, hot enough, and sufficient oxygen for combustion is present

Assuming  $\chi_A$  as unity results in a prediction for the largest possible ventilation limit fire; this may be appropriate for design fires used in life-safety hazard analysis.

### 3.17.4 Program Interface

#### *INPUT*

$W_o$  Width of the opening (m or ft)

$H_o$  Height of the opening (m or ft)

$z_o$  Height of the opening (m or ft)

$\chi$  Combustion efficiency [4]

#### *OUTPUT*

$Q_{VL}$  Fire heat release rate as limited by ventilation geometry (kW)

### 3.17.5 References

- [1] Kawagoe, K. D. & Sekine, T., "Estimation of Fire Temperature-Time Curve for Rooms," BRI Occasional Report No. 11, Building Research Institute, Ministry of Construction, Japanese Government, June 1963.
- [2] Fang, J.B., Breese, J.N., "Fire Development in Residential Basement Rooms, Interim Report," Nat. Bur. Stand. (U.S.), NBSIR 80-2120, Gaithersburg, MD 20899, 1980.
- [3] Babrauskas, V., "COMPF2--A Program for Calculating Post-Flashover Fire Temperatures," Nat. Bur. Stand. (U.S.), NBS-TN-991, Gaithersburg, MD 20899, 1979.
- [4] Tewarson, A., "Generation of Heat and Chemical Compounds in Fires," The SFPE Handbook of Fire Protection Engineering, National Fire Protection Association, Quincy, MA 02269, Chapter 1, pp. 186, 1988.



## 4 MAKEFIRE

**MAKEFIRE** is a collection of procedures designed not only to conveniently produce/edit fire files that other **FPE-tool** modules can use, but to also generate heat release rate histories for

```
QUIT SYSTEM SETUP FIREFORM MAKEFIRE FIRE SIMULATOR CORRIDOR 3rd
ROOM
?44444444444@
* FORMULA *
* FREEBURN *
* MYFIRE *
* LOOK-EDIT *
* RATES *
.))))))))-
```

Figure 4.0.1. **FPEtool** sub-menu for **MAKEFIRE**

design fires through incorporating appropriate engineering practices. There are 5 procedures within **MAKEFIRE**, four that are capable of generating files of heat release rate histories.

### 4.1 FORMULA

#### 4.1.1 Application

This procedure creates fire files with exponential or power law dependency. The module **RATES** can be used in conjunction with this procedure to provide correlation between 'real-world' fires and the typical power-law rates.

#### 4.1.2 Theory

**FORMULA** creates fire data files by describing three distinct burning phases: growth, steady-state and decay. In addition to the power law, the growth phase may also be described with an exponential eq (2). Ending conditions must be specified for each of the three user-specified burning regimes. **FORMULA** will terminate the burning regime when one of the following specifications is met: maximum time limit, maximum percentage of fuel is consumed, or maximum/minimum heat release rate.

$$\dot{Q}_{fire} = \alpha t^n \quad (1)$$

$$\dot{Q}_{fire} = e^{\beta t} \quad (2)$$

The decay phase is specified in a manner similar to the growth phase and may be thought of as a reflection of growth-phase burning.

In eq (1),  $\alpha$  is the 'growth rate' parameter which has a listing of values for roughly 25 different fuels in **RATES**. For decay phase burning, the procedure calculates eq (1) using a negative power-law integer; however, the user should still enter this decay-phase power-law integer as a positive number (the procedure will account for the negative number).

$Q_{\text{fire}}$	Fire heat release rate (kW)
$\alpha$	Fire growth constant; values for this constant may be obtained from <b>RATES</b> , NFPA 92B and the SFPE Handbook for Fire Protection Engineers [2] (kW/s <sup>2</sup> )
t	Time of fire duration since ignition (sec)
n	Power-law integer
$\beta$	Exponential constant (sec <sup>-1</sup> )

### 4.1.3 Program Notes

There is a maximum of 1,500 entries allotted to each fire file; if the file contains more entries than this they may not be accepted as a 'valid' FIRE.FIL.

As linear interpolation is used between data points in the fire file, the otherwise 'saw-tooth' nature of actual fires will tend to be 'smoothed.' This is an accepted practice per NFPA 92B [1].

It is possible to specify a fire which outputs more energy than is contained by the mass of the fuel. Entering the **total burnable mass** of fuel is a recommended option that help the user avoid this pitfall.

The fire data files created by **FORMULA** use metric units.

A familiar example of a growth phase is the 't-squared' fire where the heat release rate is described with a power law using an integer of 2 [eq (1)]. The equations are justified on the basis that they correspond to full-scale fire tests; however, the equations may not justifiably describe the burning behavior of fuels that are only 'similar' to the fuels of the original full-scale tests. An example of a fuel that is similar to an item burned in an actual full-scale test is bundled-recycled newspapers stacked 10 feet high versus filled mail bags stacked 5 feet high [1].

### 4.1.4 Program Interface

A collage of input screens is assembled in Figure 4.1.1. The individual sub-menus appear as they would to the user of the program, albeit in Figure 4.1.1 every sub-menu screen is presented simultaneously. This simultaneous presentation is only for edification purposes; the individual screens can be identified by the left-hand margins they each maintain.



Initial rate of heat release	Heat release rate at t=0 seconds, default = 0.1 kW
Total burnable mass	Fuel mass (kg or lb <sub>m</sub> )

**GROWTH PHASE**

Power law-- $Q_{\text{fire}} = \alpha t^n$	
Growth rate, $\alpha$	[1] (kW/s <sup>2</sup> )
Fire growth exponent, n	
Exponential-- $Q_{\text{fire}} = e^{\beta t}$	
Fire growth constant, $\beta$	(sec <sup>-1</sup> )

**ENDING CONDITIONS for GROWTH PHASE**

Duration	(s)
Preset burning rate	(kW)
Calculated max burning rate	
Projected fuel area	Fuel footprint from a plan (m <sup>2</sup> or ft <sup>2</sup> )
RHR per unit area	Fire heat release per unit area of fuel projected (kW/m <sup>2</sup> <sub>floor</sub> or BTU/s/ft <sup>2</sup> <sub>floor</sub> )
End on n of m	The growth phase may terminate upon 1 or 2 out of a maximum of 2 stipulated conditions (these conditions being a duration or a preset burning rate).

**STEADY-STATE PHASE**

Ending Conditions	
Time	(s)
% mass consumed	Percent total mass consumed after steady-state burning

**DECAY PHASE**

Power-law $Q_{\text{fire}} = \alpha t^n$	
Fire decay constant, $\alpha$	(kW/s <sup>2</sup> )
Fire decay exponent, n	
Exponential $Q_{\text{fire}} = e^{\beta t}$	
Fire decay constant $\beta$	(sec <sup>-1</sup> )

## ENDING CONDITIONS FOR DECAY PHASE

Duration	(s)
Preset burning rate	(kW)
% mass consumed end on n of m	Percent total mass consumed after steady-state burning The growth phase may terminate upon 1, 2 or 3 of a maximum of 3 stipulated conditions (these conditions being a duration, preset burning rate or % of mass consumed).

## *OUTPUT*

Time	(s)
Rate of heat release	Fire heat release rate (kW)
Rate of mass loss	(g/s)

### **4.1.5 References**

- [1] National Fire Protection Association, NFPA 92B, Quincy, MA 02269-9101, pp. 28-30, 1991.
- [2] Evans, D., "Ceiling Jet Flows," The SFPE Handbook of Fire Protection Engineering, National Fire Protection Association, Quincy, MA 02269, pp. 1-138 to 1-145, 1988.

## 4.2 FREEBURN

### 4.2.1 Application

This procedure, like several other procedures in **MAKEFIRE**, creates a fire file that can be imported to other **FPEtool** procedures. What makes **FREEBURN** unique among fire-file generation procedures is that *the procedure* calculates the heat release rate. Up to 5 independent fuels may be combined in the resulting heat release rate. Only one fuel must be designated as initially burning. Piloted- and auto-ignition of target fuels can be predicted from radiative heating; the target fuels must be located outside of convectively heating flow field.

### 4.2.2 Theory

There are three ignition criteria: surface temperature, radiative flux, and exposure time. In addition to ignition criteria, the procedure also considers the fuel separation distance, the width of the burning fuel items, the radiative fraction of the fuel heat release rate, and the thermophysical properties of the non-burning fuels.

#### *The target fuels:*

The easiest method to use, but one that requires expert judgement, casts the ignition criteria in terms of exposure time. The user simply identifies the time that is to elapse before burning begins.

$$\dot{Q}''_{incident,target}(t) = \sum_{j=1}^5 \frac{\dot{Q}_{emission_j}(t)}{4\pi r_{j-target}^2} \quad (1)$$

$$r_{j-target} = x_{j-target} + w_j/2 \quad (2)$$

Choosing an incident radiative flux is the second easiest method--in terms of computational time--for determining whether ignition of the target will occur. Ignition can occur when the combined radiative flux from all sources exceeds the critical incident flux of the target fuel. The critical incident flux for ignition of the non-burning fuel is given by the user. Guidance on what constitutes appropriate flux levels for particular fuels may be found in procedure **RADIANT IGNITION of a NEAR FUEL**, Section 3.12. The combined radiative flux from the flames are summed per eq (1). The distance from the center of the flame to the target is expressed as  $r_{j-target}$  in eq (2) or as the Separation distance in Figure 4.2.3. In eq (2)  $r_{j-target}$  is the sum of the distance between objects, ( $x_{j-target}$ ) plus the half-width of the burning fuel,  $w_j/2$ . The incident radiative flux at the target fuel is that fraction of the all radiative emissions from all flames that is received upon the target surface divided by the exposed target surface area. This fraction decreases as the square of the separation distance. The rapid decline of this fraction is a consequence of idealized radiative emission--uniform dispersal of energy across the surface of concentric spheres centered about the point source. As the target fuel is placed

at greater distances from the flames, the spherical surface area onto which the same amount of emitted power is dispersed increases as  $4\pi r^2$ ; this is the origin of the denominator in eq (1).  $Q_{\text{emission},j}$  is the fraction of heat release rate produced by source,  $j$  that is radiatively dispersed.  $Q_{\text{emission},j}$  is the product of the fire heat release rate and the fire's radiative heat release fraction,  $\chi_R$ .

$$T_{\text{surface}}(t_i) = T_{\text{surface}}(t_0) + \frac{1}{\sqrt{\pi k \rho c_v}} \int_0^{t_i} \frac{\dot{Q}_{\text{incident,target}}(s)}{\sqrt{(t_i - s)}} ds \quad (3)$$

Calculating ignition time by specifying a surface temperature capable of sustaining ignition is the most time consuming of three ignition criteria choices, but this choice also considers more fuel properties. The method however, is not without assumptions (see Section 4.2.3). The computations in eq (3) are based upon an energy balance. The energy balance is applied to a control volume that includes the exposed target surface and extends to an arbitrary depth below this surface. The actual depth of the control volume is relative, as long as the target remains thermally thick (see Section 3.16.2). The energy incident upon the surface of the target fuel is calculated from eq (1). Energy leaves the surface control volume by one-dimension heat conduction into the fuel. The energy remaining in the control volume heats the target fuel and raises the surface temperature. These three energy terms are combined, in a simplified manner, according to conservation of energy rules to produce eq (3).

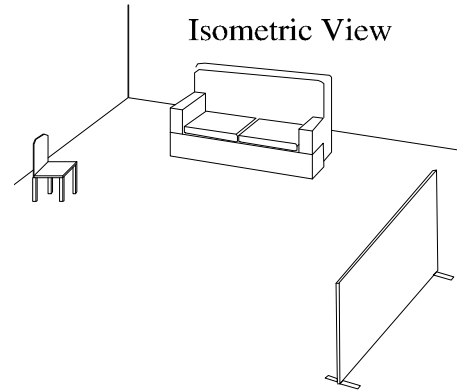


Figure 4.2.1. Illustration of fuel package geometries for **FREEBURN**

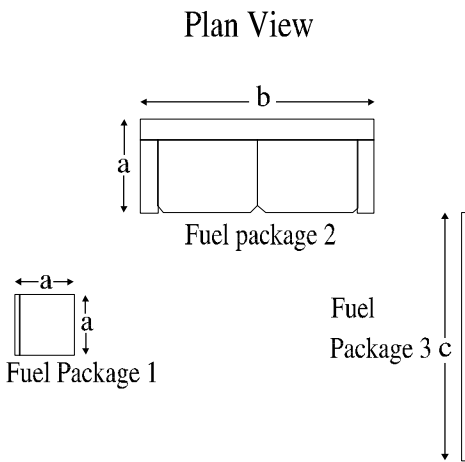


Figure 4.2.2. Fuel package widths for **FREEBURN**

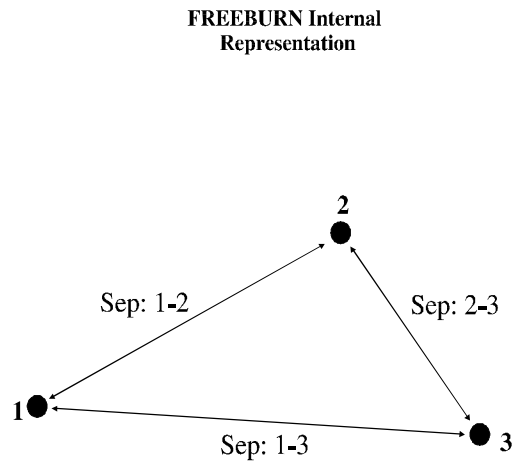


Figure 4.2.3. **FREEBURN** internal representation of fuel package separation distances

The calculation proceeds by determining the integral in eq (3) for increasingly larger times until the right-hand side of the equation equals the specified ignition temperature ( $T_s(t_i)$ ). The time of ignition ( $t_i$ ) is determined when the surface temperature,  $T_s$ , equals the user-specified ignition temperature. The effect thermal inertia ( $k\rho c_v$ ) has on the time to ignition, given that incident radiation is constant, is to reduce time to ignition with decreasing thermal inertia

***The radiating fuels:***

The user specifies a fire width for items indicated to be initially burning. This width is divided in half by the procedure and designated,  $w_j/2$ , the distance from the assumed point source of the fire to the edge of the burning object. To illustrate these parameters, Figures 4.2.1 - 4.2.3 were presented. In Figure 4.2.2, the user can enter a width of 'a' for fuel package 1, a width of  $(4a \cdot b/\pi)^{1/2}$  for package 2 (representing the diameter of a circle with equivalent area), and a width of 1 mm (representing a wall-fire flame sheet) for package 3. Figure 4.2.3 illustrates how **FREEBURN** considers user-specified separation distances.

As the size of an actual fire increases, the fire area usually increases too. **FREEBURN** accounts for a growing fire area by assuming a 1100 kW/m<sup>2</sup> (100 BTU/s/ft<sup>2</sup>) burning rate [2]. This burning rate flux, when divided into the fire heat release rate, yields a fire area. **FREEBURN** proceeds through a two-step process to arrive at its estimate of the distance from the edge of the burning fuel to the assumed flame point-source [parameter  $w_j/2$  in eq (2)]. First, **FREEBURN** takes the minimum radius from the area determined by either the preceding method or the user-specified fuel width. This radius is then limited to no greater than 0.5 m (1.64 ft). This half-meter limitation reflects the assumption that larger fires are optically thick and the flames will not allow radiation to pass through longer pathlengths.

After a fuel item ignites, the heat release rate for that item proceeds according to the fire file. When more than one item is burning, the total heat release rate of all fires is the addend of the actual heat release rate of all individual fires.

a	Dimension of an arbitrary fuel item (m)
b	Dimension of an arbitrary fuel item (m)
$c_v$	Target fuel heat capacity (kJ/(kg·K))
k	Target fuel thermal conductivity (kW/(m·K))
$Q''_{incident, target}(t)$	Total incident radiative flux from all burning fuels (kW/m <sup>2</sup> )
$Q''_{emission, j}$	Radiative component of burning fuel's heat release rate (kW/m <sup>2</sup> )
$r_{j-target}$	Distance from the center of burning fuel to the edge of the target fuel (m)
s	Dummy variable of integration
t	Time (s)
$t_i$	Time at ignition (s)
$T_{surface}(t_i)$	Surface piloted-ignition temperature (K)
$T_{surface}(t_o)$	Surface initial temperature (K)
x	Distance from edge of the burning fuel to the edge of the target fuel (m)
$w_j$	Width (or equivalent diameter) of the burning fuel (m)

$\rho$  Target fuel density (kg/m<sup>3</sup>)

### 4.2.3 Program Notes

There is no burning rate enhancement, once an item is 'ignited,' it burns as described in the fire file.

Items are assumed to be circular with an effective point of radiative emission located at the center of this circle. The circle area is initially determined from user specifications, but the **FREEBURN** can increase this area up to a radius of 0.5 m based upon an assumed heat release rate flux of 1100 kW/m<sup>2</sup>.

Auto-ignition may be predicted with this method as well. To accomplish this prediction, the target fuel auto-ignition temperature should be substituted for the piloted-ignition temperature. Values of fuel auto-ignition temperatures can be found in handbooks (see Section 1.4).

Specifying time is a zeroth-order criterion for estimating ignition, but a useful tool nonetheless for corroborated fire reconstruction work.

The incident energy flux is a first-order criterion for estimating ignition, it works similar to **RADIANT IGNITION OF A NEAR FUEL**.

The surface temperature is a second-order criterion for estimating ignition. This calculation considers the fuel to be a semi-infinite slab experiencing heat loss from the radiatively heated surface by one-dimensional conduction into the interior. There is no convective cooling modeled from the heated surface of the target fuel, nor is there consideration of emissive, reflective or transmittive radiation from or through the fuel.

As heat transfer between burning and non-burning items is via radiation, a path must exist between source and target fuel items for light to travel upon. This path may involve direct line-of-sight, as reflection and transmittance are not modeled.

It is recommended that when possible, values for  $k\rho c_v$  and  $T_{\text{ignition}}$  be obtained from the same experiment [3].

Eq (1) is more accurate as the distance from the burning fuel item to the target fuel item,  $r_{j\text{-target}}$ , increases; this coincides with the assumption of a point-source radiation term. Where the ratio of the distance to the target,  $r_{j\text{-target}}$ , over the radius of the fire,  $r_j$ , is less than 10, a small error exists. The errors are such that the actual heat flux from the burning fuels is greater than that simulated with the point-source assumption of **FREEBURN**. The magnitude of the error is no more than 7% for values of this distance ratio that are as small as 2.0 [1].

Ignition by surface temperature calculation assumes the fuel surface does not emit or reflect radiant energy, nor does the fuel material transmit any radiation through its contents. All incident energy is absorbed. For black-body fuels with piloted-ignition temperatures of 300 °C, roughly 6.5 kW/m<sup>2</sup> of

radiant energy emitted from the fuel surface is ignored.

Ignition by surface temperature calculation assumes the fuel control volume is heated as a semi-infinite slab receiving one-dimensional heat conduction. Heat losses from the fuel edges are not assumed. In some simulations with long ignition times, the temperature pulse into the fuel can reach the back surface. This penetration time can be calculated from eq (9) in Section 3.16. The implications of predicting ignition after the penetration time are dependent upon the boundary conditions at the back surface and the magnitude of the incident flux. For simulations where the incident radiative energy brings the target fuel surface temperature near--but not above--the ignition temperature, an insulated back surface can result in actual exposures igniting that will not be predicted by **FREEBURN**. This argument, however, does not consider the cooling influences of target fuel surface reradiation.

#### 4.2.4 Program Interface

The main user-input screen for **FREEBURN** appears in Figure 4.2.4; other menu screens exist for defining the ignition criterion. An explanation of the input parameter names is provided below and in the three figures of Section 4.2.2.

```

Use arrow keys to move cursor to the item to be edited, then type new
value and press Return (Enter) or F1 for help.

[Press F10 to change data set]
                                WIDTH (mm )   IGNITED AT START (Y/N)
                                RADTN (%)
                                CRIT. IGN.
FUEL PACKAGE NAME             BURN FILE
                                NAME
                                |           |           |           |
1 CHAIR                        MODERATE 750      35   0           |           |
2 SOFA                         FAST.FI 1950     35   0   600        |           |
3 WALL                         UFAST.FI 1      35   0 2000 900 750  |           |
4 NULL                         NONE        0      35   0   0   0   0   |           |
5 NULL                         NONE        0      35   0   0   0   0   0   |           |
> POSITION THE CURSOR HERE AND PRESS ENTER WHEN DONE EDITING.

```

Figure 4.2.4. **FPEtool** sub-menu of the **FREEBURN** procedure

#### INPUT

Fuel package name	Text for user's edification only
Burnfile name	Valid DOS file name. These files are produced in <b>MAKEFIRE</b> .
Width	Width (or equivalent diameter) of the burning fuel (mm or in.)
Radtn %	Percentage of the actual fire heat release rate dispersed via radiation
Critical ignition criteria	User specifies a `1', `2', or `3' depending upon definitions below
1) Ignition time	Time when ignition is prescribed to begin (s)
2) Ignition energy	Total incident flux from all burning fuels igniting target (kW/m <sup>2</sup> )
3) Ignition Temp.	

kpc	Fuel thermal inertia ( $\text{kW}^2\cdot\text{s}/(\text{m}^4\cdot\text{K}^2)$ )
$T_{\text{ignition}}$	Fuel auto- or piloted-ignition temperature ( $^{\circ}\text{C}$ or $^{\circ}\text{F}$ )
Separation	Shortest distance between fuel items (mm or in.)
Ignited at start	Indicates if fuel is burning at start of the simulation
Dataset file name	Valid DOS name for the <b>FREEBURN</b> input dataset file (.DAT)
Output file name	Valid DOS name for the <b>FREEBURN</b> output fire file (.FIR)
Output file description	Text string for user identification only
Time limit	Maximum time for the simulation to continue calculating (s)
Display interval	Interval at which output is written to the video display and printer (if so activated). Fire output file update is different; it occurs each second (s)

### *OUTPUT*

Time	(s)
Rate of heat release	(kW)
Rate of mass loss	(g/s)
Graphical Output	
$Q_{\text{fire}}$	(kW)
$\dot{m}_{\text{fire}}$	(g/s)

### **4.2.5 References**

- [1] Modak, A. T., "Thermal Radiation from Pool Fires," *Combustion and Flame*, 30,252-265, 1977.
- [2] Nelson, H.E., "FPETOOL: Fire Protection Engineering Tools for Hazard Estimation," Nat. Inst. Stand. Tech. (U.S.), NISTIR 4380, Gaithersburg, MD 20899, 1990.
- [3] Quintiere, J.G. "A Simplified Theory for Generalizing Results from a Radiant Panel of Flame Spread Apparatus," *Fire and Materials*, Vol 5 (2), pp. 52-60, 1981.

## 4.3 LOOK-EDIT

### 4.3.1 Application

**LOOK-EDIT** provides the user with a method to examine and change existing fire files (files with \*.FIR extensions). The utility of this procedure lays in its provision for quick, visual examination of fire files for appropriate shape and trends as well as correct heat release rate at peak values and endpoints. The function may be used to edit fire files line-by-line.

### 4.3.2 Theory

There is no mathematical theory. This procedure contains only instructions that allow the user to:

- pick a fire file (\*.FIR) for editing,
- display the fire file as text,
- add, modify and delete points on a line-by-line basis,
- edit the file description,
- make changes to the file permanent, and
- graphically examine the fire file.

### 4.3.3 Program Notes

This routine creates a DOS compatible fire file.

The 3 columns of data must terminate with a line containing -9,-9,-9.

The numerical output consists of only 3 columns of data; (time in seconds, HRR in kW and pyrolysis rate in g/s). At the bottom of the three columns of data are two text lines. The first line contains the file name and date; the second line contains user-specified text up to 40 characters in length that can be used for describing the file.

### 4.3.4 Program Interface

#### *INPUT*

Time	Time associated with the actual heat release rate and fuel pyrolysis rate (s)
Heat release rate	Fire heat release rate ( $Q_{\text{fire}}$ ) at time specified in previous line (kW)
Pyrolysis rate	Fuel pyrolysis rate associated with time on the first line $Q_{\text{fire}}/\Delta H_c$ ; (g/s)

## *OUTPUT*

Tabular	Tabular display of the three column of data (time, $Q_{\text{fire}}$ , and $\dot{m}_{\text{fuel}}$ )
Graphical	Graphical display of the heat release rate versus time
File	Allows the user to copy an existing fire file to a file of a new name.

## 4.4 MYFIRE

### 4.4.1 Application

This procedure creates a 'fire' file. This fire file may be imported to other simulation procedures within **FPEtool** (e.g. **UPPER LAYER TEMPERATURE, FREEBURN, FIRE SIMULATOR...**). The routine contains no significant equations. It simply provides the user with the capability of designing a fire by entering a series of discrete points linearly approximating a fire history.

### 4.4.2 Theory

The input is arranged to allow the user to enter data in terms of either heat release rate or fuel pyrolysis rate. The fuel's heat of combustion is then used to calculate the unspecified parameter.

$$\dot{m}_{pyrolysis} = \frac{\dot{Q}_{fire}}{\Delta H_{c,fuel}} \quad (1)$$

If only one parameter is specified in the input selection (see the first two options in Section 4.4.4), then the  $\Delta H_c$  (kJ/g) is calculated from an engineering method [1] that considers the percentage of wood contained in the fuel (eq 2).

$$\Delta H_{c,fuel} = (100 - \% Cellulosic) * 32.6 \frac{kJ}{g} + (\% Cellulosic) * 16.3 \frac{kJ}{g} \quad (2)$$

$\Delta H_c$	Heat of combustion (kJ/g)
$\dot{Q}_{fire}$	Fire heat release rate (kW)
$\dot{m}_{pyrolysis}$	Fuel pyrolysis rate (g/s)
% Cellulosic	Mass % of fuel composed of wood products

### 4.4.3 Program Notes

Constant heat of combustion ( $\Delta H_c$ ) is assumed. This is not always the case, even with homogeneous fuels, but the variation is generally small.

Estimation of  $\Delta H_c$  is a first-order approximation. Certain plastics have heats of combustion lower than that of cellulose; examples include polyethylene blends that contain more than 36% chlorine by mass and polyvinyl-chloride.

#### 4.4.4 Program Interface

##### INPUT

Choose one of the following modes:

q only (rate of heat release)

% of <b>FREEBURN</b> cellulosic fuel	Used to estimate $\Delta H_c$
File name for .FIR file	Valid DOS name for the fire file
Text description of fire $\leq 80$ characters	
Time	(s)
Heat release	(kW)

m only (rate of mass loss)

% of freeburn fuel that is cellulosic	Used to estimate $\Delta H_c$
File name for .FIR file	Valid DOS name for the fire file
Text description of fire $\leq 80$ characters	
Time	(s)
Mass loss	(g/s or lb <sub>m</sub> /min)

q and m (rate of heat release and rate of mass loss)

File name for .FIR file	Valid DOS name for the fire file
Text description of fire $\leq 80$ characters	
Time	(s)
Heat release	(kW)
Mass loss	(g/s or lb <sub>m</sub> /min)

q and H<sub>c</sub> (rate of heat release and heat of combustion)

File name for .FIR file	Valid DOS name for the fire file
Text description of fire $\leq 80$ characters	
Time	(s)
Heat release	(kW)
Heat of combustion	(kJ/g or BTU/lb <sub>m</sub> )

m and H<sub>c</sub> (rate of mass loss and heat of combustion)

File name for .FIR file	Valid DOS name for the fire file
Text description of fire $\leq 80$ characters	
Time	(s)
Mass loss	(g/s or lb <sub>m</sub> /min)
Heat of combustion	(kJ/g or BTU/lb <sub>m</sub> )

## *OUTPUT*

Time	(s)
Rate of heat release	(kW)
Rate of mass loss	(g/s)

### **4.4.5 References**

- [1] Nelson, H.E., "FPETOOL: Fire Protection Engineering Tools for Hazard Estimation," Nat. Inst. Stand. Tech. (U.S.), NISTIR 4380, Gaithersburg, MD 20899, 1990.

## 4.5 RATES

### 4.5.1 Application

This procedure does not create a `fire,' but rather contains data from experimentally measured fires that provides the user with numerical values for the `fire growth rate parameter ( $\alpha$ ) of **FORMULA**.

### 4.5.2 Theory

This list was assembled by Nelson [1], and is included in NFPA 92B [2].

### 4.5.3 Program Notes

The rates are a compilation of empirical equations `curve-fitted' to experimentally recorded heat release rate histories of numerous fuel items [2].

The rates described herein may not necessarily represent the burning behavior of items with similar, but not identical, characteristics of the original fuel.

### 4.5.4 Program Interface

*INPUT* -- none

*OUTPUT*

kW/m<sup>2</sup> of floor area    Fire heat release rate per floor area covered by fuel (kW/m<sup>2</sup>)

Growth Rate                      Fire growth rate parameter; see  $\alpha$  in Section 4.1.2 (kW/s<sup>2</sup>)

Fuel Description                      Text provided by the user

### 4.5.5 References

- [1] Nelson, H.E., "Fire Safety Evaluation System for NASA Office/Laboratory Buildings," Nat. Bur. Stand. (U.S.), NBSIR 86-3404, Gaithersburg, MD, 1986.
- [2] National Fire Protection Association, NFPA 92B, NFPA, Quincy, MA 02269-9101, pp. 28-30, 1991.



## 5 FIRE SIMULATOR

### 5.1 Application

This procedure consists of a single-room, two-zone, mathematical model simulating the effects created by pre- and post-flashover fires within a room equipped with a sprinkler, heat and/or smoke detector and having multiple ventilation options. The procedure is designed to provide easy-to-obtain, quick answers for fire safety professionals.

The following effects are incorporated within the model:

- temperature and smoke properties (O<sub>2</sub>, CO<sub>2</sub> and CO gas concentrations and optical density)
- heat transfer through room walls and ceilings
- sprinkler/heat and smoke detector activation time
- heating history of sprinkler/heat detector links
- smoke detector response
- entrainment of hot smoke into ceiling jet for sprinkler activation calculations
- ceiling jet temperature and velocity history at specified radius from the fire
- sprinkler suppression rate of fire
- time to flashover
- post-flashover burning rates and duration
- doors and windows which open and close
- forced ventilation

In addition, the following fire features were provided:

- fire files can be created at time of data entry
- fire files can be imported with 'point-and-click' operation
- post-flashover ventilation-limited combustion
- variable lower flammability limit
- variable smoke emissivity
- generation rates of CO/CO<sub>2</sub> pre- and post-flashover

The user may also halt the program at any user-specified time, and after sprinkler activation, and after smoke detector activation. In addition, the program will halt at flashover. At each of these halts the user may change the ventilation specifications.

### 5.2 Theory

**FIRE SIMULATOR** calculates the development of the smoke layer with the same two ordinary differential equations **ASETBX** uses. **FIRE SIMULATOR** builds however, upon **ASETBX** by considering the following features:

flashover  
 neutral plane, smoke layer interface and vent mass flow rate  
 removal of upper layer air by mechanical ventilation  
 entrainment  
 fire dimensions (diameter, elevation)  
 combustion chemistry, pre-flashover  
 combustion chemistry, post-flashover  
 post-flashover burning rate  
 carbon monoxide generation  
 sprinkler suppression  
 smoke detector activation  
 heat losses from the smoke to the compartment barriers

### 5.2.1 Flashover Definition

Flashover is '...generally defined as the transition from a growing fire to a fully-developed fire that involves all combustible items in the compartment' [22]. Flashover is a sufficiently complex phenomenon such that no single measurement is universally associated with its occurrence [7]. It is a distinct enough event though--that when observed--viewers can settle on the timing of its occurrence. Visually, flashover coincides with what is seen to be the spontaneous ignition of all combustible fuels within the room of fire origin. Flashover in a room with an open door drives the smoke layer towards the floor and large quantities of this smoke, if not flames, issue from the door, often in a pulsing manner. **FIRE SIMULATOR** assumes flashover occurs when the smoke temperature exceeds 600 °C (1112 °F).

### 5.2.2 Neutral Plane Location and Smoke Layer Interface

The neutral plane location is the level where pressure inside the ventilation opening equals the pressure outside the ventilation opening. The smoke layer interface is the level where the bottom of the smoke is found. The distinction between the two is that the neutral plane is measured *at the vent*, while the smoke layer interface can be measured almost anywhere in the room. The smoke layer interface is a characteristic value representing the average smoke level.

**FIRE SIMULATOR** does not allow the neutral plane height to fall below the smoke interface height. The neutral plane height is determined after the smoke-interface height. The smoke layer is determined per eqs (2) and (3) of the **ASETBX ROOM MODEL**. The neutral plane location, however, is determined per eqs (1) and (2) below. It is based upon a wide variety of numerical experiments with **MASS FLOW THROUGH AN OPENING** that showed the neutral plane to be fairly insensitive to vent geometries. The parameter,  $N$  represents that fraction of the opening filled with smoke, as measured from the sill.

$$N = (T - 38^\circ C) * 0.00016 + 0.51, \quad \text{when } T \leq 538^\circ C \quad (1)$$

$$N = (T - 538^{\circ} C) * 0.000036 + 0.59, \quad \text{when } T > 538^{\circ} C \quad (2)$$

### 5.2.3 Vent Mass Flow Rate

Once the neutral plane location is calculated, the vent mass flow rate is determined using eq (4) of Section 3.10. The natural ventilated flow rate is limited though, by the geometry of the vent. This limitation is calculated per the equation in Section 3.17. There can be two openings ventilating smoke in **FIRE SIMULATOR**. One vent is designated 'Inside Opening' and the other 'Outside Opening' (see Figure 5.2.1). The smoke volume, mass and enthalpy flow rates through these 'Inside' and 'Outside' Openings are presented in the program output file described in Section 5.4 under *OUTPUT*.

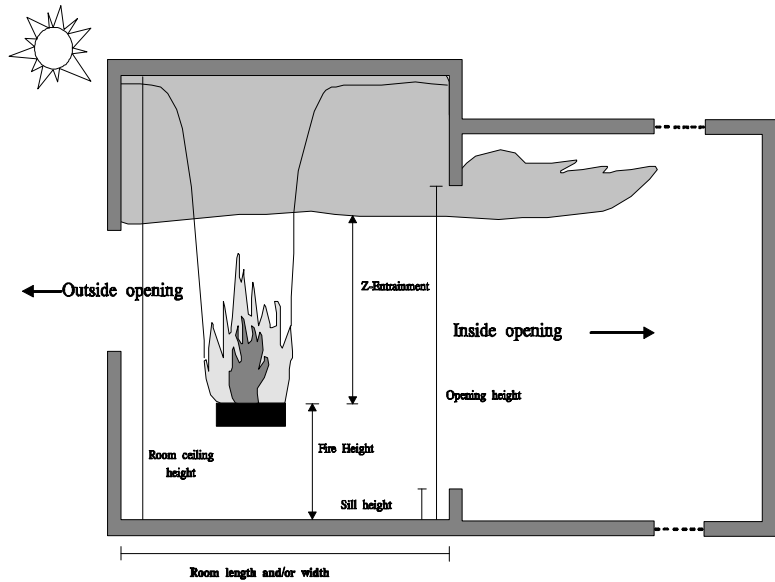


Figure 5.2.1. **FIRE SIMULATOR** geometrical descriptions

### 5.2.4 Entrainment

Entrainment is the phenomenon whereby a stationary fluid or gas is drawn into a current of fluid or gas moving through it. As entrainment proceeds, the downstream current expands in what is called a plume (Section 3.1.2). Plume entrainment is divided into two regions separated by the mean flame height (see Section 5.2.5). Below the mean flame height, entrainment is calculated by eq (3); above the mean flame height eq (4) is used. Both of these entrainment correlations use a point-source fire assumption. If a fire occupies a finite area, this area can affect the amount of entrainment. The point-source plume model [18] compensates for this simplification with the 'virtual origin' ( $z_0$ ) concept. The virtual origin is often located below the elevation of fires having small heat release rates and large-areas, and above the elevation of fires having high heat release rates. The virtual origin can be visualized as the apex of a cone whose surface is formed by the rising, expanding contour of the smoke-filled plume. To determine the virtual origin position one moves its location up or down until the cross-sectional area of the plume superimposes the burning area of the fire. Some assumptions are made in this determination. First, the rate of plume expansion is  $15^{\circ}$  degrees from the vertical (Figure 3.1.0). Second, that an equivalent, circular pyrolysis area of diameter,  $D$ , may be determined by assuming a constant pyrolysis flux rate ( $\dot{m}_f''$ ).

$$\dot{m}_{entrained} = 0.0054 \dot{Q}_C^{\frac{2}{5}} + z_0 \quad (3)$$

$$\dot{m}_{entrained} = 0.071 \dot{Q}_C^{\frac{1}{3}} (z - z_o)^{\frac{5}{3}} [1 + 0.026 \dot{Q}_C (z - z_o)^{-\frac{5}{3}}] \quad (4)$$

### 5.2.5 Fire Dimensions: Diameter, Virtual Origin and Flame Height

The fire diameter, virtual origin and flame height calculations are only exercised pre-flashover. The fire diameter (D) is obtained by using a pyrolysis flux rate representative of wood [10]. The heat release rate per unit area is 1100 kW/m<sup>2</sup> [100 BTU/(ft<sup>2</sup>·s)]. The virtual origin [eq (6b)] is obtained from Heskestad's correlation [19] and was derived from previous work on flame heights. Flame height [eq (6a)] is obtained using another Heskestad correlation [16]; it represents a mean flame height. The mean flame height is that elevation where flames appear 50% of the time. This height is somewhat greater than estimates obtained by eye [16]. The mean flame height corresponds to a temperature of 500 °C; 800 °C is found at the top of the continuous flames [20].

$$D = 2 \left( \frac{\dot{m}_f}{\dot{m}_f'' \pi} \right)^{\frac{1}{2}} \quad (5)$$

$$z_{flame} = 0.083 \dot{Q}^{\frac{2}{5}} - 1.02 D \quad (6a)$$

$$z_o = -1.02 D + 0.083 \dot{Q}_{fire}^{\frac{2}{5}} \quad (6b)$$

### 5.2.6 Compartment Combustion Chemistry, Pre-Flashover

The burning rate of a fuel inside a compartment may be enhanced by energy feedback from the hot smoke, but **FIRE SIMULATOR** and most other zone models do not account for this effect. **FIRE SIMULATOR** can however, account for a reduction in fuel burning rate due to lack of oxygen availability. The fuel burning rate is defined as the rate at which gaseous fuel particles (pyrolyzates) combine with oxygen and are converted into 'normal' combustion products. **FIRE SIMULATOR** assumes CO<sub>2</sub> and H<sub>2</sub>O are normal combustion products.

#### *Oxygen Calorimetry:*

Oxygen is consumed in the combustion process through combination with pyrolyzates. The rate that oxygen combines with pyrolyzates--per quantity of heat released by the fuel--is fairly constant (13,100

kJ/kg O<sub>2</sub>) for a wide variety of fuels. For this wide variety of fuels (notable exceptions being CO, HC≡CH and H<sub>2</sub>C=CH<sub>2</sub>), a conservation of mass balance on oxygen provides a means of calculating the fire heat release rate. This calculational method is called 'oxygen depletion calorimetry' [9] and is used in **FIRE SIMULATOR** to determine when insufficient oxygen prevents combustion of all pyrolyzates. (The pyrolysis rate is stipulated in the fire input file). Oxygen molecules from plume entrained air, the upper layer, and the mechanical ventilation system are respectively included in the oxygen mass balance. If insufficient oxygen is available for complete combustion then the fire heat release rate is limited according to what the available oxygen can support.

**Lower Flammability Limit: (LFL):**

There are two properties regarding oxygen that are necessary to maintain combustion, the total available mass (as discussed in the previous paragraph) and the concentration. The importance of this latter property becomes clearer when considering a match burning in a large warehouse. There may be more than enough oxygen within the confines of the warehouse to support complete consumption of the match, but the oxygen could be dispersed in such dilute concentrations as to be ineffective at sustaining a flame.

The LFL is one method of addressing when oxygen concentrations become too low to support combustion. Strictly speaking, the LFL applies to premixed, not diffusion flames. However the concept has enough versatility to have been successfully used in previous editions of **FPEtool**, as well as other 2-zone fire models (**CFAST** [15], **FIRST** [14]). The LFL is a rather insensitive function of fuel type in residential/office environments owing to the predominance of wood and plastic fuels. The LFL is sensitive to temperature though, and **FIRE SIMULATOR** models this phenomenon through eq (7). At ordinary room temperatures the LFL is assumed to occur below 10% oxygen by volume. At higher temperatures, such as post-flashover, the increased reaction efficiency is simulated by dropping the LFL to 2% oxygen by volume.

$$LFL_{O_2} = \max\left(LFL_{T_\infty} - \frac{(LFL_{T_\infty} - LFL_{T_{fo}})}{(T_{fo} - T_\infty)}(T - T_\infty), LFL_{T_{fo}}\right) \quad (7)$$

When, where and how **FIRE SIMULATOR** determines the fire heat release rate is a multi-step process. The rules used to calculate the heat release rate are (like the processes in nature) interdependent, yet remain a simplification of a complex process. First, **FIRE SIMULATOR** determines whether the heat release rate--as stipulated by the input fire file--is fuel-limited or oxygen-limited. The fuel-limited heat release rate is simply the value from the input fire file. The oxygen-limited heat release rate is obtained from oxygen calorimetry of available oxygen. The limiting heat release rate is then used as the source term, Q in the coupled-differential eqs (2) and (3) of **ASETBX ROOM MODEL**.

Oxygen availability is determined differently in the pre-flashover regime than in the post-flashover regime. Pre-flashover, an oxygen mass balance is conducted on three control volumes. First, oxygen is sought from the ambient air entrained into the fire plume. If insufficient, then oxygen is sought from that contained in the upper, smoke layer. Two conditions are checked before oxygen from the

smoke layer is used to support combustion. First, the mean flame height must extend into the smoke layer, and second the oxygen concentration must be greater than its LFL for that temperature. If the oxygen available in the upper, smoke layer is insufficient to complete combustion, then oxygen is sought from the mechanical ventilation system. If the available oxygen is still insufficient then the fire heat release rate is limited to that what is sustainable. Post-flashover, available oxygen is sought from two sources. The first source is from air drawn through the natural vent openings (Section 3.17 **VENTILATION LIMIT**) and the second source is mechanical ventilation. No plume is modeled post-flashover; the smoke layer is driven down almost to the floor and gases are assumed well mixed. The fire is extinguished if the heat release rate is less than 0.1 kW for more than 5 consecutive seconds.

Oxygen concentration in the smoke layer is computed using mass conservation eq (8). Oxygen mass into the smoke-layer control volume comes from the plume [eq (10)]. Mass out of the smoke layer leaves either through the inside or outside opening (Figure 5.2.1) or mechanical ventilation duct [eq (11)]. No oxygen generation is assumed eq (12); oxygen depletion is accounted for with eq (13).

$$\frac{d[m_{O_2}]}{dt} = \dot{m}_{O_2,in} - \dot{m}_{O_2,out} + \frac{\text{rate of } O_2 \text{ mass}}{\text{Generation}} - \frac{\text{rate of } O_2 \text{ mass}}{\text{Depletion}} \quad (8)$$

$$\frac{d[m_{O_2}]}{dt} = \frac{\dot{m}_{O_2,t+\Delta t} - \dot{m}_{O_2,t}}{(t + \Delta t) - t} \quad (9)$$

$$\dot{m}_{O_2,in} = \dot{m}_{entrained} * 0.23 \frac{\text{kg } O_2}{\text{kg air}} \quad (10)$$

$$\dot{m}_{O_2,out} = \dot{m}_{O_2,natural vents} + \dot{m}_{O_2,mechanical vents} \quad (11)$$

$$\frac{\text{rate of } O_2 \text{ mass}}{\text{Generation}} = 0.0 \quad (12)$$

$$\frac{\text{rate of } O_2}{\text{Depletion}} = \dot{Q}_{fire} \left( \frac{\text{kg } O_2}{13,100 \text{ kJ}} \right) \quad (13)$$

### **Carbon Monoxide Generation:**

**FIRE SIMULATOR** considers the fuel be a generic composite of plastic and wood; this presumed mix represents fuels present in most office/residential/commercial occupancies. From this fuel mixture, combustion is assumed to produce 50 % molar product water and 50 % molar product

carbon species. The two carbon species of combustion that **FIRE SIMULATOR** accounts for are CO<sub>2</sub> and CO.

$$CO \& CO_2 \text{ Volume \%} = \frac{(100 - O_2\% - N_2\%)}{2} * [1 + (0.61 * 1 - \Delta H_c \text{ FACTOR})] \quad (14)$$

$$\Delta H_c \text{ FACTOR} = \text{maximum}(0, \text{minimum}(1, \frac{\Delta H_c - 17,000}{17,000})) \quad (15)$$

$$\frac{\text{Molar Generation}}{\text{Rate of CO}} = \left( \frac{CO \& CO_2}{\text{Volume \%}} \right) * \left( \frac{\text{Moles}}{\text{Pyrolyzates}} \right) \left( \frac{\chi_{CO/CO_2}}{1 + \chi_{CO/CO_2}} \right) \frac{\dot{Q}_{fire}}{\Delta H_c} \quad (16)$$

$$\frac{\text{Molar Generation}}{\text{Rate of CO}_2} = \left( \frac{CO \& CO_2}{\text{Volume \%}} \right) * \left( \frac{\text{Moles}}{\text{Pyrolyzates}} \right) \left( \frac{1}{1 + \chi_{CO/CO_2}} \right) \frac{\dot{Q}_{fire}}{\Delta H_c} \quad (17)$$

While the ratio of carbon atoms predicted to form CO versus those atoms predicted to form CO<sub>2</sub> ( $\chi_{CO/CO_2}$ ) is calculated from a user input (see CO/CO<sub>2</sub> molar ratios in Sections 5.4.1 and 5.4.2), the number of total carbon atoms formed from combustion is calculated from the oxygen depletion level. This fact is seen from eq (14) where the N<sub>2</sub> concentration is assumed to be constant at 79%. The remainder (21% - O<sub>2</sub>% is divided by 2 to account for the half molar product of water. Carbon monoxide is not a significant product of complete combustion and only a minor constituent in the pre-flashover burning regime, nonetheless is considered because it is highly toxic and generated in lethal concentrations post-flashover. The reasons for higher CO generation in post-flashover appear to be thermodynamic; higher temperatures and reduced oxygen concentrations in the post-flashover regime favor CO production rates to those in pre-flashover. Current research work in this area is continuing [21,12,13]. The default values for the CO/CO<sub>2</sub> molar ratio parameter ( $\chi_{CO/CO_2}$ ) represent best estimates for composite fuels [11].

### 5.2.7 Post-Flashover Burning Rate

In pre-flashover, when the fire size is limited it usually due to a lack of available oxygen from a shortened plume. The plume is shortened by the descending smoke layer. In post-flashover the fire size is also limited by the available oxygen, but the cause is due to a lack of ventilation area, not plume entrainment. The ventilation limit imposed on the heat release rate is described in **VENTILATION LIMIT** (Section 3.17) and eq (21).

#### ***Post-Flashover Duration:***

The post-flashover duration is determined before **FIRE SIMULATOR** begins the first post-flashover

time-step. The first assumption is that all exposed fuels will burn. The post-flashover burning duration is divided into three regimes [10]. The parameters available to the user for influencing post-flashover duration are: fuel thickness, fuel load density, fuel orientation (whether vertical or horizontal), the percentage of fuel burned and the heats of gasification ( $L_g$ ) and combustion ( $\Delta H_c$ ). The distinction between horizontal and vertical fuels merely serves as a useful categorization to the user; there is no advantage assigned to fuel orientation within the simulation.

After receiving user-specified, post-flashover inputs, the program calculates the flashover duration. These calculations proceed in successive steps, looking at the first 300 seconds, the next 900 seconds and finally an open-ended time frame. Post-flashover will last 300 seconds if any fuel thickness is described with a dimensional thickness less than or equal to 6.4 mm (1/4 inch). Post-flashover will last 1200 seconds if any fuel allotment has a dimensional thickness greater than 6.4 mm and less than 25.4 mm (1 inch). For fuels over 25.4 mm thick an open-ended duration is calculated per (19). The term,  $Q_{fuel}$  in eq (19) is determined from eq (22) where  $Q_{fuel, initial}$  is determined from eq (20). The post-flashover fuel burning rate is the lesser of the fuel-limited eq (18) or the vent-limited eq (21) burning rate.

### ***Post-Flashover Heat Release Rate ( $Q_{fire}$ ):***

The rate of heat released by the post-flashover fire depends upon the user specified and model calculated parameters appearing in eqs (18), (20) and (21). The parameters available to the user for influencing the post-flashover heat release rate are the heat of gasification ( $L_g$ ), the heat of combustion ( $\Delta H_c$ ), the amount of exposed fuel area ( $Area_{fire}$ ) and the ventilation opening sizes. These may be changed at the flashover halt. The parameter that the user can not alter is  $Q''_{incident}$ , the combined radiative and convective heat flux onto the unburned fuel from the fire.  $Q''_{incident}$  is 80 kW/m<sup>2</sup> during ventilation limited burning, 60 kW/m<sup>2</sup> during fuel controlled burning. From eq (18), it can be seen that the fuel-limited, post-flashover heat release rate ( $Q_{fire}$ ) can differ among each of the three regimes due to differences in  $Q''_{incident}$  and exposed fuel surface area.

$$\dot{Q}_{fire_{FO}} = \frac{\dot{Q}''_{incident} Area_{fire} \Delta H_c}{L_{g,work}} \quad (18)$$

$$t_{duration_{post-flashover}} = \frac{Q_{fuel, remaining}}{\dot{Q}_{fire}} \quad (19)$$

$$Q_{fuel, initial} = FuelFlux * Area_{fuel} * (\% Fuel Burned) * \Delta H_c \quad (20)$$

$$\dot{Q}_{fire_{VL}} = 3000 \frac{kJ}{kg} \cdot \sum_{i=1}^n \left( \frac{1}{2} A_{o_i} \sqrt{H_{o_i}} \right) \frac{kg}{s} + \dot{m}_{mechanicalventilation} \quad (21)$$

$$Q_{fuel, remaining} = Q_{fuel, initial} - \int_0^{300} \dot{Q}_{fire, 6mm} dt - \int_{300}^{1200} \dot{Q}_{fire, 25mm} dt \quad (22)$$

$$m_{consumed} = \frac{1}{\Delta H_c} \int_0^{t^2} \dot{Q}_{fire}(t) dt \quad (23)$$

Once the fire heat release rates for each post-flashover time stage are determined, they are compared against what heat release rate can be supported by available oxygen, limited accordingly, and summarily returned to the two coupled ordinary differential equations (described in **ASETBX**) that solve for smoke depth and temperature.

**FIRE SIMULATOR** also considers char-forming behavior. Charring is important to the post-flashover burning rate because it inhibits fuel gasification by shielding unpyrolyzed fuel from radiative sublimation. **FIRE SIMULATOR** correlates the amount of charring in post-flashover according to heat of combustion ( $\Delta H_c$ ) using eq (24). Wood and other fuels with low  $\Delta H_c$  are assumed to char more. Wood, with a heat of combustion about 17 MJ/(kg·K) will have a 'working' heat of gasification ( $L_{g,work}$ ) effectively double that of the post-flashover, user-specified heat of gasification ( $L_{g,work}$ ). This simulated charring reduces post-flashover heat release rates eq (18).

$$L_{g,work} = \frac{35,714 kJ}{kg} * \frac{L_g}{\Delta H_c} \quad (24)$$

### Post-Flashover fuel mass consumed ( $m_{consumed}$ ):

The fuel mass consumed within each of the three post-flashover time regimes is determined from eq (23).

## 5.2.8 Sprinkler Activation and Fire Suppression

The sprinkler/detector algorithm considers the entrainment of warm, smokey air into the plume (depicted as condition 2 in Figure 5.2.2). The net result of this entrainment is to accelerate the time to detector activation. The implementation of this warm-air entrainment algorithm does not begin until the hot layer thickness exceeds that of the ceiling jet. Before this point, the temperature and velocity predictions within the jet are identical to those obtained from **SPRINKLER/**

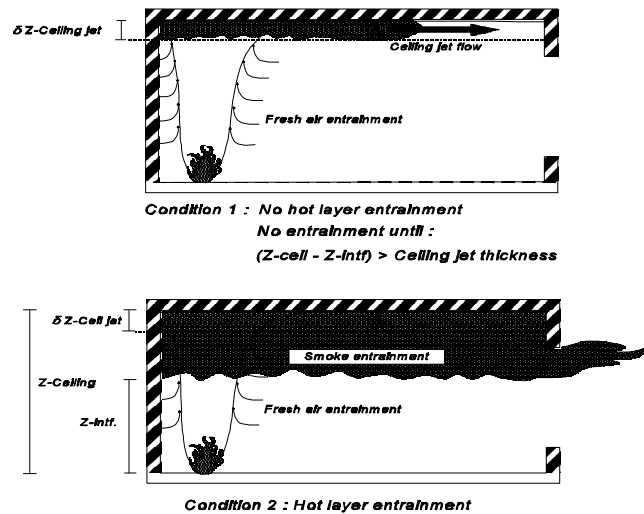


Figure 5.2.2. Warm-air plume entrainment interactions with smoke layer interface elevation

**DETECTOR RESPONSE** [Section 3.14, eqs (3) - (6)]. The ceiling jet thickness is taken as  $0.12(z_{\text{ceiling}} - z_{\text{fire}})$  [24]. Prediction of ceiling jet velocities and temperatures in plumes entraining warm-air keys upon relocating a pseudo-fire ( $\dot{Q}_{\text{intf}}$ ) and a pseudo-fire height ( $z_{\text{intf, pseudo}}$ ) at the base of the smoke layer where warm air entrainment begins. This pseudo-fire height accounts for the virtual origin location (described in Section 5.2.4) and any mass accumulation in the smoke layer during the last time-step. The heat release rate of the pseudo-fire is conceptually equivalent to the energy flow rate in the plume of the original fire where the plume intersects the bottom of the smoke layer. The heat release rate of this pseudo-fire ( $\dot{Q}_{\text{intf},1}^*$ ) is then changed to  $\dot{Q}_{\text{intf},2}^*$  in account of temperature differences between plume gases at smoke-layer interface level and plume gases at flame level. In eq (29), the value  $z_{\text{ceil, pseudo}}$  is used as the value  $H$  in eqs (1) - (6) of Section 3.14.

$$\dot{Q}_{\text{intf},1}^* = \frac{\dot{Q}}{(\rho c_p T)_{\infty}} \sqrt{g z_{\text{intf}}^5} \quad (25)$$

$$\dot{Q}_{\text{intf},2}^* = \left[ \frac{(1 + C_T \dot{Q}_{\text{intf},1}^{*2/3})}{\zeta C_T} - \frac{1}{C_T} \right]^{3/2} \quad (26)$$

$$z_{\text{intf,pseudo}} = \left[ \frac{\zeta \dot{Q}_{\text{intf},1}^* C_T}{\dot{Q}_{\text{intf},2}^{*1/3} [(\zeta - 1)(\beta + 1) + \zeta \dot{Q}_{\text{intf},2}^{*2/3} C_T]} \right]^{2/5} z_{\text{intf}} \quad (27)$$

$$\dot{Q}_{\text{intf}} = \dot{Q}_{\text{intf},2}^* (\rho c_p T)_{\text{warm air}} \sqrt{g z_{\text{intf, pseudo}}^5} \quad (28)$$

$$z_{\text{ceil, pseudo}} = z_{\text{ceil}} - z_{\text{intf},1} + z_{\text{intf, pseudo}} \quad (29)$$

In summary, ceiling jet properties during warm-air entrainment are accomplished with the **SPRINKLER/DETECTOR RESPONSE** algorithm, but with the warm-air properties replacing the normally cool air [eq (28)]. This replacement occurs through a transformation process outlined in Figure 5.2.3.

One other consideration accounts for sprinklers located in positions where jet velocities are not normal. Examples of this circumstance are sidewall sprinklers and sprinklers behind deep beams. In circumstances such as these the ceiling jet velocities can be somewhat reduced. The user may specify what percentage of the nominal ceiling jet velocity is to be used at the sprinkler location. The default value is 50 percent.

### *Sprinkler Suppressed Heat Release Rate:*

The simulated suppression of the fire heat release rate due to water spray-sprinkler action was empirically developed from experimental data [6]. The correlation eq (30) considers a series of sprinkler suppression tests and fits a mathematical curve such that the predicted suppression rate is slower than the slowest measured suppression rate. The predicted suppression rate is also conservative in that some of the experimental fires were shielded from the water spray either by the structure of the crib or by a desk. The time constant ( $\dot{w}''$ ) representing the water-spray density rate is user adjustable.

Suggested values for  $\dot{w}''$  range from 130 sec--a water-spray density of 0.07 mm/s (0.1 gpm/ft<sup>2</sup>)--to 435 sec--corresponding to a water-spray density of 0.13 mm/s (0.2 gpm/ft<sup>2</sup>) [8].

$$\dot{Q}_{fire}(t) = \dot{Q}_{fire}(t_{activation}) \exp\left[\frac{-(t - t_{activation})}{(3\dot{w}'')^{-1.85}}\right] \quad (30)$$

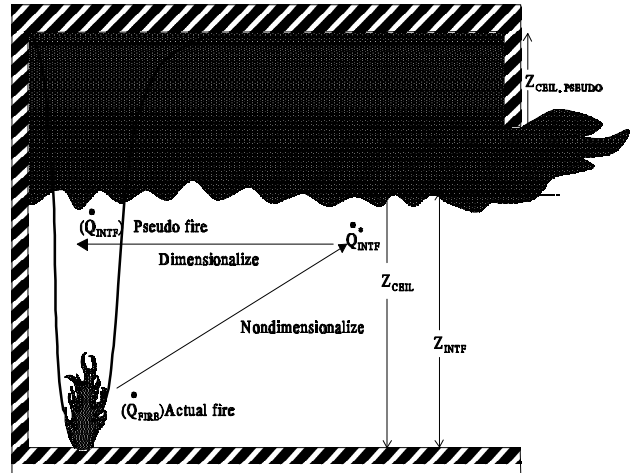


Figure 5.2.3. Conceptual procedure for warm-air plume entrainment

## 5.2.9 Smoke Detector Activation

Simulation of smoke detector activation follows procedures identified for **SPRINKLER/DETECTOR RESPONSE**, except that the smoke detector has an infinitely small response thermal index (resulting in an instantaneous response time). The user can not adjust the jet velocity to account for smoke detector location as was possible with heat detectors, but the user can adjust the activation temperature. The smoke detector activates when the ceiling jet temperature at the radial location of the smoke detector attains the activation temperature. An activation temperature of 13 °C (23 °F) above the initial detector temperature (21 °C) is the default value [17].

## 5.2.10 Heat Losses from the Smoke to the Compartment Barriers

### *Pre-flashover:*

The heat loss from the gas layer to the surfaces of the compartment is calculated after the simultaneous solution of smoke layer thickness and temperature [eqs (2) and (3)] of the **ASETBX ROOM MODEL**]. The process of calculating the heat losses to the room surfaces begins with determining an average wall temperature eq (31). This temperature represents heat contributions from conduction, convection and radiation components. After  $T_{wall}$  is obtained, an overall heat transfer coefficient,  $h_k$ , is calculated. The description on how this heat transfer coefficient is calculated is

found in **UPPER LAYER TEMPERATURE** (Section 3.16). The surface temperature and overall heat transfer coefficient are then combined with smoke temperature to solve for the total heat loss passing into the wall surfaces from the smoke gases eq (32). Heat loss through the ceiling is calculated in the same manner as the heat loss through the walls.

$$T_{surface} = T_{\infty} + \frac{(h_c + 4\epsilon\sigma T^3)(T - T_{\infty})}{h_k + h_c + 4\epsilon\sigma T^3} \quad (31)$$

$$\dot{Q}_{walls_{convection}} = h_k A_{walls} (T - T_{surface}) \quad (32)$$

### **Post-flashover :**

The heat loss calculations post-flashover follow the same process as executed in pre-flashover burning, but with the following changes:

Smoke emissivity is taken as unity

Heat loss from the smoke layer gases is not assumed to occur into those portions of the walls and ceiling that are burning, and the area of these surfaces that are burning is subtracted from the user-defined total-exposed-fuel surface area.

It was discovered [1] that pre-flashover heat losses through the floor were minor relative to the overall heat losses through the upper compartment surfaces. Therefore, convective heat losses per eq (32) are not calculated for the floor. Radiation heat losses to the floor are calculated though. In the radiation calculation, the emissivity ( $\epsilon$ ) is linearly adjusted with temperature in a manner analogous to the LFL adjustment. This adjustment assumes increasing soot-volume fraction with increasing temperature.

$A_o$	Area of the vent opening (m <sup>2</sup> )
$A_{wall}$	Area of surface denoted by subscript, excluding vent areas (m <sup>2</sup> )
$\beta$	Constant related to plume flow (.913) [18]
$C_T$	Constant related to plume flow (9.115) [Zukoski 18]
$c_p$	Heat capacity of gas or fluid denoted by subscript (kJ/kg/ΔK)
$D$	Effective or equivalent fire diameter (m)
$g$	Earth's surface acceleration constant (9.81 m/s <sup>2</sup> )
$h_c$	Convective heat flow coefficient (20 Kw/m <sup>2</sup> )
$h_k$	Overall heat transfer coefficient for surfaces limited by conduction (Kw/m <sup>2</sup> /ΔK)
$H_o$	Height of vent opening-- $z_{soffit} - z_{sill}$ (m)
$\Delta H_c$	Heat of combustion based on CO <sub>2, gas</sub> and O <sub>2, gas</sub> as products (kJ/kg)
$L_g$	Effective heat of gasification (kJ/kg)
$L_{g,work}$	Working heat of gasification (kJ/kg) (a concept used to account for charring)
$LFL_{T,fo}$	Lower flammability limit at flashover temperature
$\dot{m}_{entrained}$	Mass of gas entrained into the plume (kg/s)

$m_i$	Mass of 'i' molecules (kg)
$\dot{m}_f$	Fuel pyrolysis rate (kg/s)
$\dot{m}_f''$	Fuel pyrolysis flux rate (kg/s/m <sup>2</sup> )
$\dot{m}_{out}$	Mass flow rate of hot gas out of the room (kg/s)
$N$	Fraction of ventilation opening filled with smoke measured up from the sill
$Q_{fire}$	Fire heat release rate (kW)
$Q_{fuel}$	Energy available from the fuel after complete combustion (kJ)
$Q_{incident}''$	Incident energy on the fuel (kW/m <sup>2</sup> )
$Q_{intf,1}^*$	Nondimensional actual fire heat release rate (Froude number) <sup>1/2</sup>
$Q_{intf,2}^*$	Nondimensional fire heat release rate at the smoke interface
$Q_c$	Fraction of fire heat release rate convected into the plume (kW)
$Q_{surface}$	Heat lost from the control volume to the room surfaces (except floor) (kW)
$t$	Time (seconds)
$t_{activation}$	Time when the sprinkler/detector activates (sec)
$T$	Temperature of the control volume (smoke) gases (°C or °F)
$T_{\infty}$	Ambient air temperature at simulation start (21 °C)
$T_{FO}$	Flashover temperature (600 °C)
$\Delta T$	$T - T_{\infty}$ (°C)
$\dot{w}''$	Water spray density constant (0.07 mm/s)
$W_{vent}$	Vent width (m)
$z$	Elevation in the fire plume measured from the floor (m)
$z_o$	Fire virtual origin (m)
$\epsilon$	Smoke layer emissivity
$\zeta$	Temperature ratio ( $T_{warm\ gas}/T_{\infty}$ )
$\rho_{\infty}$	Density of gas or fluid denoted by subscript (kg/m <sup>3</sup> )
$\sigma$	Stephan-Boltzmann constant ( $5.676 \cdot 10^{-8}$ W/(m <sup>2</sup> ·K <sup>4</sup> ))
$\chi_{ij}$	Molar fraction of species 'i' to species 'j'

### 5.3 Program Notes

Pre-flashover burning rate is user specified; **FIRE SIMULATOR** can reduce this burning rate due to oxygen starvation but it can not enhance the burning rate due to enclosure effects or radiation feedback.

Radiation feedback, the process where high temperature smoke emits radiative energy sufficient to enhance fuel burning rates, is not considered in pre-flashover burning.

Post-flashover enhancement of CO generation rates are estimated, but a generally accepted post-flashover CO generation model is neither fully modeled nor fully understood at the time of publication.

A reasonable value for the Response Time Index (RTI) of a quick-response (QR) sprinkler is  $50 \text{ (m}\cdot\text{s)}^{1/2}$ .

The plume model does not consider the fire to be a distributed source (the fire is assumed to be a point source). This simplification produces the greatest error when entrainment heights are short. This error is somewhat compensated for with the virtual origin concept (discussed in Section 5.2.5).

Even if doors to a room are closed, very few rooms are 'hermetically sealed.' Providing some ventilation opening in each room to simulate the inevitable voids and cracks present in actual construction is good practice.

Rooms with very tall ceilings ( $r \leq 0.2 \cdot z_{\text{ceiling}}$ ) can nullify the axisymmetric plume assumption because rising smoke can contact the room walls.

Buoyant gas transport time from the fire to the bottom of the layer is not modeled.

Caution should be used when evaluating fires in rooms larger than room sizes existing in verified databases. Caution should also be used in rooms having geometrical aspect ratios or shapes markedly different from room shapes in the experimentally verified databases. The smoke-filling model **CORRIDOR** becomes more appropriate for use than the **FIRE SIMULATOR** model when the aspect ratio of the floor area deviates from a 'square' geometry to that resembling a corridor. It is with the informed judgement of the modeler to determine at what point this transition occurs. The level of detail needed--as well as the physics of the problem--should influence the decision as to what model is used.

The ambient conditions are fixed at standard pressure (101, 325 Pa), ambient gas concentrations (21% O<sub>2</sub>, 79% N<sub>2</sub>) and room temperature (21 °C).

One may account for the reduced pyrolysis rate of charring fuels in post-flashover by increasing the working heat of gasification. This is accomplished by setting the heat of combustion close to the value for wood (~ 17 kJ/g).

It is assumed that the fuels have a  $\Delta H_{c, O_2} \sim 13.1 \text{ MJ/kg oxygen}$ , although this is not the case for CO, ethene (H<sub>2</sub>C=CH<sub>2</sub>) and acetylene (HC≡CH), among select other fuels. The exception for these three fuels is probably due to the multiple aliphatic carbon-bonding. Representative values for the  $\Delta H_{c, O_2}$  may be found in Drysdale [5] or fire safety handbooks (see Section 1.4).

Predicted smoke flow rates may be inaccurate when the fire occurs on an extreme upper or lower floor of a multi-story building due to stack effect.

$\lambda_c$  is a variable representing heat losses from the hot gas layer. These heat losses include convective (eq 32) and radiative losses to the walls and ceiling, as well as radiative losses to the floor. The heat losses associated with  $\lambda_c$  are separate and distinct from the radiative heat losses from the fire ( $\chi_r$ ).

Both  $\lambda_c$  and  $\lambda_r$  are normalized, or divided by, the convective fraction of the fire heat release rate.  $\lambda_r$  is always less than or equal to one.  $\lambda_c$  can be greater than one as in the case of a large fire that peaked and is decaying in strength. If in this case the walls are hotter than the smoke temperature then the walls can return heat to the smoke layer in a quantity greater than the actual fire heat release rate.

$\lambda_{c, \max}$  limits heat loss to the walls. This is used because the heat loss algorithm of eq (32) is correlational and can overestimate wall losses at early times in the fire. Eq (32) is also inappropriate for barriers with high thermal conductivity or low thermal thickness (e.g. glass or metal).

The flame height estimates apply to standard ambient conditions, buoyancy-driven and low-momentum fires. The estimates are valid for  $Q_{\text{fire}}^2/D^5 \leq 1 \cdot 10^{14}$  (Q is in kW and D is in m).

The HVAC input parameter '*ventilation rate*' describes the volume of gases removed from the upper layer of the compartment per hour. The units of volume are measured in rooms; the American customary units for this parameter are therefore '*air-changes-per hour*.' No density compensation between heated and ambient temperature is necessary because the ventilated gases are assumed to be ambient (21 °C) temperature when they arrive at the fan. The air ventilated from the upper layer of the room is considered to be replaced by an equal mass of air into the lower layer. This replacement air is considered to contain '*normal*' concentrations of ambient oxygen. The '*combustion efficiency*' parameter considers how much of the 21% oxygen comprising the replacement air is available for supporting combustion.

The output parameter '*Vision*' refers to the distance through a smoke layer that a person can see approximately 5% of the light emitted from the source.

## 5.4 Program Interface

The simultaneous keystroke '*Control-Q*' will exit a user from any point in the program expecting an alphanumeric input.

**FIRE SIMULATOR** is broken into 5 sub-menu items. These menu items allow the user to:

- Create/Revise a case*
- Run an Existing case*
- Lining Material*
- Hazard Warning*
- Translate to New Format*

The *Create/Revise a case* allows the user to either start a new input file from '*scratch*', or to *Revise an Existing Case*. It is much quicker to revise an existing case. This is accomplished by either '*clicking*' on or typing in an existing input file name. *Run an Existing Case* simply allows the user to execute an existing input file. *Lining Material* allows the user to change or add to the existing



Sidewall	(Y/N)
Jet velocity flow reduction	As a % of unconfined jet velocity
Sprinkler fire suppression	(Y/N)
$\dot{W}_{\rho, \text{sprinkler water}}''$	Water discharge rate (mm/s or gallon/(min·ft <sup>2</sup> ))
Smoke detector response	(Y/N)
Radial distance	(m or ft)
Smoke temperature at detection	(°C or °F)
Sidewall	(Y/N)
Jet velocity flow reduction	As a % of unconfined jet velocity
Fire Characteristics	
Heat of combustion	(kJ/kg or BTU/lb <sub>m</sub> ) [4]
Height at base of flames	Lowest elevation fuel freely entrains air (m or ft)
Extinction coefficient	(m <sup>2</sup> /g or ft <sup>2</sup> /lb <sub>m</sub> )
Flashover temperature	(°C or °F)
Minimum O <sub>2</sub> required for burning	Pre-flashover LFL <sub>Oxygen</sub> (volume %)
Minimum O <sub>2</sub> required for post-flashover	Post-flashover LFL <sub>Oxygen</sub> (volume %)
Fire file	
pre-existing fire file (*.FIR)	Choose existing fire file from specified directory
spontaneously generate fire file	
Time, Q <sub>fire</sub>	Up to 1,500 entries (ESCAPE to finish) (s, kW)
Fire file name	(* .FIR) DOS file name, extension is automatic
Text describing fire file	Text string describing the fire
Freeburn CO/CO <sub>2</sub> ratio	Molar ratio in fuel-limited burning
Vitiated CO/CO <sub>2</sub> ratio	Molar ratio in vent-limited burning
Radiant fraction	Radiative fraction of fire heat release $\lambda_r$
Pre-flashover $\lambda_{c, \text{max}}$	Maximum ratio of the instantaneous wall heat losses to fire generated heat release rate
Vent (INSIDE or Vent1)	Smoke moves from room of origin into the building
Flag indicating the presence of a vent	Y or N
Height	(m or ft)
Width	(m or ft)
Sill height	(m or ft)
Vent (OUTSIDE or Vent2)	Smoke moves from room to building exterior
Flag indicating the presence of a vent	Y or N
Height	(m or ft)
Width	(m or ft)

Sill height (m or ft)

HVAC (Y/N)  
Combustion efficiency % of `normal' replacement air available as oxidizer  
Ventilation rate Number of room air changes per hour

### 5.4.2 Post-Flashover

Opportunity to Revise: Inside Opening  
Height of top of opening (m or ft)  
Width (m or ft)  
Sill height (m or ft)

Opportunity to Revise: Outside Opening  
Height of top of opening (m or ft)  
Width (m or ft)  
Sill height (m or ft)

Opportunity to Revise: Combust. chemistry.  
Heat of gasification Energy needed to pyrolyze fuel (kJ/g)  
Heat of combustion Effective heat of combustion (kJ/g)

Fuel Quantity Data  
Fuel load Fuel mass per floor area of room (kg/m<sup>2</sup> or lb<sub>m</sub>/ft<sup>2</sup>)  
% of fuel burnable Also the % of fuel that has burned  
Total horizontal exposed fuel Based upon floor area (%)  
Total vertical exposed fuel Based upon wall area (%)  
Horizontal surface area > 6 mm Based upon floor area (%)  
Vertical surface area > 6 mm Based upon wall area (%)  
Horizontal surface area > 25 mm Based upon floor area (%)  
Vertical surface area > 25 mm Based upon wall area (%)

Revise duration of the run (sec)

Filenames  
Data file name Valid DOS input-file name having extension .DAT

Output file name	Valid DOS file name for the spreadsheet file
Halt flags	
At specified time	(s)
After sprinkler activation	(s)
After smoke detector activation	(s)

## *OUTPUT*

Temperature	Characteristic of average smoke temp. (°C or °F)
Layer	Height of smoke layer bottom above floor (m or ft)
O2	Average for the smoke layer (molar or volume %)
CO	Average for the smoke layer (molar or volume %)
CO2	Average for the smoke layer (molar or volume %)
L. frac <sub>actual</sub>	Minimum of $\{\lambda_c, \lambda_{c, \max}\}$
L. frac <sub>calculated</sub>	$\lambda_c$ , see program notes Section 5.3.
RHR	Fire heat release rate (kW)
Mass loss	Fuel pyrolysis rate (kg/s)
Fl ht.	Mean flame height above base of flames (m or ft)
Entrain	Fire HRR <i>supportable</i> by plume entrained O <sub>2</sub> (kW)
Ent. mass	Mass of lower layer air entrained to the plume (kg)
O2 req.	LFL for sustaining combustion per eq (7)
Vent	Enthalpy mass flow of VENT1 and VENT2( kW)
Vent1	Enthalpy mass flow of inside vent (kW)
Vent2	Enthalpy mass flow of outside vent (kW)
Hvacvent	Enthalpy mass flow of mechanical ventilation (kW)

OD	Visibility through the smoke [4] ( $m^{-1}$ )
Vision	Distance 5% of emitted light is visible (m or ft)
Smkflow1	Smoke flow of inside opening ( $m^3/s$ or $ft^3/s$ )
Smkflow2	Smoke flow of outside opening ( $m^3/s$ or $ft^3/s$ )
Rm. lining	Room barrier surface per eq (31) ( $^{\circ}C$ or $^{\circ}F$ )
Vent. limit	Heat release rate limitation (see Section 3.17) (kW)
Det. jet. F.	Ceiling jet temp. at smoke detector ( $^{\circ}C$ or $^{\circ}F$ )
Det. jet. V.	Ceiling jet velocity at smoke detector (m/s or ft/s)
As. jet. F.	Ceiling jet temperature at heat detector ( $^{\circ}C$ or $^{\circ}F$ )
As. jet. F.	Ceiling jet velocity at heat detector (m/s or ft/s)
As. link F.	Heat detector link temperature ( $^{\circ}C$ or $^{\circ}F$ )

## 5.5 References

- [1] McCaffrey, B.J., Quintiere, J.G., Harkelroad, M.H. "Estimating Room Temperatures and the Likelihood of Flashover using Fire Test Data Correlations," Fire Technology, Vol. 17, No. 2, 98-119, May 1981.
- [2] Rockett, J.A., "Fire Induced Gas Flow in an Enclosure," Combustion Science and Technology, Vol. 12, p. 165, 1976.
- [3] Kawagoe, K. D. & Sekine, T., "Estimation of Fire Temperature-Time Curve for Rooms," BRI Occasional Report No. 11, Building Research Institute, Ministry of Construction, Japanese Government, June 1963.
- [4] Tewarson, A., "Generation of Heat and Chemical Compounds in Fires," SFPE Handbook of Fire Protection Engineering, 1st Ed.," National Fire Protection Association, Quincy, MA 02269, pp. 1-195, 1988.
- [5] Drysdale, D.D., "Fire Dynamics," John Wiley and Sons, New York, pp. 462, 1983.

- [6] Madrzykowski, D., Vettori, R.L. "A Sprinkler Fire Suppression Algorithm for the GSA Engineering Fire Assessment System, Nat. Inst. Stand. Tech. (U.S.), NISTIR 4833, Gaithersburg, MD 20899, 1992.
- [7] Thomas, P.L., Bullen, M.L., "On the Role of kpc<sub>v</sub> of Room Lining Materials in the Growth of Fires," *Fire and Materials*, Vol. 3, (2), pp. 68-73, June 1979.
- [8] Evans, D. D., "Sprinkler Fire Suppression Algorithm for HAZARD," Nat. Inst. Stand. Tech. (U.S.), NISTIR 5254, Gaithersburg, MD 20899, August 1993.
- [9] Huggett, C. "Rate of Heat Release - Implications for Engineering Decisions by C. Huggett," *Engineering Applications of Fire Technology Workshop Proceedings*. April 16-18, 1980, Nat. Bur. Stand. (U.S.) NBS, Gaithersburg, MD 20899; co-sponsored by the Society of Fire Protection Engineers and Center for Fire Research, H.E. Nelson, Editor, Boston, MA 1980.
- 1[0] Nelson, H.E., "FPETOOL: Fire Protection Engineering Tools for Hazard Estimation," Nat. Inst. Stand. Tech. (U.S.), NISTIR 4380, Gaithersburg, MD 20899, 1990.
- [11] Op cit, pp.93-95.
- [12] Bryner, N.P., Mulholland, G.W., "Smoke Emission and Burning Rates for Urban Structures," Defense Nuclear Agency, Washington, DC, *Atmospheric Environment*, Vol. 25A, No. 11, pp. 2553-2562, 1991.
- [13] Gottuk, D.T., Roby, R.J., et al., "Study of Carbon Monoxide and Smoke Yields From Compartment Fires with External Burning," Combustion Institute, Proceedings of the Symposium International on Combustion--24th, July 5-10, 1992, Sydney, Australia, pp. 1729-1735, 1992.
- [14] Mitler, H.E. and Emmons, H.W., Documentation for CFC V, the fifth Harvard computer fire code, Nat. Bur. Stand. (U.S.), NBS-GCR-81-344, Gaithersburg, MD, pp. 187, 1981.
- [15] Jones, W.W. and Peacock, R.D., Technical Reference Guide for FAST version 18, Nat. Inst. Stand. Tech. (U.S.), NIST TN 1262, Gaithersburg, MD, 1989.
- [16] Heskestad, G., "Fire Plumes," *The SFPE Handbook of Fire Protection Engineering*, 1st Ed., National Fire Protection Association, Quincy, MA 02269, pp. 1-108, 1988.
- [17] Heskestad, G., Delicatsios, M.A., "Environments of Fire Detectors--Phase I. Effect of Fire Size, Ceiling Height and Material," Nat. Bur. Stand. (U.S.), NBS-GCR-77-86, Gaithersburg, MD 20899, 1977.

- [18] Zukoski, E.E., Kubota, T., Cetegen, B., "Entrainment in the Near Field of a Fire Plume. Final Report," Nat. Bur. Stand. (U.S.), NBS-GCR-81-346, Gaithersburg, MD 29899, November 1981.
- [19] Heskestad, G., "Luminous Heights of Diffusion Flames", Fire Safety Journal, Vol. 5, (2), pp. 103 - 108, 1983.
- [20] McCaffrey, B.J., "Purely Buoyant Diffusion Flames--Some Experimental Results," Nat. Bur. Stand. (U.S.), NBSIR 79-1910, Gaithersburg, MD 20899, 1979.
- [21] Pitts, W., et al. "Production Mechanisms for CO in Enclosure Fires," Combustion Institute/Eastern States Section, New Orleans, LA, March, pp. 102-106, 1993.
- [22] Walton, W.D., Thomas, P.H. "Estimating Temperatures in Compartment Fires," The SFPE Handbook of Fire Protection Engineering, 1st Ed., National Fire Protection Association, Quincy, MA 02269, pp. 1-108, 1988.
- [23] National Fire Protection Association, NFPA 92B, NFPA, Quincy, MA 02269-9101, pp. 92B-25, 1991.
- [24] Alpert, R. L., "Calculation of Response Time of Ceiling-Mounted Fire Detectors," Fire Technology, Vol 8:(3), National Fire Protection Association, Quincy, MA, pp. 181-195, 1972.

## 6 CORRIDOR

### 6.1 Application

This procedure can be used to estimate the characteristics of a smoke wave as it propagates along the ceiling of a corridor away from a steady-state smoke source. The estimated smoke characteristics are: velocity, position, temperature, thickness, and gas concentrations. The term `corridor' is used to describe the procedure, but the terms hallway, aisle, concourse and other descriptions of a space apply equally as well provided the space contains a propagating smoke wave.

### 6.2 Theory

This routine employs conservation of mass to an expanding gas control volume within a corridor. The control volume receives entraining smoke. The smoke expands horizontally from buoyant forces (Figure 6.0.1). The control volume begins at the opening to the corridor and ends at the front of the smoke wave. The control volume contains only the mass of the smoke and entrained air [eq (1)]. The wave front velocity is calculated by a correlational expression [eq (6)] abstracted from experimental tests [2]. This equation is a significant simplification of the transient smoke-wave problem [6,7], but it justifiably serves as a first-order engineering approximation of the phenomenon [1].

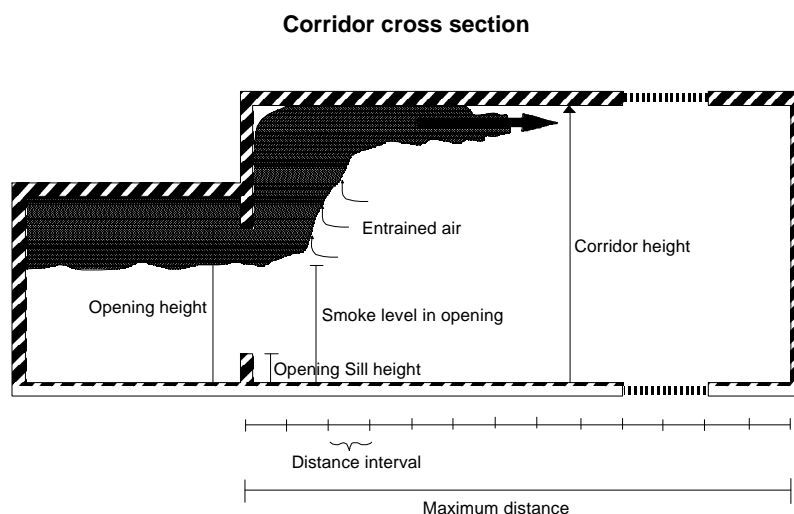


Figure 6.0.1. **CORRIDOR** geometry in cross-section

This equation is a significant simplification of the transient smoke-wave problem [6,7], but it justifiably serves as a first-order engineering approximation of the phenomenon [1].

$$\dot{m}_{wave} = \dot{m}_{room} + \dot{m}_{entrainment} \quad (1)$$

$$\dot{m}_{entrained} = 71 \eta_{entrainment} \dot{Q}_{room}^{\frac{1}{3}} z^{\frac{5}{3}} \quad (2)$$

Given that the velocity of the wavefront is obtained with eq (6), the position of the wavefront at the

next time step is determined from the classical displacement eq (5). The entrained air is calculated from an approximate method [eq (2)]; no detailed experiments on door jets yet provide a verifiable correlation for this phenomenon.

$$\dot{m}_{room} = \dot{V}_{room} \frac{T_{\infty}}{T} \rho_{\infty} \quad (3)$$

$$\dot{Q}_{room} = \dot{m}_{room} c_p (T - T_{\infty}) \quad (4)$$

The wave front velocity decreases with time not due to modeling of viscous effects, but to modeling energy losses. Energy loss from the smoke to the walls is modeled with an effective heat transfer coefficient,  $h_{eff}$ . The effective heat transfer coefficient (eq 9) considers convective and radiative losses. This convection coefficient (eq 9) defaults to a value suggested by the original authors [2], and a value that also produces a best fit to experimental data [5]. The radiative coefficient ( $h_{radiation}$ ) results from a linearization of the fourth-power temperature dependency [eq (10)]. A correction was added to  $h_{radiative}$ ,  $(-4T_{\infty})$ , in order to eliminate non-physical behavior at ambient smoke temperatures. The smoke temperature used in determining the radiative coefficient is a spatially averaged value obtained through integration along the length of the wave [eq (11)].

$$x(t+\Delta t) = x(t) + \int_t^{t+\Delta t} \bar{v} dt \quad (5)$$

$$v_{front}(t) = v_o \left[ \frac{T_{\infty}}{T} \exp(-3Kx(t)) + B \right] \quad (6)$$

$$B = \frac{T - T_{\infty}}{T} \exp(-6Kx) \quad (7)$$

$$K = \frac{h_{eff} W_{corridor}}{3 \dot{m}_{wave} c_p} \quad (8)$$

Only after the wave position is determined can the smoke temperature used in the radiative heat loss calculation be used. The smoke temperature as a function of position,  $x$ , along the wave is calculated by using a simple exponential decay relationship [eq (12)].

$$h_{effective} = h_{convective} + h_{radiative} \quad (9)$$

$$h_{radiative} = \epsilon \sigma (\bar{T}^3 + \bar{T}^2 T_{\infty} + \bar{T} T_{\infty}^2 - 3 T_{\infty}^3) \quad (10)$$

$$\bar{T} = \frac{1}{(L-x_o)} \int_{x_o}^L T(x) dx \quad (11)$$

$$T(x) = T_{\infty} + (T - T_{\infty}) \exp(-3Kx) \quad (12)$$

The depth of the corridor wave ( $\delta$ ) is obtained by applying a mass and energy balance to the entrained smoke [eq (2)]. A correction factor, ( $\zeta$ ), serves to weakly thicken the smoke-wave depth at higher temperatures and early stages in the progression. This correction was included per the original authors' suggestion [2].

$$\delta = \frac{\dot{m}_{wave} t T}{T_{\infty} \rho_{\infty} \xi W_{corridor}} \quad (13)$$

$$\xi = x + \frac{1}{3K} \ln\left(\frac{T_{\infty}}{T} + \left(1 - \frac{T_{\infty}}{T}\right) \exp(-3Kx)\right) \quad (14)$$

$c_p$	Heat capacity of the wave gases (kJ/(kg·K))
$h_{effective}$	Effective, overall heat transfer coefficient (kW/(m <sup>2</sup> ·K))
$h_{convective}$	Convective heat transfer coefficient (kW/(m <sup>2</sup> ·K))
$h_{radiative}$	Radiative heat transfer coefficient (kW/(m <sup>2</sup> ·K))
$K$	Ratio of heat loss to heat gain; eq (8) m <sup>-1</sup>
$\ln$	Natural logarithm transformation
$\dot{m}_{entrained}$	Clean-air mass flow rate entrained into the door-spill plume (kg/s)
$\dot{m}_{room}$	Smoke mass-flow rate from the fire-room into the corridor (kg/s)
$\dot{m}_{wave}$	Mass-flow rate of entrained air and smoke (kg/s)
$Q_{room}$	Enthalpy of $\dot{m}_{room}$ (kW)
$t$	Time in the simulation (sec)
$T$	Temperature of smoke-wave front as it leaves the fire-room (K)
$T_{\infty}$	Temperature of the ambient, corridor air (K)
$V_{room}$	Smoke volume-flow rate out of the room (m <sup>3</sup> /s)
$\bar{V}_{front}$	Velocity of the smoke wave (m/s)
$v_o$	Velocity of the smoke wave leaving the fire-room (m/s)
$\bar{v}$	Average velocity between timesteps, t and t+ $\delta t$ (m/s)
$x_t$	Position of the front of the smoke-wave at time t (m)
$x_{t+\Delta t}$	Position of the smoke-wave front at time t+ $\Delta t$ (m)
$W_{corridor}$	Width of the corridor (m)

$\delta$	Depth of the corridor wave (m)
$\xi$	Smoke wave length adjustment factor (m)
$\eta_{\text{entrainment}}$	Influences entrainment amount per eq (2)
$\rho_{\infty}$	Ambient air density (kg/m <sup>3</sup> )

### 6.3 Program Notes

Conditions of the smoke entering the `corridor' are steady-state.

Increasing mass of cool air entraining into the smoke plume reduces the buoyancy of the developing smoke wave. If this behavior continues, a point is eventually reached where propagation is no longer an accurate description of the smoke movement phenomena (and a more appropriate description of the smoke filling would be described with the traditional 2-zone-filling model). **CORRIDOR** notifies the user when this transition should be considered.

The entrainment factor,  $\eta$ , defaults to 1.0. This value corresponds to smoke entrainment from a cylindrical shape plume. For wide soffits where the spill plume into the corridor space more closely resembles line-fire entrainment, higher values of  $\eta$  should be used. This is an area in need of further research.

Convective heat transfer from the hot gas to the compartment surfaces is a user-specified constant. For rough surfaces and high smoke-source velocities the heat transfer coefficient may be increased from the default value of 20 W/(m<sup>2</sup>·K).

The corridor is not intended to have any large obstructions, vestibules or branching corridors opening onto it. The procedure is only useful to the point where the smoke reaches a branch in the corridor, a turn in the corridor, the end of a corridor, or where the smoke expands to touch the floor. No `return wave' or filling is simulated.

The procedure is sensitive to the smoke velocity at the source to the corridor; the `*Smoke level in the opening*' is a user-specified parameter strongly influencing this velocity when flashover created volume flows issue from standard size door openings [0.81m (32 in.)].

Ambient conditions are fixed. Air is the assumed entrained fluid; gases with different thermodynamic properties will not behave similarly.

Initial conditions ( $T$ ,  $\dot{m}_{\text{smoke}}$ , smoke concentrations) for this routine may be obtained from **FIRE SIMULATOR** or most other zone-compartment fire models.

Depth is the least precisely predicted parameter of the procedure [5].

The procedure has been tested against 3 sets of experimental data that included large- and medium-sized fires in 15 m (50 ft.) corridors and tunnels hundreds-of-meters long with good results.

Comparisons are graphed [5] and original data are available [2,3,8].

The mathematics considers only one-dimensional smoke movement. Although this routine may be used to estimate smoke flow in a space with any sized floor area, the application was correlated from and verified on floor aspect ratios common to corridors and tunnel spaces.

## 6.4 Program Interface

If the user wishes to 'backup' in the data entry process, this reversal may be accomplished by simultaneously pressing the 'Control' and 'Q' keys at any point where the program expects non-filename, keyboard input.

If the user wishes to terminate the simulation during execution this may be accomplished by pressing the 'F3' key.

### *INPUT*

Spreadsheet file name Any valid DOS filename

Convective heat coefficient Recommended range: 10 - 30 W/(m<sup>2</sup>·K)

Smoke level in opening Neutral plane elevation in the exit leading to the corridor (m or ft)

Smoke temperature Characteristic smoke temperature entering the corridor (°C or °F)

Smoke flow Smoke temperature (m<sup>3</sup>/s or ft<sup>3</sup>/min)

CO Carbon monoxide concentration (parts per million)

CO<sub>2</sub> Carbon dioxide concentration (% by volume)

O<sub>2</sub> oxygen concentration (% by volume)

Entrainment factor Parameter ' $\eta_{\text{entrainment}}$ ' in eq (2)

Smoke emissivity Black-body representation factor

Smoke flow in 1 dirct. or 2 1 direction if at end of hall; 2 directions if in middle of hall

Opening height (m or ft)

Opening width	(m or ft)
Opening sill height	(m or ft)
Corridor height	(m or ft)
Corridor width	(m or ft)
Maximum distance	Calculations cease when the wave is beyond this distance (m or ft)
Distance interval	Distance interval that calculations are modeled at (m or ft)
Time interval	Interval for screen and/or file output (s)

### *OUTPUT*

Time	Simulation time (sec)
Position of smoke front	(m or ft)
Velocity of smoke front	(m/s or ft/s)
Smoke depth	Average value over the length of wave, not a point value (m or ft)
Smoke temperature @ intvl	Refers to the distance interval (°C or °F)

## **6.5 References**

- [1] Steckler, K.D., "Fire Induced Flows in Corridor--A Review of Efforts to Model Key Features," Nat. Inst. Stand. Tech. (U.S.), NISTIR 89-4050, Gaithersburg, MD 20899, 1989.
- [2] Hinkley, P.L., "Work by the Fire Research Station on the Control of Smoke in Covered Shopping Centers," proceedings of the Conseil International du Bâtiment (CIB) W14/163/76 (U.K.) 24 p. September 1975.
- [3] Heskestad, G. and Hill, J.P., "Experimental Fires in Multi-Room/Corridor Enclosures, NBS-GCR-86-502, Gaithersburg, MD 20899, 1986.
- [4] Stroup, D.W., Madrzykowski, D., "Conditions in Corridors and Adjacent Areas Exposed to Post-Flashover Room Fires, Nat. Inst. Stand. Tech. (U.S.), NISTIR 4678, Gaithersburg, MD, 1991.

- [5] Nelson, H.E., Deal, S., "Corridor: A Routine for Estimating the Initial Wave Front Resulting from High Temperature Fire Exposure to a Corridor," Nat. Inst. Stand. Tech. (U.S.), NISTIR 4869, Gaithersburg, MD 20899, July 1992.
- [6] Emmons, H. "The Ceiling Jet in Fires," Nat. Inst. Stand. Tech. (U.S.), NIST-GCR-90-582, Gaithersburg, MD 20899, October 1990.
- [7] Chubotov, M.V., Zukoski, E., et al. "Gravity Currents With Heat Transfer Effects," NBS-GCR-87-522, Gaithersburg, MD, September 1986.
- [8] Heseldon, A.J., Hinkley, P.L., "Smoke Travel in Shopping Malls - Experiments in Cooperation with Glasgow Fire Brigade, Parts 1 and 2; Fire Research Note 832, Fire Research Station, Borehamwood, Herts, UK, 1970.



## 7 3rd ROOM

### 7.1 Application

This procedure estimates the time to human untenability from heat and inhalation exposure in a space experiencing smoke infiltration from a steady-state source.

### 7.2 Theory

The untenability/lethality estimates of human response to smoke and heat are correlated from laboratory-animal response to smoke and heat. Smoke conditions in the target room are predicted using door-ventilation techniques similar to those described in CCFM [2].

#### 7.2.1 Vent Flows

The door ventilation techniques used in **3rd ROOM** differ from the techniques developed in CCFM in that the former iterates on the conservation of mass while the latter iterates on the conservation of mass and energy. Smoke conditions within **3rd ROOM** are predicted by applying conservation of mass to steady-state source terms. There is one leakage area connecting the 3rd room (or 'target room') to an 'adjacent space.' This leakage area does not change size during the simulation (one can not open or close a door); conditions on the 'fire' side of the leakage area are assumed constant; the smoke leakage rate is assumed constant. Mass conservation is achieved by iterating on the difference between the target room floor-level pressure and the adjacent space pressure at same elevation. The pressure at the floor of the target room is assumed to be identical to the pressure out-of-doors at this same elevation.

The user is given an opportunity to explore the effects ambient pressure exerts on fluid flow by manipulating the

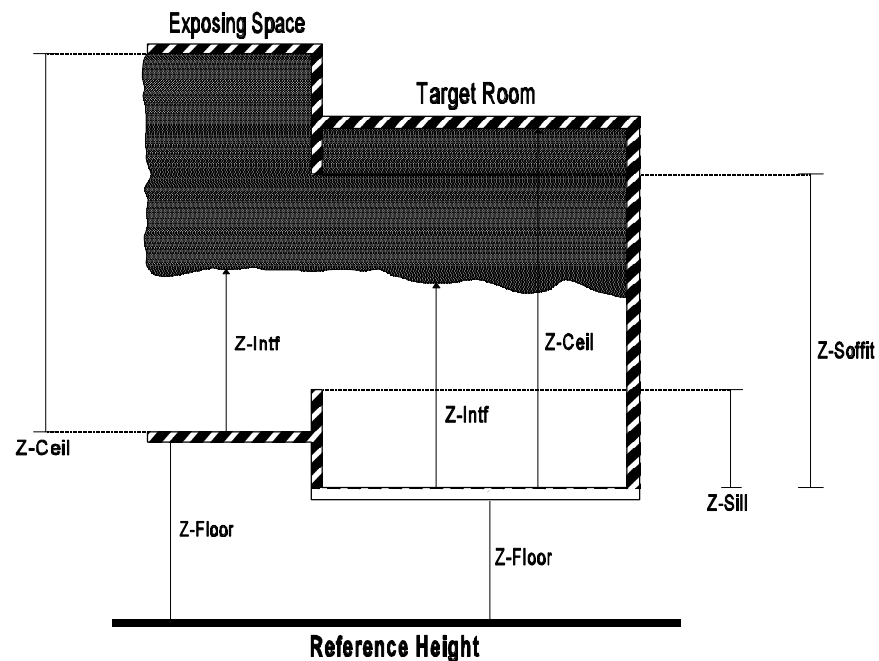


Figure 7.0.1. **3rd ROOM** input parameter geometries.

reference elevation. The reference elevation is, from the procedure's point of view, the datum or 'zero' height (Figure 7.0.1). It also is the elevation where the program assumes the reference-pressure measurement was taken. The importance of correctly fixing the reference pressure and reference elevation resides in vent flow predictions. The reference pressure together with the procedure's 'guess' of the trans-room pressure difference at floor level are used to calculate static pressure profiles across the vents (Figure 7.0.2). The cross-vent pressures ( $\Delta P_{1,2}$ ) are then used in the Bernoulli derived orifice eq (1) for vent flow predictions.

$$\dot{m} = \rho v A_{leakage} = \rho C \sqrt{\frac{\Delta P_{1-2}}{\rho}} A_{leakage} \quad (1)$$

In eq (1), the cross-vent pressures ( $\Delta P_{1-2}$ ) are determined from static pressure gradients within the elevation of an arbitrary slab of flowing fluid. (There are 6 flow slabs in Figure 7.0.2, each slab contains fluid that is well mixed and moving in the same direction). The pressure difference ( $\Delta P_{1-2}$ ) is represented by the horizontal distance between the solid- and dashed-pressure-profile lines on the right-hand side of Figure 7.0.2. The subscripts '1-2' represent sides 1 and 2 of the ventilation area (e.g. '1' can be the exposing space and '2' can be the target room space). In eq (1), the density of the fluid flow slab is  $\rho$ , and C is a fitting constant normally taken between 0.65 and 1.0.

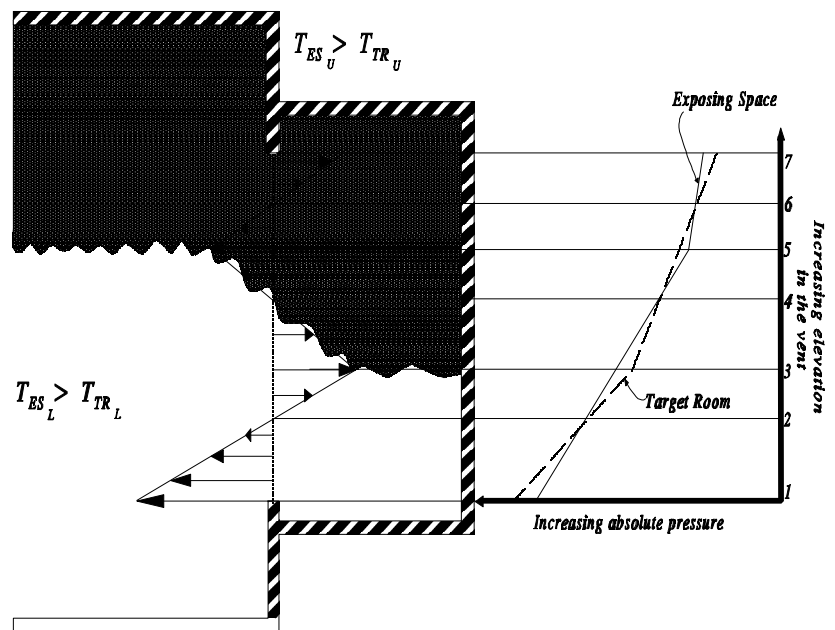


Figure 7.0.2. Delineation of vent-flow slabs and cross-vent pressure profiles

The vent flow predictions are described in great detail by Cooper, Forney [2]; therefore they are presented here briefly. The vent flows can be perceived as moving in slabs having uniform temperature. The slabs are divided by either a change in temperature (a layer interface), a change in pressure (a neutral plane), or the physical limits of the vent (sill and soffit). The maximum possible number of slabs in a vent is illustrated in Figure 7.0.2. Once the slabs are identified, the flow destination is determined. Flow from the slab may be deposited totally in the upper layer, totally in the lower layer, or the flow can split depositing into both layers according to the temperature of the slab [3]. The slab mass is deposited without entrainment; after all slabs are deposited, a variable audits for mass conservation and verifies that closure occurs. If closure does not occur within the specified tolerance ( $1 \cdot 10^{-10}$ ) a new cross-vent pressure is guessed and the iteration process repeats. Iterations

are converged using the bisection method; the virtue of this slower process being reliability. After convergence of mass conservation, gas species concentrations are determined.

Energy conservation is addressed after mass flow is conserved and species are deposited. The temperature of the smoke is determined after ceiling and wall heat transfer are calculated. The method of heat transfer is almost identical to that of **FIRE SIMULATOR**. First, a surface temperature is estimated from considerations of radiative, convective and conductive losses to the walls and ceiling, respectively. Next heat is removed from the smoke--based upon Newton's heat loss formula--using an overall heat transfer coefficient [Section 3.16 -- eq (7)]. No heat transfer to the floor is considered.

### 7.2.2 Viability Analysis

After the room smoke conditions are determined, the influence of this smoke on the viability of a theoretically exposed human is addressed. Heat loading considerations are first, then gas loading.

#### *Heat Loading:*

There are two primary pathways towards human incapacitation from heat, long-term exposure (heat stroke) and shorter-term trauma (burns). The separation between these regimes occurs at about 120 °C (250 °F) [9]. **3rd ROOM** does not consider long-term, heat-stroke degradation, but burn trauma is considered from both convective and radiative contributions.

The heat loading calculations predict skin burn trauma. Nonetheless, skin burns are a significant insult and their formation notes the onset of significant fire-created hazard. Heat loading is calculated not through a temperature criterion, but rather, through heat accumulation. The rate of heat absorption is integrated over the exposure time to yield the net heat accumulation; this quantity is compared to an empirical threshold value for burn formation [4]. When the integrated quantity is greater than the empirical quantity, burns are predicted.

The method is verified in the sense that the empirical equation is correlated to experimental results. However, the method does not apply to temperatures below 120 °C for

#### Convective Heat Transfer as f(T smoke)

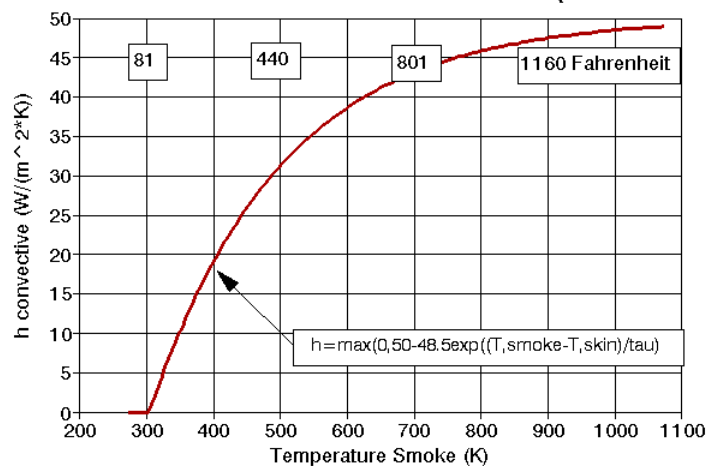


Figure 7.0.3. Convective heat transfer exponential dependence upon temperature

reasons described above, nor does the method have experimental verification at fluxes over 75 kW/m<sup>2</sup>. The 75 kW/m<sup>2</sup> flux represents extreme conditions that can be tolerated only for short durations even with a full ensemble of firefighting turnout equipment.

When calculating the heat loading onto an individual in direct contact with the smoke layer, both convection and radiation are considered. The radiative component assumes a unit emissivity and unit configuration factor. The convection component assumes an exponentially varying heat transfer coefficient from 0 to 50 W/(m<sup>2</sup>·K) over the temperature range 20 °C to 750 °C (70 °F to 1380 °F) (Figure 7.0.3). These values agree with previously reported natural convection heat transfer coefficients [5,7]. The value for  $\tau$  in Figure 7.0.3 is 200 °C<sup>-1</sup>. Skin temperature is taken as 318 K (45 °C); this is the threshold temperature for skin burns.

For calculations of heat loading onto an individual located in the lower layer--only radiative heating is considered. The emissivity of the hot layer is assumed to vary linearly with temperature. The emissivity is taken as a minima of 0.4 at 20 °C (70 °F) and a maximum of 1.0 at 873 °C (1600 °F). The radiation configuration factor for emission from the smoke layer to the individual assumes the layer to emit as a flat plate onto an element located on the floor at the middle of the room [eq (2)].

$$F_{1-2} = \frac{2}{\pi} * \left( \left( \frac{L1}{\sqrt{D^2 + L1^2}} \right) * \tan^{-1} \left( \frac{L2}{\sqrt{D^2 + L1^2}} \right) + \left( \frac{L2}{\sqrt{D^2 + L2^2}} \right) * \tan^{-1} \left( \frac{L1}{\sqrt{D^2 + L2^2}} \right) \right) \quad (2)$$

### ***Inhalation Gas Loading:***

The second type of degradation estimated to affect human viability is inhalation gas loading. Toxic gas calculations are independent of any heat loading calculations. The need for inhalation gas hazard analysis is warranted since 65 percent of fire incapacitations in the United States are estimated to occur from inhalation of toxic concentrations of gas [6,9,11]. Roughly 30% of fire deaths are attributable to burn trauma [6,11].

Inhalation gas loading calculations begin with the gas species concentrations determined from the vent flow routines. Similar to the heat loading calculations, the inhalation calculations consider each layer separately. Inhalation calculations proceed toward estimates of tenability (unconsciousness) and lethality. The following discussion now focuses on the calculational procedure for the upper layer, but the arguments apply with equal relevance to the lower layer.

Three gases are considered: CO, O<sub>2</sub> and CO<sub>2</sub>. Of these, CO is the most influential. At CO concentrations above 1300 ppm the model begins degrading human viability; this value is consistent with results obtained when hydrogen cyanide (HCN) is also in the smoke. The presence of HCN is considered because of the 'wood-plastic' fuel mixture that **FIRE SIMULATOR** assumes and because it represents conservative fire-hazard analysis. The following items--among others--will generate hydrogen cyanide in measurable quantities: wool, cotton, linen, acrylics and polyurethane.

The influence of CO<sub>2</sub> is to potentiate the effects of CO. Direct degradation of human viability from CO<sub>2</sub> is not simulated because of the high concentrations of CO<sub>2</sub> required to produce lethality. Lethality from CO<sub>2</sub> in normal atmospheres does not typically occur until CO<sub>2</sub> concentrations exceed roughly 40 % by volume; incapacitation, however, is possible from lower CO<sub>2</sub> exposure levels [10]. A two minute exposure to 10% CO<sub>2</sub> can induce incapacitation [8]. Inhalation of CO<sub>2</sub> at levels up to 5% by volume increases a person's respiratory rate and this in turn increases CO respiration. The chemical toxicity model reproduces this effect by accounting for the presence of CO<sub>2</sub> in concentrations up to 5% by volume. Above 5% CO<sub>2</sub> by volume, no increased effects are simulated. Mathematically, these effects are represented in eqs (3) - (5).

$$FED_{CO}(t) = \frac{(CO_{t+\Delta t} + CO_t)}{2} \cdot \frac{\Delta t}{DCO} \quad (3)$$

$$DCO = \bar{CO} \cdot \frac{80,000 \cdot (1 - 1 \cdot 10^{-5}) \bar{CO}_2}{\bar{CO} - 1300} \quad \text{if } \bar{CO}_2 \leq 50,000 \text{ ppm} \quad (4)$$

$$DCO = \frac{\bar{CO} \cdot 40,000}{\bar{CO} - 1300} \quad \text{if } \bar{CO}_2 > 50,000 \text{ ppm} \quad (5)$$

It is the absence, not presence, of oxygen, that results in oxygen toxicity (hypoxia). The model begins simulating hypoxia at O<sub>2</sub> concentrations slightly below 6% by volume [4].  $\bar{O}_2$  is the average value of O<sub>2</sub> between successive time-steps, t and t + Δt.

$$FED_{O_2}(t) = ((5.8 - \frac{[O_{2,t+\Delta t} + O_{2,t}]}{2}) * \Delta t) \frac{1}{9.2} \quad \text{if } \bar{O}_2 < 5.8 \quad (6)$$

In summary, the inhalation module considers the influences created by the presence, or lack, of three gases (with the presence of a fourth gas (HCN) assumed, but not tracked). The simulated effects of gas loading are normalized against a lethal exposure-dose. This lethal exposure-dose was extrapolated from experimental rodent data. The extrapolation was obtained by first correlation human response at low exposure-doses to rodent response at low exposure-doses. Then, human response at lethal exposure-doses was extrapolated from exposure-doses lethal to rodents. The final equation for inhalation gas loading appears in eq (7) and was obtained from the HAZARD I gas-toxicity model [4]. When  $FED_{3-GAS, t+\Delta t} \geq 0.5$ , unconsciousness is predicted; when  $FED_{3-GAS, t+\Delta t} \geq 1.0$ , lethality is predicted. The individual terms in eq (7) are obtained per eqs (3) and (6).

$$FED_{3Gas, t+\Delta t} = FED_{3Gas, t} + FED_{O_2, t} + FED_{CO, t} \quad (7)$$

$A_{\text{leakage}}$	Area of a vent opening (m <sup>2</sup> )
C	Orifice coefficient (0.65-1.0)
CO	Mole percent CO (also volume % in ideal gases)
CO <sub>2</sub>	Mole percent CO <sub>2</sub> (also volume % in ideal gases)
D	Vertical distance from the smoke layer to the floor (m)
F <sub>1-2</sub>	Configuration factor from the smoke to a centroidal floor-level point
FED	Fractional Effective Dose
L1	Room length measured in a direction perpendicular to L2 (m)
L2	Room width measured in a direction perpendicular to L1 (m)
$\dot{m}$	Air mass flow rate (kg/s)
$\tan^{-1}$	Arctangent transformation
O <sub>2</sub>	Mole percent oxygen (also volume % in ideal gases)
P <sub>1-2</sub>	Pressure change across a vent (Pa)
t	time (sec)
$\Delta$	Discrete change in a variable
$\rho$	Material density (kg/m <sup>3</sup> )
v	Material velocity (m/s)

### 7.3 Program Notes

The vent area accommodating smoke leakage may be either small voids around a door or a completely open vent. The representation of this vent area, to the **3rd ROOM** procedure, is one of constant horizontal cross-section.

The target room is assumed to have a constant horizontal cross-section.

The smoke conditions entering the '**3rd ROOM**' are constant in time.

The initial exposing space conditions may be obtained from **CORRIDOR**.

The mass-flow slab entering the room splits according to rules based upon flow stream temperatures [3].

Hot, vitiated plumes spilling into the room will not ignite.

Ventilation through horizontal openings is not simulated.

No entrainment into the spill-plume of the target room is modeled.

The most appropriate reference height is the height of the target room floor set to a value of zero.

Smoke flow is assumed nonviscous; modeling smoke flow at reference pressures that are orders of magnitude greater than standard atmospheric is not valid.

Heat loss from the smoke to the room surfaces assumes heat transfer through the barriers is limited by conduction; heat transfer through metal barriers is therefore not well characterized.

Untenability can result from hypoxia at concentrations of O<sub>2</sub> as high as 13 percent. Extended exposure to concentrations of O<sub>2</sub> below 10 percent can result in brain damage [6,12].

The tenability and lethality inhalation gas estimates assume that exposure to a layer is continuous; the calculations do not consider an individual who alternates their exposures between upper and lower layers.

The inhalation gas model was developed from data taken primarily from rats, not human exposures.

Human respiratory rate effects CO toxicity. Given identical CO exposures, the same individual when jogging uphill becomes unconscious before he/she will when walking on level ground (Figure 7.0.4). **3rd ROOM** toxicity analysis does not consider human respiratory rate.

No mechanical ventilation is modeled.

The heat loading calculations have significant uncertainties because of unknowns that the presence of clothing introduces, because of the variability in individual constitutions regarding heat loading and because of the lack of experimental data.

Most clothing will delay the onset of skin blister formation.

Gas concentrations in the exposing space are calculated based upon an assumed exposing space volume of  $1 \cdot 10^{14} \text{ m}^3$ . As the volume of the target room increases to an order-of-magnitude comparable with the exposing space volume, feedback will develop wherein the assumed constant concentrations in the exposing space will be affected by changing concentrations in the target room.

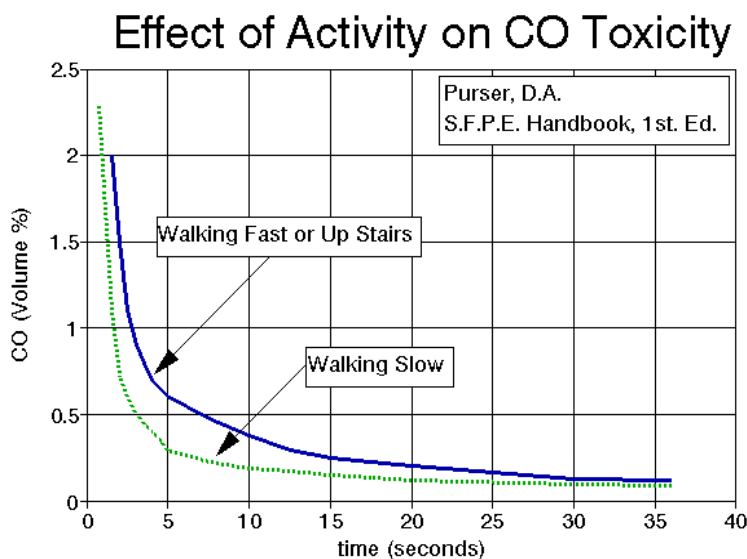


Figure 7.0.4. Effect of human activity on time to incapacitation via CO toxicity

## 7.4 Program Interface

The user may quickly exit their data entry process by simultaneously pressing the `Control' and `Q' keys. This procedure works at any point where non-filename alphanumeric input from the keyboard is expected by the program.

### INPUT

#### 7.4.1 Reference Parameters

Reference height	Height where Reference pressure measurement was taken (m or ft)
Reference pressure	Out-of-doors pressure measured at Reference height (Pa or psi)
Reference T	The temperature at the target room floor ( $^{\circ}\text{C}$ or $^{\circ}\text{F}$ )
Simulation duration	Duration of the simulation (sec)
Time step	Interval that the simulation marches forward in time with (sec)

#### 7.4.2 Target Room Parameters

Floor height	(m or ft)
Ceiling height	(m or ft)
Room length	(m or ft)
Room width	(m or ft)
Smoke layer height	(m or ft)
Upper layer T	( $^{\circ}\text{C}$ or $^{\circ}\text{F}$ )
Lower layer T	( $^{\circ}\text{C}$ or $^{\circ}\text{F}$ )
Barrier materials properties	User may choose from a pre-existing list or define their own material with $k$ , $\rho$ , $c_p$ and $\delta$
$A_{\text{surface}}$	Material surface area, ( $\text{m}^2$ or $\text{ft}^2$ )
$k$	Material thermal conductivity ( $\text{kW}/\text{m}/\text{K}$ )
$\rho$	Material density ( $\text{kg}/\text{m}^3$ )
$c_p$	Material heat capacity ( $\text{kJ}/\text{kg}/\text{K}$ )
$\delta$	Material thickness (m or ft)
Lower layer O2	(mol or volume %)
Upper layer O2	(mol or volume %)
Lower layer CO2	(mol or volume %)
Upper layer CO2	(mol or volume %)
Lower layer CO	(ppm)
Upper layer CO	(ppm)

### 7.4.3 Exposing Space Parameters

Floor height	Floor height above reference height (m or ft)
Ceiling height	Height of ceiling above exposing space floor (m or ft)
Smoke layer height	Height of bottom of smoke layer bottom above floor (m or ft)
Upper layer T	(°C or °F)
Lower layer T	(°C or °F)
Lower layer O2	(mol or volume %)
Upper layer O2	(mol or volume %)
Lower layer CO2	(mol or volume %)
Upper layer CO2	(mol or volume %)
Lower layer CO	(ppm)
Upper layer CO	(ppm)

### 7.4.4 Leakage Area Parameters

Top of leakage area	Height of the soffit above the target room floor (m or ft)
Bottom of leakage area	Height of the sill above the target room floor (m or ft)
Leakage area	(m <sup>2</sup> or ft <sup>2</sup> )

### *OUTPUT*

Interface height	Elevation of the bottom of the smoke layer (m or ft)
Temperature, up. layer	Temperature in the target room (°C or °F)
Temperature, low layer	Temperature in the target room (°C or °F)
Oxygen, up. layer	(mol or volume %)
Oxygen, low layer	(mol or volume %)
Carbon dioxide, up. layer	(mol or volume %)
Carbon dioxide, low layer	(mol or volume %)
Carbon monoxide, up. layer	(mol or volume %)
Carbon monoxide, low layer	(mol or volume %)
3-Gas FED, up. layer	Fractional effective dose based on 3 gas toxicology
3-GAS FED, lower layer	Fractional effective dose based on 3 gas toxicology
Heat FED, upper layer	Fractional effective dose based on heat loading
Heat FED, lower layer	Fractional effective dose based on heat loading
CO FED, upper layer	Fractional effective dose based on CO gas toxicology
CO FED, lower layer	Fractional effective dose based on CO gas toxicology

## 7.5 References

- [1] Nelson, H.E., Deal, S., "Corridor: A Routine for Estimating the Initial Wave Front Resulting from High Temperature Fire Exposure to a Corridor," Nat. Inst. Stand. Tech. (U.S.), NISTIR 4869, Gaithersburg, MD 20899, July, 1992.
- [2] Cooper, L.Y., Forney, G.P., "The Consolidated Compartment Fire Model (CCFM) Computer Code, Application CCFM. Vents-Part III: Catalog of Algorithms and Subroutines," Nat. Inst. Stand. Tech. (U.S.), NISTIR 4344, Gaithersburg, MD 20899, July 1990.
- [3] Op cit, pp. flogo2-flogo17.
- [4] Bukowski, R.W., Peacock, R.D., et al., "Technical Reference Guide for the HAZARD I Fire Hazard Assessment Method," Nat. Inst. Stand. Tech. (U.S.), NIST HANDBOOK 146, Volume II, Gaithersburg, MD, June 1989.
- [5] Khalifa, A.J.N., Marshall, R.H., "Validation of Heat Transfer Coefficients on Interior Building Surfaces Using a Real-Sized Indoor Heat Test Cell," International Journal of Heat and Mass Transfer, Vol 33 (10), pp. 2219-2236, 1990.
- [6] Kimmerle, G., "Aspects and Methodology for the Evaluation of Toxicological Parameters During Fire Exposure," JFF/Combustion Toxicology, Vol. 1, pp. 8, February 1974.
- [7] Mitler, H., Rockett, J.A., "User's Guide to FIRST, A Comprehensive Single-Room Fire Model," Nat. Bur. Stand. (U.S.), NBSIR 87-3595, Gaithersburg, MD 20899, September 1987.
- [8] Purser, D.A. "Toxicity Assessment of Combustion Products," SFPE Handbook of Fire Protection Engineering, NFPA, Quincy, MA 02269, pp. 1-212, 1988.
- [9] Op cit, pp. 1-200 & pp. 1-206.
- [10] Levin, B.C. et al., "Synergistic Effects of Nitrogen Dioxide and Carbon Dioxide Following Acute Inhalation Exposure in Rats," Nat. Bur. Stand. (U.S.) NBSIR 89-4105, Gaithersburg, MD 20899, pp. 7, 1989.
- [11] Berl, W.G., Halpin, B.M., "Human Fatalities from Unwanted Fires," Nat. But. Stand. (U.S.), NBS-GCR-79-168, Gaithersburg, MD 20899, December 1988.
- [12] Environmental Protection Agency, "Hazardous Materials Incident Response Operations: 165.5, Envir. Prot. Agency, (U.S.)--Office of Emergency and Remedial Response--Emergency Response Division, Washington, DC, Section, Respiratory Protection Chapter, pp. 2, July 1993.

## 8 INDEX

$\alpha$ .....	53, 76, 78, 91
$\lambda_c$ .....	17, 19, 106, 107, 109, 111
$\lambda_r$ .....	17, 19, 107, 109
$\sigma$ .....	105
$\chi$ .....	73
actual heat release rate .....	6, 17, 58, 69, 82, 86
ambient gas concentrations .....	18, 106
average temperature .....	21
burn trauma .....	125, 126
ceiling jet .....	4, 7, 11, 25, 27-29, 31, 59-61, 79, 93, 101-103, 112, 121
characteristic temperature .....	18
conduction .....	60, 81, 83, 84, 103, 104, 129
configuration factor .....	126, 128
continuous flame height .....	30
control volume .....	12, 13, 46, 47, 66, 68, 70, 81, 84, 98, 105, 115
convection .....	7, 17, 51, 58, 103, 116, 126
convective heat transfer .....	117, 118, 125
corridor .....	4-6, 8, 9, 11, 75, 106, 115, 117-121, 128, 132
dose .....	127, 128, 131
effective heat of combustion .....	18, 110
effective width .....	32-34
egress .....	11, 20, 22, 32-34, 50
energy feedback .....	96
entrainment . . . . .	5, 13, 15, 16, 18, 20-22, 25, 26, 28-31, 49, 50, 59, 60, 93-95, 99, 101-103, 106, 114, 118, 119, 124, 128
entrainment height .....	16, 21, 25, 26, 29, 60
fire heat release rate .	4, 1, 4, 17-19, 21, 22, 26, 27, 29, 31, 49, 50, 53, 59-61, 63, 64, 68, 69, 72, 73, 76, 79, 81, 82, 84, 86, 88, 91, 97, 98, 103, 105, 107, 111
fire height .....	102
flame height .....	30, 31, 49, 51, 95, 96, 98, 107, 111
fluid .....	15, 20, 23, 37, 39, 48, 56, 95, 104, 105, 118, 123, 124
freeburn .....	1, 5, 6, 53, 75, 80-85, 88, 89, 109
fuel burning rate .....	96, 100
heat loading .....	125, 126, 129, 131
heat of combustion .....	16-18, 26, 30, 59, 72, 77, 88, 89, 100, 101, 104, 106, 109, 110

heat of gasification	100, 101, 104, 106, 110
heat release rate	4, 1, 4, 6, 17-19, 21, 22, 26, 27, 29-31, 49, 50, 52, 53, 58-61, 63, 64, 68, 69, 72, 73, 75, 76, 78-84, 86-88, 91, 96-103, 105, 107, 109, 111, 112
heat transfer	17, 49, 67, 68, 83, 93, 103, 104, 116-118, 121, 125, 126, 129, 132
ignition	11, 25, 41, 42, 52, 53, 76, 80-85, 94
jet	4, 7, 11, 25-29, 31, 58-61, 79, 93, 101-103, 109, 112, 121
jet temperature	11, 25-27, 29, 60, 61, 93, 103, 112
lethality	123, 126, 127, 129
mean flame height	30, 49, 95, 96, 98, 111
oxygen calorimetry	96, 97
plume temperature	11, 22, 29, 31
pyrolysis	4, 6, 26, 30, 46, 47, 59, 86, 88, 95-97, 105, 106, 111
pyrolyzate	15, 73
radiation feedback	3, 17, 105
radiative fraction	19, 53, 80, 109
radiative heat transfer	49, 117
radiative ignition	53
second item	52, 54
smoke flow	11, 46, 55-57, 106, 112, 119, 129
smoke interface	94, 105
smoke layer interface	13, 15, 17, 94, 101
specified directory	109
stack effect	38, 39, 47, 56, 106
tenability	4, 126, 129
theoretical fire heat release rate	26, 27, 29, 31, 49, 59, 61
theoretical heat of combustion	17, 18, 26, 30, 59
thermally thick	41, 44, 64, 67, 81
toxic	6, 99, 126
toxic gas	126
upper layer temperature	6, 11, 18, 47, 66, 88, 104
vent flow	46, 55, 56, 124, 126
viability	4, 1, 5, 125-127
virtual origin	95, 96, 102, 105, 106

wall heat losses .....	109
zone fire model .....	18